QATAR UNIVERSITY

COLLEGE OF ENGINEERING

BREAKTHROUGH ASSESSMENT AND KINETIC STUDY OF THE UPFRONT NITROGEN REMOVAL USING LITHIUM CYCLE

BY

ABDULLAH A. OMAR

A Thesis Submitted to

the College of Engineering

in Partial Fulfillment of the Requirements for the Degree of

Master of Science in Environmental Engineering

January 2024

COMMITTEE PAGE

The members of the Committee approve the Thesis of

Abdullah A. Omar defended on 26/11/2023.

Fares AlMomani, Professor of Chemical Engineering, College of Engineering
Thesis/Dissertation Supervisor

Abdul Shakoor, Research Assistant Professor, Center for Advanced Materials
Thesis/Dissertation Co-Supervisor

Mustafa Nasser, Research Professor, College of Engineering
Committee Member

Muneer Baabbad, Research Associate, College of Engineering
Committee Member

Approved:

Khalid Kamal Naji, Dean, College of Engineering

ABSTRACT

Omar, Abdullah, A., Masters : January : [Thesis 2024], Master of Science in Environmental Engineering

Title: Breakthrough Assessment and Kinetic Study of The Upfront Nitrogen Removal Using Lithium Cycle

Supervisor of Thesis: Fares, A., AlMomani.

As Qatar continues to rely on the exportation of liquefied natural gas (LNG) as its primary source of economic growth, new technologies must be investigated to improve the economic appeal and production capacity of traditional LNG plants. This research work aims to investigate the feasibility of a proposed lithium cycle (Li-Cy) that partially removes nitrogen from the natural gas (NG) stream via chemi-sorption using lithium (Li) metal. Nitridation experiments conducted at 60, 80 and 100 ^{o}C showed the middle temperature to be the optimal condition for operation, yielding lithium conversion and nitrogen uptake rate of up to 80% and 19 mmol/g, respectively, after 30 minutes of moisture treatment and 2 hours of reaction time (F: 0.1 L/min, P: 1 atm). Meanwhile, hydrolysis trials proved using steam as a water source to react with lithium nitride (Li_3N) could quickly convert almost all (98%+ conversion) solid particles into lithium hydroxide (LiOH) after 2 hours of reaction time. Experimental results were fit into kinetic models with the obtained areic reactivity of growth being 0.202 and 125 mol/m^2.min, respectively. Preliminary economic evaluation of the proposed Li-Cy showed that given the current prices of ammonia and electricity, NH_3 production would return 0.654 and 0.515 USD/kg Li under ideal (100% conversion) and real scenarios, respectively, both of which are higher than the estimated electrolysis cost of 0.468 USD/kg Li, translating to an annual net profit of approximately 6, 10, 16, 21 and 26 MM USD for a plant capacity of 1, 2, 3, 4 and 5 MTPA, respectively, from the ammonia production alone.

DEDICATION

This work is dedicated to my dear mother, who has encouraged me to pursue higher education and continues to cheer for me for the smallest achievements in my life.

May I continue to keep you proud and smiling <3

ACKNOWLEDGMENTS

First and foremost, I would like to acknowledge the Qatar National Research Fund (QNRF) for making this research work possible under the GSRA grant (**GSRA8-L-2-0411-21011**) and Qatar University for providing all the needs to achieve the requirements of this study.

On a personal note, I would like to give special thanks to my supervisor, Dr. Fares Al-Momani, who was more patient with me than I would have been with myself and providing me with all the needed guidance and useful feedback to move forward, and I cannot forget the great assistance provided to me by the lab technicians Mr. Saied, who was always there to help me with managing and maintaining the experimental setups, Mr. Khaled and Mr. Sivaprasad who were also available to help.

TABLE OF CONTENTS

DEDICATION iv

ACKNOWLEDGMENTS v

LIST OF TABLES viii

LIST OF FIGURES ix

CHAPTER 1: INTRODUCTION 1

1.1 Background Information 1

1.2 Objectives 6

1.3 General Chemistry 6

1.3.1 *Nitridation of Lithium* 7

1.3.2 *Hydrolysis of Lithium Nitride* 8

1.3.3 *Electrolysis of Lithium Hydroxide* 9

1.4 The Applicability of the Li-Cy 12

1.4.1 *Nitridation of Lithium* 13

1.4.2 *Hydrolysis of Lithium Nitride* 15

1.4.3 *Electrolysis of Lithium Hydroxide* 16

1.4.4 *The Li-Cy: Against the Current & the Alternatives* 20

CHAPTER 2: METHODOLOGY 33

2.1 Materials & Equipment 33

2.2 Experimental Procedure 35

2.2.1 *Nitridation* 35

2.2.2 *Hydrolysis* 37

2.3 Calculations & Analysis 38

2.4 Kinetic Models 40

CHAPTER 3: RESULTS & DISCUSSION 42

3.1 Nitridation of Lithium Metal 42

3.1.1 *Ribbon-shaped Lithium Experiments* 42

3.1.2 *Granule-shaped Lithium Experiments* 44

3.1.3 *Kinetic Model* 56

3.2 Hydrolysis of Lithium Hydroxide 63

3.2.1 *Temperature & Heating Rate Experiments* 63

3.2.2 *Reaction Time Experiments* 67

3.2.3 *Kinetic Model* 69

CHAPTER 4: ECONOMIC CONSIDERATIONS 71

CHAPTER 5: PROSPECTS, LIMITATIONS AND FUTURE CHALLENGES 81

5.1 Nitridation 81

5.2 Hydrolysis 82

5.3 Electrolysis 84

CONCLUSION 90

REFERENCES 91

LIST OF TABLES

Table 1. Thermochemistry Data for Relevant Species 6

Table 2. Summary of the Most Relevant Reactions in the Proposed Li-Cy 7

Table 3. Summary of Research Literature on the Three Steps of the Li-Cy 18

Table 4. Summary of Results Using Adsorbents for N_2/CH_4 Mixtures Separation..... 24

Table 5. Summary of Results Using Membranes for N_2/CH_4 Mixtures Separation 26

Table 6. Summary of the Different Technologies and Candidates for UNR 29

Table 7. Preliminary Nitridation Experiments on Lithium Ribbons..... 43

Table 8. LiC% and NUR With Temperature and Flow Rate Changes 44

Table 9. The Reaction Rate Expression ($d\alpha/dt$) for The 18 Different Scenarios..... 59

Table 10. Notations for The Reaction Rate Law Expressions 59

Table 11. Experimental Results of Lithium Nitridation (T: 80 ^oC, P: 1 atm)..... 61

Table 12. Hydrolysis Results of Temperature Trials by CHNS Analysis 67

Table 13. Summary of Analysis Results, LNC% and AP for The Time Trials..... 68

Table 14. Summary of The Main Economic Benefits of Ammonia 78

Table 15. Percentage Increase in Annual Profits 80

Table 16. Summarized points for future work 88

LIST OF FIGURES

Figure 1. Conventional LNG plant 1

Figure 2. Proposed lithium cycle (Li-Cy) for upfront nitrogen removal 4

Figure 3. Publications' volume of literature regarding lithium chemisorption 5

Figure 4. Different alternatives for UNR according to recent research 21

Figure 5. Nitridation reaction column (a) and hydrolysis water container (b) 35

Figure 6. Nitridation experimental setup 37

Figure 7. Hydrolysis experimental setup 38

Figure 8. Effect of temperature on LiC% for different flow rates 47

Figure 9. Effect of temperature on NUR for different flow rates 47

Figure 10. Effect of flow rate on LiC% for different temperatures 48

Figure 11. Effect of flow rate on NUR for different temperatures 49

Figure 12. Extent of chemisorption demonstrated by lithium metal surface consumption for sliced (a) and clustered (b) granules 50

Figure 13. Effect of slicing lithium clusters into individual granules for chemisorption on lithium conversion (a) and nitrogen uptake rate (b) 51

Figure 14. Reaction time trials for the flow rate of 0.05 L/min and T = 60 ^{o}C (a) and 80 ^{o}C (b) 51

Figure 15. Nitridation time experiments at 60 ^{o}C (a), 80 ^{o}C (b) and 100 ^{o}C (c) (P: 1 bar, F: 0.1 L/min, t_A: 30 minutes), and all compared (d) 54

Figure 16. Effect of reaction temperature of 60 (a), 80 (b) and 100 (c) ^{o}C on formation of LiOH layer (F: 0.1 L/min, t_A: 30 minutes, t_{Rxn}: 140 minutes, P: 1 bar) 55

Figure 17. Effect of sample activation time on the lithium conversion to Li_3N (T: 80 ^{o}C, P: 1 atm, F: 0.1 L/min, t_{Rxn}: 120 minutes) 56

Figure 18. Fitted kinetic model of spherical particles with inward growth-controlled

rate at the internal interface (T: 80 ^{o}C, P: 1 atm) 62
Figure 19. Kinetic model fitting into nitridation experimental data at 80 ^{o}C and 1 atm under the assumptions of a) spehrical-internal interface-inward growth b) cylindrical-internal interface-inward growth c) spherical-external interface-inward growth d) cylindrical-external inerface-inward growth e) spherical-external interface-outward growth f) cylindrical-external interface-outward growth. 63
Figure 20. Burned filter and sample 65
Figure 21. Reactor gradual temperature increase (ST: heater's set temperature) 65
Figure 22. Change in Li_3N powder's color to LiOH for 20 (a), 40 (b), 60 (c), 80 (d), 100 (e) and 120 (f) minutes 69
Figure 23. Fitted kinetic model for powdered samples for the hydrolysis of lithium nitride at 80 ^{o}C and 1 atm 70
Figure 24. Block diagram visualizing the economic benefit of upfront nitrogen removal 73
Figure 25. Lithium regeneration loop 77
Figure 26. Li-O-H system's potential diagram 85
Figure 27. Potential setup considering connecting the three-cycle steps for continuous operation 87

CHAPTER 1: INTRODUCTION

1.1 Background Information

Liquefied natural gas (LNG) has quickly matured and is now an important component of the global energy market (Economides & Wood, 2009). Reports showed that the LNG trade has quadrupled in the last two decades. Even as it grows, the LNG industry faces numerous challenges and threats that must be addressed for the industry to grow not only in volume but also in value (Hafezi et al., 2021).

Figure 1 summarizes the unit operation within the conventional LNG plant. In general, the NG processing and liquefaction include complicated unit operations including phase separation, impurities removal (e.g., CO_2 and H_2S), dehydration, mercury removal, separation of heavy hydrocarbons (C^{3+}), and then liquefaction. The cold section is the pillar of the liquefaction process and consumes roughly 60% of the total energy demand. This section is comprised of the refrigeration cycles (C_3MR or SMR, etc.), fractionation unit, nitrogen removal unit (NRU), and helium extraction unit. Shaft's work used to operate compressors accounts for the majority of the total energy demand in this section. Although the NG liquefaction process is well established, there is much innovation to be added that could further optimize the production process and increase the profit. Therefore, heat integration and process optimization are commonly used to reduce energy demand in the LNG process.

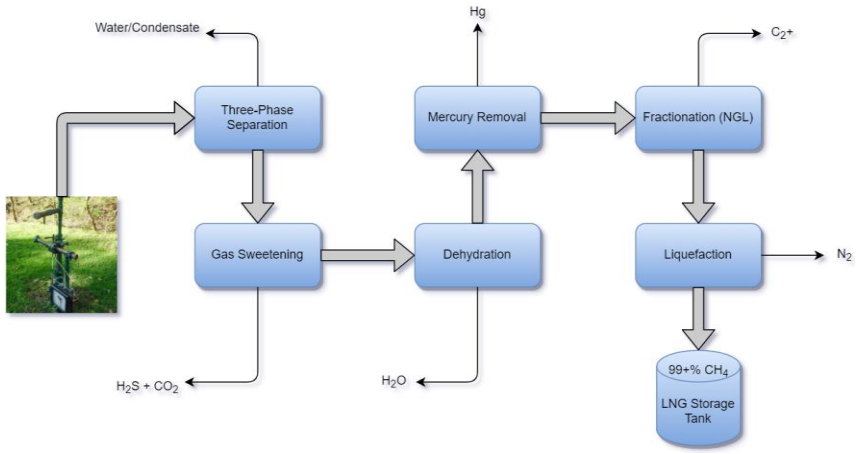

Figure 1. Conventional LNG plant

One particular area of research that could be optimized within an LNG production plant is the nitrogen removal/rejection unit (NRU), which is usually placed at the tail end of the plant to remove nitrogen impurities from the LNG (Lim et al., 2013). The LNG standards call for stringent and lower nitrogen specifications as nitrogen content >1mol% in LNG tanks can cause safety hazards and risk of rollover. The removal of nitrogen from NG in the cold section is usually implemented via separation processes based on molecular, thermodynamic, and/or transport properties between nitrogen and the hydrocarbons (mostly methane). Cryogenic distillation is the most commonly used NRU in commercial LNG plants (Kuo et al., 2012). The process relies on the difference between the boiling points (B.P) of NG (B.P ~ 111.7 ^{o}K) and nitrogen (B.P ~77.3 ^{o}K). This process is reliable and consistently exhibits superior performance in achieving hydrocarbon recovery up to 99+%. However, it has a lot of challenges including the high cost of the refrigeration equipment, the requirements for shaft work to operate gas compressors, and the process is complicated and required a lot of maintenance (Kuo et al., 2012). In addition, removing nitrogen after liquefaction generally increases the energy requirements and reduces the production capacity.

Recently, upfront nitrogen removal (UNR) was proposed as a promising alternative to NRU. The fundamental of UNR is based on separating nitrogen from NG at the hot section, which operates at temperature ranges of 0 to 100 ^{o}C. This would save energy, increase the production capacity and reduce the costs associated with the cooling process. According to (Almomani et al., 2021), the UNR in the LNG plants can lead to significant energy cost savings due to the removal of nitrogen, which moves as an inert gas through the plant. This occupies volume in the plant that could be used for increasing the NG capacity to subsequently increase the energy load on the plant.

The literature review outlines numerous processes for UNR including (1) physical separation technologies such as adsorption (Hu et al., 2021; Kennedy & Tezel, 2018; Y. J. Wu et al., 2015), membrane separation (K. Lokhandwala et al., n.d.; Wang et al., 2018; S. Wu et al., 2020) hybrid processes and distillations (Nagesh Rao & Karimi, 2017) (2) Chemical Separation Technologies (Friesen et al., 2000; Q. Gu et al., 2018; Z. Li et al., 2019) including Absorption

(Z. Li et al., 2019) and lithium-based adsorption (Q. Gu et al., 2018; Z. Li, 2018) and (3) Gas Hydrate Technology (Ballard & Sloan, 2002; Chatti et al., 2005; Dong et al., 2014; Jhaveri & Robinson, 1965). A detailed discussion of all these processes will be presented in a later subsection in this chapter.

The lithium-based adsorption process was found to be a promising technology for reducing the N_2 content from NG to less than 2%. **Figure 2** illustrates the steps included in the Lithium Cycle (Li-Cy), which consist of the chemisorption of nitrogen (Chem_{N_2}) (Q. Gu et al., 2018; Perth & 2018, 2018), hydrolysis of lithium nitride (Hyd_{Li3N}) (Goshome et al., 2015; Jain et al., 2017; Tang et al., 2021; Yamaguchi et al., 2020), and electro-winning (Elec.-w) of the final product to precipitate lithium metal for further reuse (Laude et al., 2010; Takeda et al., 2014; Tang & Guan, 2021). In such a process, lithium reacts with N_2 in NG producing Li_3N. The generated Li_3N undergoes hydrolysis process to generate Li(OH), which can be further reacted to recover and recycle the lithium. Although lithium is the least reactive metal in the alkali group, extensive experimental works have been done since mid of the 20th century elucidating the feasibility of reacting lithium with gases through varying degrees. Water vapor was found to prompt these reactions by reacting with lithium to form a dark layer of Li(OH) and generate hydrogen as a side product (Deal & Svec, 1953; Irvine & Lund, 1963). It was observed that the reaction rate of lithium with other gaseous such as O_2, CO_2 and N_2 was enhanced in the presence of water vapor (M. M. Markowitz & Boryta, 1962; Mcfarlane & Tompkins, 1962). According to (Shang & Shirazian, 2018), the dissociation of water aids in the formation of a LiOH layer on the lithium surface, which provides more active edge sites for approaching gas molecules attachment. While the results of the previously mentioned research may be prone to inaccuracies due to outdated methodologies and less sophisticated equipment, they still prove the existence of the interaction between the lithium metal and gas molecules which was theoretically established by chemists.

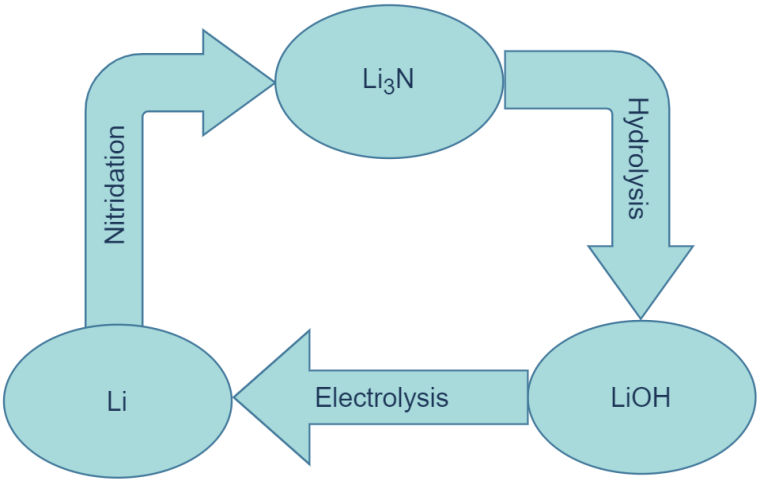

Figure 2. Proposed lithium cycle (Li-Cy) for upfront nitrogen removal

In the context of modern applications of lithium solid for gas chemisorption, lithium was found to be a good medium for hydrogen gas storage through lithium hydride species which can undergo reverse reactions to produce hydrogen (Banger et al., 2018; Ichikawa et al., 2004; Napán & Peltzer Y Blancá, 2012). Lithium solid was also used for CO_2 capture integrated with power generation as in Li-CO_2 batteries (X. Li et al., 2016; Qiao et al., 2017) and for the production of lithium oxide which can be used as a flux in ceramic glazes. **Figure 3** shows the trend of the publications in the last century on the use of lithium for the chemisorption of nitrogen gas in ambient conditions to produce lithium nitride (Li-N_2) and the chemisorption of nitrogen gas from a mixture with methane (Li-N_2-CH_4) to improve the NG quality. It was noted that while the nitridation reaction is well documented in the literature, particularly in the presence of moisture, and is mostly performed by chemists, its use to remove nitrogen from NG streams is less common. The feasibility of this process was recently highlighted through both experimental and theoretical testing (Z. Li, 2018). The thermodynamic favorability of the reaction was also confirmed by (Q. Gu et al., 2018). Moreover, patents for the usage of lithium for the chemical sorption of nitrogen from NG were issued (CHIE et al., 2012; V & SAI, 2018).

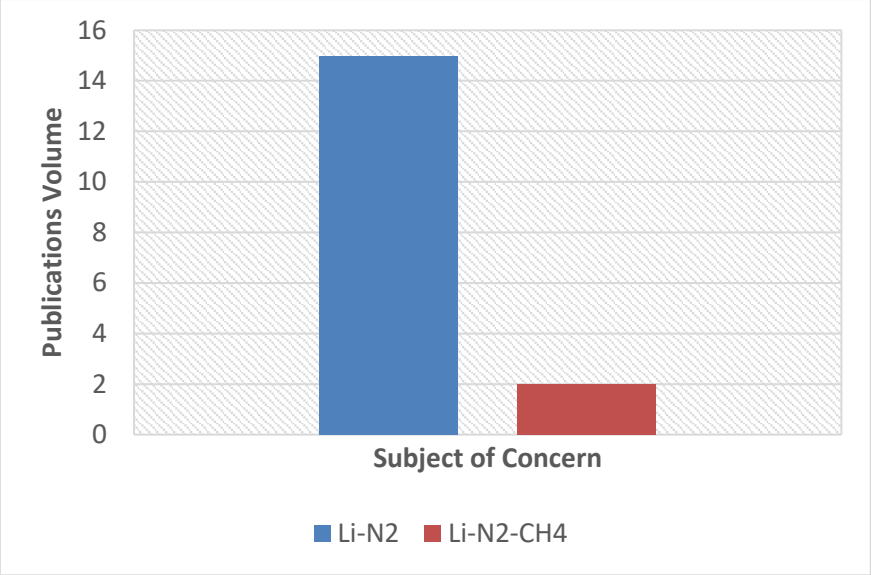

Figure 3. Publications' volume of literature regarding lithium chemisorption

Nitrogen removal from NG using lithium solid chemisorption is a promising and novel process. The theoretical nitrogen uptake can reach up to 24 mmol/g Li, which is higher than any other reported methods. According to (Z. Li, 2018), lithium solid chemisorption can achieve a 100% conversion of lithium to lithium nitride in a mixture of N_2/CH_4. Additionally, the regeneration of the lithium occurs by reacting the lithium nitride with water, which produces ammonia as a side product (Jain et al., 2017). This increases the economic attractiveness of this method. The aforementioned literature review suggests that Li-Cy is a promising technology for URN from NG. While the use of lithium metal to adsorb nitrogen was conducted in previous research for chemistry studies (M. M. Markowitz & Boryta, 1962), safety hazard studies (Maroni et al., 1981), as a medium to store renewable energy (Brockhinke et al., 2014) and even as an intermediate in ammonia production (McEnaney et al., 2017), little to no research investigates lithium chemisorption applicability and economic feasibility with NG under real operation conditions. Therefore, this study focuses on the use of Li-Cy for nitrogen removal for the purpose of utilizing it for a mixture of gases in general and NG in specific. It aims to evaluate the literature research work on the aforementioned Li-Cy steps, including the process chemistry, applicability, economic feasibility, and the challenges and limitations that may be faced during the integration with a real LNG plant. The findings of this research help pave the

way for the development of will-defined Li-Cy, which has the potential to be a viable option among the many options for UNR from NG.

1.2 Objectives

Based on the previous analysis, the objectives of this study are:

1- Establishing the reaction kinetics for the nitridation of lithium, hydrolysis of lithium nitride and if possible, the electrolysis of lithium hydroxide as a full cycle (Li-Cy)

2- Obtaining reaction data and fitting them into newly found/novel kinetic models that do not simplify the relationship between the thermodynamic and morphologic variables

3- Investigating the economic feasibility of the proposed Li-Cy as a method of upfront nitrogen removal in the context of baseload LNG plants in Qatar

The extent to which these objectives will be achieved depends on the time constraints and the occurrences of interruptions/inconveniences to the project work, but the ultimate objective is to prove the feasibility of the proposed Li-Cy as an UNR technology for baseload LNG plants to reduce energy costs and increase production capacities.

1.3 General Chemistry

This section briefly summarizes the relevant reactions expected to occur in the proposed Li-Cy. It is important to highlight that many other reactions can occur with regards to Li involving H_2, O_2 and CH_4, but will not be competitive (Q. Gu et al., 2018). Due to differences in free energy reactions, a hierarchy is established, which prioritizes competitive reactions. Given the novelty of the subject, there is minimal literature that investigates these reactions within the context of NG treatments. That being said, **Table 1** contains the extracted thermochemistry data for the relevant species in the Li-Cy (*NIST Chemistry WebBook,* n.d.), and **Table 2** provides a summary of its most relevant reactions.

Table 1. Thermochemistry Data for Relevant Species

Species	S^0 (J/mol.^{o}K)	ΔH_f^0 (kJ/mol)
$Li_{(s)}$	29.09	0
$N_{2\,(g)}$	191.61	0

Species	S^0 (J/mol.°K)	ΔH_f^0 (kJ/mol)
$Li_3N_{(s)}$	62.66	-164.56
$H_2O_{(l)}$	69.95	-285.83
$H_2O_{(g)}$	188.84	-241.83
$LiOH_{(s)}$	42.81	-484.93
$LiOH_{(l)}$	47.97	-474.42
$NH_{3\,(g)}$	192.77	-45.94
$O_{2\,(g)}$	205.15	0

Table 2. Summary of the Most Relevant Reactions in the Proposed Li-Cy

Reaction	Type	Temperature Cond.	Note
$6Li_{(s)} + N_{2(g)} \rightarrow 2Li_3N_{(s)}$	Spontaneous Exothermic Nitridation	25 – 100 °C	Does not occur at such low temperatures without prior activation by moisture (vapor H_2O).
$Li_3N_{(s)} + 3H_2O_{(g)} \rightarrow 3LiOH_{(s)} + NH_{3(g)}$	Spontaneous Exothermic Hydrolysis	25 – 100 °C	A highly exothermic reaction that requires cooling. Produces ammonia as a side product (side benefit).
$LiOH_{(l)} \rightarrow Li_{(s)} + {}^1/_2\,H_2O_{(l)} + {}^1/_4\,O_{2(g)}$	Non-spontaneous Endothermic Electrolysis	>325 °C	Energy-intensive step, utilizing electric current at elevated temperatures to regenerate Li metal at the cathode.

1.3.1 Nitridation of Lithium

In the first step of the cycle, lithium metal is exposed to nitrogen gas at low temperature, below the melting point, to yield lithium nitride as expressed by **Eq. 1**. The enthalpy of formation, entropy change, and Gibbs free energy change at 25 °C for a single mol of lithium nitride are 164.6 kJ/mol, -121.1 J/mol.°K, and -128.5 kJ/mol, respectively. These values are extracted/calculated from the NIST Chemistry WebBook (*NIST Chemistry WebBook*, n.d.).

$$6Li_{(s)} + N_{2(g)} \rightarrow 2Li_3N_{(s)} \quad (1)$$

This reaction is exothermic and spontaneous. However, according to (Jeppson et al., 1978), it does not occur with dry nitrogen and required the presence of water moisture (≥10 ppm). The water moisture activates the surface of lithium and produces the white to gray-colored lithium

hydroxide and lithium hydride, or hydrogen (Shang & Shirazian, 2018). The reaction with moisture has two benefits: the creation of a lithium hydroxide layer that promotes a more active edge site for the nitridation reaction to occur (Z. Li, 2018), and the release of energy (375 kJ/mol) that is used as the activation energy for the nitridation reaction (Q. Gu et al., 2018). Based on the existing research literature, there is conflictual evidence on the likelihood of lithium reacting to nitrogen in dry conditions. For instance, (Mcfarlane & Tompkins, 1962) argue that it is possible for the reaction to occur, while (Meyer M. Markowitz & Boryta, 2002) assert that lithium will remain stable for days. (Wayne Ronald Irvine, 1961) confirmed that the moisture pre-treatment significantly enhances the reaction rate.

While **Eq. 1** describes the primary reaction that occurs when lithium is exposed to nitrogen, when thinking about NG, it can be helpful to imagine other relevant species besides nitrogen (i.e., impurities) such as H_2, CO_2, and O_2. For example, (Q. Gu et al., 2018) summarized 21 reactions that include lithium, lithium hydride, and lithium hydroxide with the aforementioned gases and calculated the activation energy for each reaction. Notably, most of these reactions do not theoretically or experimentally occur due to the favorability of reactions with low activation energies. Some of them, however, may occur and are highlighted with their Gibbs-free activation energies in **Eqs. 2 – 4**. These reactions involve LiH and LiOH species, which may be present due to moisture pretreatment. They are thus more likely to react with N_2 to generate Li_3N as well.

$$6LiH + N_2 \rightarrow 2Li_3N + 3H_2 \qquad \Delta G = 13.4\ \frac{kJ}{mol} \tag{2}$$

$$3LiH + N_2 \rightarrow Li_3N + NH_3 \qquad \Delta G = 96.4\ \frac{kJ}{mol} \tag{3}$$

$$3LiOH + N_2 \rightarrow Li_3N + N(OH)_3 \qquad \Delta G = 327.6\ \frac{kJ}{mol} \tag{4}$$

1.3.2 Hydrolysis of Lithium Nitride

The “used adsorbent” can be regenerated in two different ways, hydrolysis and hydrogenation methods. The hydrolysis method differs from the hydrogenation of Li_3N, which uses H_2 gas instead of water to produce ammonium (Goshome et al., 2015; Yamaguchi et al., 2020). While not the focus of this study, hydrogenation can be an alternative to hydrolysis. As demonstrated

by **Eq. 5**, in the hydrolysis method, the Li_3N reacts with water in a violent exothermic reaction to produce lithium hydroxide and ammonia as a side product.

$$Li_3N_{(s)} + 3H_2O_{(g)} \rightarrow 3LiOH_{(s)} + NH_{3(g)} \quad (5)$$

The hydrolysis reaction can occur at room temperature with thermodynamic parameters ΔH, ΔS, and ΔG of -610.6 kJ/mol, -307.9 J/mol.°K, and -518.8 kJ/mol, respectively (*NIST Chemistry WebBook*, n.d.). As concluded from the enthalpy of the reaction, this reaction is exothermic and spontaneous as confirmed by the research by (Jain et al., 2017) on ammonia production by lithium nitride hydrolysis. Following this reaction, it was noted that the reactor temperature and pressure increased from room temperature and 0.1 Pa to 80 °C and 0.8 MPa, respectively. It was confirmed through the same study that the reaction can reach 100% conversion at room temperature and generate hydrogen gas. In **Eq. 5**, water must be in vapor phase form to avoid an excessive dissipation of energy that could dissociate the formed NH_3. Moreover, as ammonia is fairly soluble in water at the desired reaction conditions the reaction should be conducted using water vapor on solid surfaces away from water liquid to allow the ammonia gas to escape (Hales & Drewes, 1979). The hydrogenation of lithium nitride is also expected to happen simultaneously with the hydrolysis process. This is due to the presence of H_2 as an impurity in the NG stream or as a side product from the aforementioned reactions. As demonstrated in **Eq. 6**. The reaction will consume lithium nitride and hydrogen gas to produce lithium hydride and ammonia.

$$Li_3N_{(s)} + 3H_{2(g)} \rightarrow NH_{3(g)} + 3LiH_{(s)} \quad (6)$$

However, this reaction was reported to occur at relatively high temperatures up to 500 °C (Goshome et al., 2015; Tang et al., 2021; Yamaguchi et al., 2020). If lithium hydride forms, it can always be turned into lithium nitride by reacting with nitrogen per **Eqs. 2** & **3**. Though, this reaction is not expected to be significant due to the limited reaction conditions.

1.3.3 Electrolysis of Lithium Hydroxide

The hydrolysis of lithium nitride primarily yields lithium hydroxide (LiOH), which must be processed to generate Li that can be used again for the chemisorption step. Most industrial

generation of lithium by electrolysis is conducted with LiCl-KCl molten salt mixtures. In this step, a eutectic mixture of LiOH-LiCl is introduced as the analyte inside the electrochemical cell at elevated temperatures. The anode and cathode half-reactions occur according to **Eqs. 7** & **8**, respectively. Then, **Eq. 9** describes the overall reaction. This reaction is the most complex in the cycle in terms of reactor setup, conditions, and complexity. The heating and electricity flow requirements also make the maintenance process more complicated.

$$OH^- \rightarrow e^- + {}^1/_2\, H_2O + {}^1/_4\, O_2 \qquad E^0 = -0.4\ V \tag{7}$$

$$Li^+ + e^- \rightarrow Li \qquad E^0 = -3.05\ V \tag{8}$$

$$LiOH \rightarrow Li + {}^1/_2\, H_2O + {}^1/_4\, O_2 \qquad E^0 = -3.45\ V \tag{9}$$

The cell potential of the reaction indicates that it is not spontaneous and requires an electric current. The reported potentials for **Eqs. 7 – 9** are standard values at 25 ^oC, and the melting points for LiOH and LiCl are 462 and 605 ^oC, respectively. (Levin & McMurdie, 1975) note that LiOH-LiCl has a eutectic melting point of 325 ^oC with a molar concentration between 70% to 30%. The operating temperature inside the reactor for this step is expected to be quite high. This significant increase in temperature from standard conditions (300+ ^oC) seems to only have a small impact on the dissociation potential, which was reported to be 3.05 V at 380 ^oC (Laude et al., 2010) and 2.9 at 350 ^oC (Takeda et al., 2014). Conversely, (Tang & Guan, 2021) identified the potential to be 2 V at 400 ^oC, which was explained by their use of liquid Sn as the cathode. This was a modification that seems to decrease the dissociation potential. The electrolysis efficacy of LiOH in molten salt is measured by the Faraday efficiency of the cell. Within this context, it is defined as the ratio between the actual amounts of metal (Li) deposited at the cathode by a current divided by the theoretical amount of the same metal deposited according to Faraday's law of electrolysis (*Faraday's Laws of Electrolysis | Definition, Example, & Facts | Britannica*, n.d.) (**Eq. 10**). Where n is the number of moles precipitated on the electrode, t is the total time the current was constantly applied, F is the Faraday constant, and v is the valency.

$$n = \frac{It}{Fv} \tag{10}$$

One area of concern noted in the literature is the undesirable precipitation of Li_2O on the cathode. This hinders the regeneration of Li as it reacts with LiOH via the spontaneous reaction outlined in **Eq. 11**. This reaction harms Li recycling and reduces the yield. When the Li_2O precipitates on the cathode, less surface area is available for Li to form. This can be prevented by adding a porous membrane to block the LiOH from traveling to the cathode section (Tang & Guan, 2021).

$$Li + LiOH \rightarrow Li_2O + {}^{1}/_{2}\, H_2 \qquad \Delta G^0 = -96.9\ \frac{kJ}{mol} \tag{11}$$

As water (H_2O) is a side product in **Eq. 9**, a possible interfering reactant present in the moisture with an electrolysis potential of 1.23 V (less than the main reaction), it is expected to have a negative effect on the reaction conditions. This uses up some of the electric currents, which leads to a decreased current efficiency as suggested by (Laude et al., 2010). The current efficiencies in the electrolysis of LiOH were reported to range from 38% (Laude et al., 2010) up to >80% (Takeda et al., 2014; Tang & Guan, 2021).

Given the nature of such reactions discussed in this section, it is concluded that such a pathway that starts with lithium metal and undergoes a regeneration cycle for continuous operation in an LNG plant is theoretically possible with attention to the highlighted details and the concerning reaction conditions. Some of these conditions include temperature, pressure and energy requirements. It was observed that the required temperature and pressure are within operating conditions of the hot section in the LNG plant. That being said, integrating and operating such a cycle with an LNG plant will require better knowledge of the limitations and challenges that will be discussed in a later section. For example, hydrolysis of lithium nitride must be performed on a pure lithium nitride sample to avoid the evolution of hydrogen gas but given that complete conversion in the nitridation step on a large-scale setup could be very difficult to achieve, it would be wise to account for the increase in reactor pressure that will inevitably build-up due to the "undesired" gas production. Regardless, most of these challenges can be easily remedied by simple solutions such as modifications to the reactors and higher bed volume with high surface area to compensate for "inactive" lithium that is not converted in the

calculations to obtain the effluent methane purity.

1.4 The Applicability of the Li-Cy

This section focuses on analyzing techniques and technologies that use lithium metal (Li) to support the proposed lithium-based cycle. The majority of the research work that was examined whether experimental or theoretical, widely differs from the perspective of this work. For example, the research typically focused on presenting the nitridation reaction between Li and nitrogen (N_2) or establishing an ammonia production process or cycle, rather than formulating a cycle for the UNR from the LNG plant. However, this research can be beneficial for this case as collecting the associated outcomes supports the visualization of the possible approach and performance of the cycle. Thus, this section aims to gather practical information, data, and results about one or more steps of the proposed lithium-based cycle. This helps to finalize the circumstances and conditions required for ensuring the practicability and reliability of the lithium-based cycle. This section will serve as a summary of the work done that demonstrates the feasibility of the Li-Cy in each step, and a more critical discussion regarding the accuracy, reliability of reviewed literature and the limitations and challenges of associated technology will be further discussed in Chapter 5. Lastly, much like the previous section, this section is divided into three parts, which encompass the three reactions of the lithium-based cycle.

Interestingly, there is research work in the literature that targets a similar desired goal for the upgrading of NG, though it primarily focuses on removing impurities instead of the possibility of a cycle. (Q. Gu et al., 2018) presented an approach for NG purification by using pre-treated lithium with moisture as a material for adsorbing the impurities from the NG stream. The performance of lithium as an adsorbent for selective separation when exposed to different gas mixtures was studied theoretically. The density functional theory (DFT) calculations were used for the reactivity analysis. Additionally, the temperature-programmed kinetic Monte Carlo calculation method (TP-KMC) was used to analyze the effectiveness of the lithium to adsorb the impurities in the streams of the gas mixtures containing methane. The results highlighted thermodynamic favorability and confirmed the separation approach to occur spontaneously and provided outstanding conclusions that it may potentially achieve a high purity methane stream.

The main problem with these results however was the reliance on the Arrhenius law for studying and predicting the reaction kinetics, which is problematic for several reasons, not the least of which is the assumption of temperature-independence of the reaction free energy (Michle et al., 2011). Nevertheless, the researchers found that the main mechanism influencing the process is the reaction between the captured gases and the components produced after the exposure of lithium to moisture. The TP-KMC calculations highlighted how the binary mixture of N_2 (10%) and methane at 35 ℃ and 0.1 MPa can be effectively separated after operating the system for 70 minutes. This achieved a high purity of methane stream and collected N_2 as a solid (lithium nitride, Li_3N). The desired selectivity can still be achieved at higher temperatures due to the maintained differences in reaction kinetics. When the temperature is increased the reaction slightly increases and the separation time decreases (Q. Gu et al., 2018). It should be reminded that the pressure of the proceeding and succeeding units (dehydration, NGL recovery, liquefaction) operate at much higher pressures. The NG dehydration unit is commonly operated at 70 bar and can go up to 200 bar (Netušil & Ditl, 2012), which would only make the nitridation process more attractive as the chemisorption would positively benefit from higher pressures.

1.4.1 Nitridation of Lithium

The nitridation of the Li reaction is considered to be the first reaction in the proposed cycle. This specific step was introduced as the first step in work that focused on the N_2 reduction reaction and the ammonia production process or cycle. For instance, (Jain et al., 2017) introduced Li metal as a test start material for the nitridation process at room temperature in a differential scanning calorimetry (DSC). The DSC profile of the nitridation reaction indicated how exposing fresh Li to N_2 with pressure no less than 0.8 MPa starts the reaction. After that, the reaction continuously occurred and an exothermic peak was identified at a temperature of approximately 50 ℃, which increased from room temperature. The DSC profile and the X-ray diffraction analysis (XRD) pattern in this work confirmed the complete transition of Li to Li_3N as no endothermic peak was observed at 180 ℃ (the melting point for Li). Additionally, the metal surface of the Li affects the characteristics of the nitridation, meaning that it has a clear

influence on the temperature and pressure needed for the reaction to occur. When the Li is exposed to air for 6 hours, the reaction could not be initiated at room temperature even when the pressure of N_2 increased to 1 MPa. The required temperature for a reaction increased when the Li sample was exposed to the air for 6 hours. After the sample was exposed to the air for 24 hours, the temperature reached values closer to the melting point of Li.

The relation between temperature and reactivity was also studied. It was found that the preheated Li (at 100 ℃) required less pressurized N_2 (0.5 MPa) than the non-preheated Li (0.8 MPa) (Jain et al., 2017). The required pressure can be less than 0.35 MPa when preheating the Li to higher temperatures such as 150 ℃. While thermodynamically the reaction can proceed at room temperature with a pressure of 0.1 MPa, it has activation energy to overcome. Given that, high pressure is essential for the initiation of the reaction. As a result, for the reaction to occur at lower pressure values, the Li needs to be heated to higher temperatures.

(McEnaney et al., 2017) presented the nitridation of Li reaction as part of a proposed ammonia production cycle. The cycle was principally designed based on the Li-N-O-H phase diagram, which is constructed with a reference pressure of 1 bar, a pH of 1, a temperature of 300 ^{o}K, and a Li^{+} ion concentration of 10^{-6} M. Throughout the cycle steps, it is possible to adjust for optimized conditions because the diagram's energy differences are quite large. Consequently, the physical state of the cycle is not greatly affected by parameter changes. Importantly, before the nitridation reaction, voltage is applied to the Li sample to produce an electronically activated surface. Then, it is exposed to N_2 gas in a tube furnace with a maintained temperature range between 22 and 100 ℃. Next, the Li_3N product is created.

The outcome of the nitridation reaction was pronounced beginning at the ammonia production point, meaning that the conversions were based on the ammonia production from reacting the product of the nitridation reaction with water. The conversion was analyzed at three different temperatures of the nitridation reaction including 22, 50, and 100 ℃ and in two different time frames of 30 minutes and 12 hours (McEnaney et al., 2017). Increasing the temperature of the nitridation reaction led to higher conversion values. Additionally, exposing the N_2 flow to 100

℃ for 30 minutes produced conversion values greater than 80%. In contrast, exposing the N2 flow for 12 hours resulted in near-complete conversion values. Moreover, XRD analysis substantiated the presence of Li_3N and traces of LiOH and Li_2O, which resulted from transferring the Li sample from the electrochemical cell to the furnace tube of N_2. The exposure of O_2 and H_2O found in the atmospheric air seemed to increase the rate of the nitridation reaction.

1.4.2 Hydrolysis of Lithium Nitride

This section focuses on the hydrolysis of Li_3N, which is the second reaction in the proposed cycle. In the research literature, the reaction was discussed within the context of ammonia production reactions or cycles. (Jain et al., 2017) presented a new experimental approach using nitride hydrolysis for the production of ammonia, a hydrogen storage material comprised of 17.8 wt% of hydrogen at temperatures lower than 100 ℃. Hydrolysis controls the atmosphere at a temperature of 80 ℃, and the Li_3N must react with the water vapor rather than the liquid water. This approach converts nitrides to receive ammonia through exhaust heat, solar heat, or thermal energy. The conversion was conducted in a simple reactor system that turns heated water into water vapor, which then passes through a metallic filtrate with a Li_3N sample. As an initial trial, the experiment was performed with a pressure of 0.1 Pa and at room temperature in the reactor system with a closed chamber. This was repeated multiple times to optimize the reaction conditions. The optimized temperature for the reaction to occur was 80 ℃, with a considerably high amount of Li_3N consumption and the lowest possible hydrogen generated value. Importantly, the XRD analysis substantiated the LiOH as a product of the hydrolysis reaction and the calculations confirmed a reaction fraction of 95% after 2 hours of reaction at 80 ℃.

(McEnaney et al., 2017) examined an innovative production procedure for ammonia to find a substitute for the Haber-Bosch process, which is an energy-intensive and unsustainable approach for ammonia production. The hydrolysis reaction was conducted between Li_3N and de-ionized water (10 mL) in scintillation vials. The determination and quantifying of ammonia

were accomplished using two approaches with high accuracy: the colorimetric test connected to the ultraviolet-visible light spectroscopy (UV-Vis) and Fourier transform infrared spectroscopy (FTIR). The results of this proposed cycle, depending on the individual step, exhibited an 88.5% current efficiency for ammonia yield. Moreover, the results of the ammonia conversion achieved high values of more than 80% when the temperature of the nitridation reaction was 100 ℃ after 30 minutes of exposure to N_2. Higher values were obtained when the exposure to N_2 was for 12 hours at different temperatures. The source of the N_2 in the cycle was also confirmed using FTIR, which came from the provided gaseous N_2 and not from an unexpected source.

1.4.3 Electrolysis of Lithium Hydroxide

This subsection focuses on the electrolysis of LiOH, which is the final step of the Li cycle. In the research literature, this reaction was investigated within the context of the techniques used for hydrogen storage. (Takeda et al., 2014) explored the practicality of Li recovery from LiOH by electrolysis in molten chloride. This was aimed at forming a system for hydrogen storage and transportation. A potential diagram for the Li-H-O system formed, which was dependent on thermodynamic data. The recovery of Li from LiOH cannot be accomplished if the molten salt from the electrolysis had LiOH as one of the components. This is because the recovered Li from the electrolysis will react with the LiOH available in the molten salt generating Li_2O. In this approach, it was preferable to assemble the components of the experimental setup in the Quartz tube to prevent the direct contact of freshly generated Li with LiOH. Instead, molten LiCl–42 mol% KCl or molten LiCl–17 mol% KCl–26 mol% CsCl were used as the molten salt. Then, the LiOH was inserted into the anode section away from the Li metal, which is deposited in the cathode section.

Following this approach, the Li metal was collected at the end of the electrolysis. The hydrogen generated from reacting Li with water also enabled the calculation of the lithium deposition current efficiency (Takeda et al., 2014). The two proposed molten salts, through different conditions, were used to analyze their impact on the cathode and anode reactions as well as the

overall electrolysis. The temperature of the molten salt did not have a strong effect on the cathode current efficiency. Using LiCl–KCl or LiCl–KCl–CsCl molten salts at lower temperatures also did not cause a major difference in the cathode current efficiency, which can reach a value up to 84 to 86%.

(Laude et al., 2010) proposed a three-step cycle designed to ensure an efficient hydrogen supply from LiH. The cycle process is based on recycling the LiOH, which is the by-product of the LiH hydrolysis (i.e., first step). The electrolysis of LiOH (i.e., second step) is considered to be the recycling reaction, where Li metal is created through a hydrogeneration reaction (i.e., third step). The researchers also focused on the electrolysis of the LiOH, which was conducted in a quartz reactor at 380 ℃ using a LiOH-LiCl mixture as the molten salt. This achieved 37.9% current efficiency. During electrolysis, constant values of current electrolysis (1.5 A) and current density (1.5 A/cm^2) were used. The amount of hydrogen generated from dropping the collected Li metal from the electrolysis enabled the determination of the amount of metal generated. The first 30 minutes of the experiment exhibited a low current efficiency (12.5%) due to the moisture in the LiOH-LiC1 mixture. Then, after 16 minutes the current efficiency increased to 37.9% and the metal produced was established as Li by the differential scanning calorimetry. Moreover, with the cyclic voltammetry measurement, the anode behavior exhibited no LiC1 dissociation and no anode corrosion as there were no corresponding peaks and only one main reaction was identified ($\mathrm{LiOH} \rightarrow \mathrm{Li^+} + \mathrm{e} + \frac{1}{2}\mathrm{H_2O} + \frac{1}{4}\mathrm{O_2}$) (Laude et al., 2010). Conversely, for the cathode, only one reaction was determined ($\mathrm{LiOH} + \mathrm{e} \rightarrow \mathrm{OH^-} + \mathrm{Li}$), which confirmed the Li metal deposition. Although other peaks were found, it is likely only due to some water electrolysis and impurities. The non-generation of Cl_2 was also confirmed with the KI solution test.

(McEnaney et al., 2017) demonstrated how the LiOH electrolysis in the LiCl–KCl/LiOH–LiCl molten salt mixture is a step in the cycle for ammonia production. The setup used for the electrolysis was designed to ensure that there was no direct contact between the produced Li with LiOH, H_2O, or O_2 to avoid any possible side reactions. Depending on the melting

temperature of the molten salt mixture, the temperature of the electrolysis was maintained at 450 ℃ to ensure the liquid phase of the molten salt. Additionally, cyclic voltammetry was used to analyze the behavior of the electrolysis process. It was determined that the total cell potential for LiOH was approximately 3.0 V, which is consistent with the theoretical values of 2.8 V at 427 ℃. The current efficiency of the LiOH electrolysis associated with Li production was examined and the average yield reached 88.5%.

As highlighted, each article provided its perspective on one or more of the reactions of interest. Analyzing the research helps to understand the exact conditions and circumstances needed for the reactions as well as the outcomes. As such, the following **Table 3** summarizes the relevant research conclusions that should be considered.

Table 3. Summary of Research Literature on the Three Steps of the Li-Cy

Step	Literature work	Advantages or beneficial conclusions	Drawbacks, concerns, or areas of improvement
Nitridation	(Q. Gu et al., 2018)	• Specific semi-related scope of work, utilizing Li as an adsorbent for NG upgrading. • In 70 minutes of operation at 35 ℃ and 0.1 MPa, a high purity methane stream can be achieved.	• No experimental work was provided.
	(Jain et al., 2017)	• A confirmation of the complete transition from Li to Li_3N, by the DSC profile, and XRD analysis. • The reaction was performed at 55°C and 0.8 MPa and was completed in 15 minutes.	• Preheating Li to reduce the required pressure for the nitridation reaction, when lithium is exposed to air for hours, needs further investigation.

Step	Literature work	Advantages or beneficial conclusions	Drawbacks, concerns, or areas of improvement
	(McEnaney et al., 2017)	• Conversion efficiency calculations and XRD analysis confirmed the transition from Li to Li_3N. • Conversion efficiency reached more than 80%, after 0.5 h of reaction at 100 ℃.	• The results of the conversion of the reaction are related to the NH_3 production, meaning that there are no separate results represented for the reaction, which could have been helpful in comparison with other approaches. • The complete conversion was only achieved when the reaction between Li and N_2 was for 12 h.
Hydrolysis	(Jain et al., 2017)	• Well-represented setup that provides easy collecting of LiOH. • A high value of Li_3N consumption reached 95% after the reaction was performed at 80℃.	• The experimental setup requires a vacuum pressure, which can be hard to achieve in some circumstances. • It is mandatory to control the atmosphere of the reaction properly and to work with water vapor. • The setup needs modifications for it to work in continuous production and be applicable in the industry.
	(McEnaney et al., 2017)	• High-accuracy analysis methods were applied.	• The setup needs extra investigation for it to work continuously. • As this step was mainly focused on ammonia production, the LiOH yield was not elaborately demonstrated.
Electrolysis	(Takeda et al., 2014)	• Cathode's current efficiency reached 84-86%. • Using molten salts that do not have LiOH and a setup that prevents the direct contact of LiOH with generated Li.	• At the graphite anode used, there was CO_2 generation. • Possible Cl_2 generation.

Step	Literature work	Advantages or beneficial conclusions	Drawbacks, concerns, or areas of improvement
	(Laude et al., 2010)	• No CO_2 generation. • KI solution test was performed, and it was found that No Cl_2 production on the anode confirmed no LiCl decomposition.	• Not very high current efficiency, 37.9%, that needs improvement. • Chemical crossing in the Castner cell causes current loss. • Using molten salt that has LiOH as one of its components could be a reason for the low current efficiency. • The remaining moisture in the LiOH-LiCl mixture wasted 30 minutes.
	(McEnaney et al., 2017)	• An average current efficiency to Li of 88.5% • This work pointed out experimental details for collecting Li from the electrolysis reaction and properly preparing it for the nitridation reaction. • Comparable value of total cell potential for LiOH. • Cell stability was tested. • Negative results for the Cl_2 generation test.	• The used graphite rods can cause CO_2 generation.

1.4.4 The Li-Cy: Against the Current & the Alternatives

After discussing each step of the proposed Li-Cy, it is worth briefly discussing what it is supposed to replace/enhance and the other currently researched technologies in the separation of CH_4/N_2 gas mixture. After a literature review of the most recently published work in the last couple of years, the most prevalent technologies are summarized in **Figure 4**, which classifies such technologies into physical, chemical, and gas hydrate formation. Hybrid technology is possible and is discussed by the work of (Almomani et al., 2021) who present several designs that incorporate multiple technologies into one LNG plant. The technology in the figure can all

be operated in the hot section of the LNG plant (ambient temperatures), hence they are the best candidates for UNR, and more research is still being conducted into their selectivity and performance, so while they may not all be competitive with current practice, they are the focus of the scientific community in this subject.

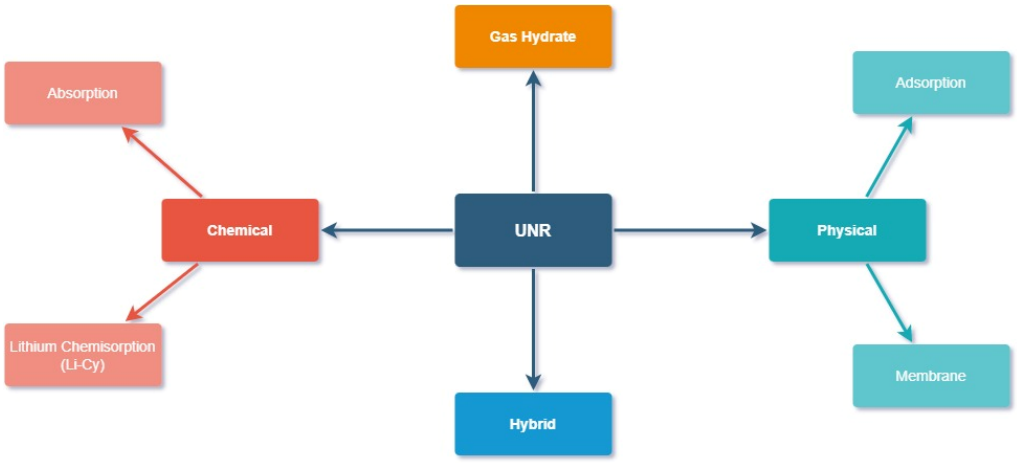

Figure 4. Different alternatives for UNR according to recent research

Physical separation processes rely on differences between N_2 and CH_4 in terms of physical properties, such as volatility, van der Waals forces, and molecular size among others. The most important and commonly used technology in nitrogen separation from NG is cryogenic distillation, and it essentially consists of a series of heat exchangers, compressors, a refrigerant, and a distillation column in which the CH_4-N_2 stream is cooled to extremely low temperatures such that methane liquefies due to its boiling point of -162 ^oC while nitrogen remains mostly gaseous due to its lower boiling point of -196 ^oC by a refrigeration cycle that utilizes mixed refrigerants and propane, before being directed to the distillation column where they are naturally separated the same way as a regular distillation column (volatility differences), though at low temperatures, hence the "cryogenic" term. Cryogenic distillation is currently the go-to option for most operating LNG plants due to its well-established nature and reliability in achieving high-quality LNG with satisfactory heating values and energy recovery ratios. The main "problem" with such technology is, unsurprisingly, the vast amount of monetary

investment due to the high energy demands of the liquefaction, which is ultimately manifested in fuel requirements. This is usually moderated by the utilization of nitrogen-rich methane gas streams as fuel which are produced at the LNG plant, due to having low qualities are not feasible to sell, but these can only do so much. Even when utilizing such gas streams for fuel demands, it is reported that most of the LNG plant costs are attributed to the cold section of the plant, which includes the liquefaction and distillation units. This technology's intense energy demands are the driving force behind the authors' proposal of the Li-Cy in which the nitridation of lithium is documented to occur at ambient temperatures, that is in the hot section of the LNG plant. The Li-Cy would be able to remove nitrogen without the need for cooling, and if such technology manages to remove N_2 even partially, serious economic savings could be made, which will be further discussed in a later section.

Given the economic appeal of upfront nitrogen removal, it is worth discussing the different candidate technologies to achieve it. Most literature investigated focuses on two processes, namely adsorption and membrane technology, and a summary of the different options along with some of their reviewed performances is found in **Table 4 & Table 5**. it should be noted that the numbers of the process performances are extracted from preferred papers, that is work based on: a) Experimental results: because they are more representative of real scenarios and no assumptions or simplifications are made regarding the removal process and b) N_2-containing mixture gas' separation process since research exists that investigates the removal of acidic gases among others, but for the sake of comparison with the proposed Li-Cy, our interest only lies in the separation between N_2 and CH_4.

Adsorption is driven by the van der Waals attraction forces between one of the NG components and the surface of the adsorbent, either natural or synthetic. Existing literature contains the usage of many types of materials for CH_4-N_2 separation, such as activated carbon (AC) (Yao Li et al., 2019), zeolites (Kencana et al., 2022; Y. Wu et al., 2021), metal-organic frameworks (MOFs) (Chang et al., 2021; C. Zhang et al., 2022; Zheng et al., 2022), and carbon molecular sieves (CMS) (Ghazi-MirSaeed & Matavos-Aramyan, 2020), and reviewed work published in the recent few years is summarized in **Table 4**. However, the selection process must be

conducted carefully since they may (and often do) differ in selectivity of which component. For example, (Tu et al., 2022) propose and test out a nickel-based MOF called Ni-BPZ for the separation of a binary mixture of CH_4/N_2. The authors reported a methane selectivity and uptake rate of 6.6 and 1.56 mmol/g respectively at ambient temperature and pressure. While this may initially seem competitive with other options, this study's adsorbate is methane and not nitrogen, which might only make sense in the context of retrieving methane from coal mine gas (hence the binary mixture). However, to enhance NG streams which are ~90% in methane content by the time they arrive in the adsorption unit, CH_4-selective adsorbents are highly uneconomical. This is because large amounts of adsorbents would be required which would lead to high costs of both initial one-off purchase of adsorbent and the regeneration step. Unfortunately, much of the existing literature regarding adsorbents for the separation of N_2/CH_4 mixtures for the purpose of fuel enhancement prioritize methane selectivity over nitrogen. (Ghazi-MirSaeed & Matavos-Aramyan, 2020) target the rejection of N_2 utilizing silica-modified CMS derived from pistachio and walnut and achieve a relatively low selectivity of 2.1 though it is one of the highest regarding N_2 adsorption. This may also imply the superiority of CMS over other adsorbent materials when the to-be-rejected component is required to be nitrogen. The existing literature of using adsorption for N_2/CH_4 separation is also compromised by two additional crucial pieces of information: firstly, most of such research if not all conducts the experiments on equimolar feeds, which is unrepresentative of NG in LNG prior to the cold section, and secondly, many rely on numerical and theoretical calculations to determine mixture selectivities instead of experimental results. For example, the Ideal Adsorbed Solution Theory (IAST) is often used (Chang et al., 2021; Kencana et al., 2022; Yao Li et al., 2019; Y. Wu et al., 2021), which is a theoretical method commonly used to calculate said selectivities using only adsorption results for individual pure components, but such a method assumes homogenous gas molecules distribution on the adsorbent surface and similarity in surface area occupation for that of the mixture molecule and the pure gas molecule, which was proven not to be necessarily the case in many systems (Krishna & Van Baten, 2021).

Table 4. Summary of Results Using Adsorbents for N_2/CH_4 Mixtures Separation

Adsorbent	Feed Conditions	Favored Component	Separation	Reference
MOF: Ni(4-DPDS)$_2$CrO$_4$	T: 25 ºC P: 1 bar CH_4:N_2: 50:50	CH_4	Selectivity: 7.3 Uptake: 0.95 mmol/g	(Zheng et al., 2022)
MOF: Co(AIP)(BPY)$_{0.5}$	T: 25 ºC P: 5 bar CH_4:N_2: 50:50	CH_4	Selectivity: 7.3 Uptake: 1.03 mmol/g	(C. Zhang et al., 2022)
MOF: SBMOF-1	T: 25 ºC P: 1 bar CH_4:N_2: 50:50	CH_4	Selectivity: 11.5	(Chang et al., 2021)
Zeolite: Ag-ZK-5(n)	T: 25 ºC P: 1 bar CH_4:N_2: 50:50	CH_4	Selectivity: 11.8 Uptake: 1.6 mmol/g	(Kencana et al., 2022)
Zeolite: NaY (Amine-modified)	T: 25 ºC P: 1 bar CH_4:N_2: 50:50	CH_4	Selectivity: 6.5	(Y. Wu et al., 2021)
AC	T: 25ºC P: 1 bar CH_4:N_2: 50:50	CH_4	Selectivity: 7.62 Uptake: 1.01 mmol/g	(Yao Li et al., 2019)
CMS: Silica-modified and pistachio/walnut-derived	T: 25 ºC P: 40 bar	N_2	Selectivity: 2.1 Uptake: 8.8 mmol/g	(Ghazi-MirSaeed & Matavos-Aramyan, 2020)

Membranes have also been investigated in the separation of NG components as summarized in **Table 5** of the last two years in literature. Membrane technology is based on the rejection of certain components and permeation of others by semi-permeable "barriers" due to differences in molecular sizes of approaching gas components. While membranes are often traditionally made from polymers (K. A. Lokhandwala et al., 2010), other options in recent literature look into other materials such as zeolites (Alam et al., 2020; Yanmei Li et al., 2021), and increasingly, mixed matrix membranes (Z. Gu et al., 2021; Montes Luna et al., 2021; Yousef et al., 2021), which are synthetic membranes made from the combination of organic polymers

with inorganic materials to enhance its performance and selectivity. Unlike adsorption, membrane technology does not require a regeneration step, making it more attractive economically, and more importantly, summarized reviewed research in **Table 5** shows the membrane research to be more oriented towards the removal of nitrogen than adsorption literature. This is a positive aspect because the pressure drop across membranes is often significant, and it is preferred to preserve the methane pressure as high as possible to minimize required energy demands for compression in later stages, and for this reason, N_2 permeable membranes are more appropriate. Otherwise, when the membrane is CH_4-selective, it is essential to recompress the gaseous product afterward (K. A. Lokhandwala et al., 2010). One criticism that could be levied against much of the currently existing research regarding membrane usage for nitrogen-methane separation is the method of determining the selectivity. Ideally, to get reliable results that could be made to argue in their favor, membranes would have to be experimentally tested with gaseous mixtures replicating compositions similar to those of the NG, and then measuring the effluent concentration/composition to calculate the selectivity by the mol fractions method. Instead, it was more common to simply measure individual gas permeability through the membrane and use theoretically-derived equations to calculate hypothetical mixture (Z. Gu et al., 2021; Yousef et al., 2021). The accuracy of these results is shaken by the deviancy of the experiments from realistic gas influents expected to be encountered in an LNG plant, and as previously stated, it is difficult to safely assume that individual gas molecules interact with solid phases the same way they would as a part of a mixture. This is proven by the work of (Yanmei Li et al., 2021), who compare such "ideal" calculated selectivities with experimental results from mixture feeds and notice the ideal ones to be noticeably larger. The authors report an N_2/CH_4 selectivity of 13.5 for an equimolar gas mixture at room temperature and 3 bar. Furthermore, reviewed literature on membrane technology repeats some of the flaws witnessed in adsorption, which are low-pressure values of the feed gas not representative of the NG stream in LNG plants and equimolar compositions in the rare cases where mixtures are tested instead of predicted by theoretical equations from individual gases permeation tests. According to (Baker & Lokhandwala, 2008), a selectivity of

at least 17 toward N_2 must be achieved to reduce an NG stream from 10% to 4% N_2, and as of currently, this selectivity is rarely achieved by membrane technology despite its seemingly obvious superiority to adsorption. A selectivity of 28 was reported by (Yu et al., 2021), but their mixture contained 20% N_2, making the selectivity calculated overestimated if compared to 10% N_2 NG. (Montes Luna et al., 2021) report a selectivity of 22.4 towards N_2, which does pass the threshold, which may suggest that innovations in preparing MMMs is the most productive pathway for this technology, but it is hard to say due to the insufficient amount of work investigating such issue as the material type with similar adsorption conditions. Membranes are reported to be most effective when multiple units in series are installed (Almomani et al., 2021), which will increase the cost of installation, operation and maintenance of the technology while also increasing the recompression demands.

Table 5. Summary of Results Using Membranes for N_2/CH_4 Mixtures Separation

Membrane	Feed Conditions	Favored Component	Separation	Reference
CMS: PI-LPSQ	T: 35 ºC P: 1 bar CH_4:N_2: 80:20	N_2	Selectivity: 28	(Yu et al., 2021)
MMM: PBI-CLINOm	T: 35 ºC P: 3.4 bar CH_4:N_2: 90:10	N_2	Selectivity: 22.4	(Montes Luna et al., 2021)
MMM: ZIF-8@VR	-	CH_4	Selectivity: 3.1	(Z. Gu et al., 2021)
MMM: CNTs/PES	P: 4 bar	CH_4	Selectivity: 1.62	(Yousef et al., 2021)
Zeolite: SAPO-34	T: 25 ºC P: 3 bar	N_2	Selectivity: 4.4	(Alam et al., 2020)
Zeolite: SSZ-13	T: 25 ºC P: 3 bar CH_4:N_2: 50:50	N_2	Selectivity: 13.5	(Yanmei Li et al., 2021)

Though these are the most relevant in research, other technologies have been reported for the

separation of N_2/CH_4 mixtures. One of the newer technologies in this application is the formation of gas-hydrates, which are in essence mostly water that is turned to ice by changing pressure and temperature while exposed to the target gases. Some of the gaseous components (methane) are trapped in the "cage-like" structure in the process, while other components are allowed to flow outside the hydrate container, therefore recovering the methane. Extracting the entrapped gaseous molecules is done by reversing the process, liquefying the hydrate, and releasing the gas. The most important and determining parameter in this process is the hydrate formation pressure, which is different for both nitrogen and methane. Though relatively new, gas-hydrate technology has been investigated in the enhancement of coal-mine gas containing low amounts of methane, increasing the methane molar fraction from 0.5 to 0.7 at 2 ^oC and 10 – 14 bar (Dong et al., 2014), The same quality improvement was also achieved at 4 ^oC and 15 – 45 bar when using promoters (SDS & THF) (Cai et al., 2018). (Sun, Chen, et al., 2019) utilized natural polyphenols as promoters and reported an almost doubled methane composition (34% ➔ 61%) and a methane separation factor of 5.31 at 1 ^oC and 55 – 90 bar. The use of promoters is common in this technology to encourage hydrate formation and reviewed literature includes some examples of chemicals reported to enhance CH_4 recoveries such as amino acids (Q. Zhang et al., 2021) and alkyl polyglucosides (Sun, Azamat, et al., 2019). Although intriguing, gas-hydrate technology has not been proven from literature to process NG with relatively low nitrogen content (<10%) and most of the reported results deal with low-quality NG. More research is required in this area to study the technology's performance on UNR in the hot section of an LNG plant containing mostly methane and lower hydrocarbons with low amounts of nitrogen before making any confident state in the feasibility of the process. That being said, gas-hydrates were investigated for another purpose, though relevant to the subject of LNG, and that is the storage and transport of NG by using gas-hydrates as mediums which are reported to increase the economic efficiency when compared to liquid phase storage and transport (C. Chen et al., 2022; Ge et al., 2022).

Besides the physical processes discussed so far, nitrogen could also be removed chemically, and this always entails a chemical interaction occurring between some component of the NG

with material brought in contact with it, either solid or liquid (solvent) phase. The most obvious and relevant example of this is the nitridation reaction which is the first step of the Li-Cy proposed in this work. This process is advantageous over physical adsorption due to its highly selective nature of it. When exposed to both major gaseous components of NG (CH_4+N_2), experimental results revealed that no methane sorption was detected while the nitrogen uptake rate calculated was 22 – 24 mmol/g (Z. Li, 2018), which is magnitudes higher than most of those recorded in literature. This extremely high selectivity towards nitrogen is demonstrated by the energy of activation values for the reactions of lithium with nitrogen compared with methane, with the former having a lower value of 87 KJ/mol (compared to 106 KJ/mol) (Q. Gu et al., 2018). Additionally, regeneration of Li in the proposed cycle involves hydrolysis of Li_3N which yields ammonia (and possibly H_2) (Jain et al., 2017; McEnaney et al., 2017) which will later be proven to be such a huge economic benefit that it can offset the cost of the electrolysis of LiOH (the final step of the cycle) plus a profit. Lithium nitridation does not require multistage operation like membranes do, however it must undergo sorbent regeneration like adsorption, with the latter having no positive aspect/economic side-products. With research regarding adsorption centered around methane separation, and membrane technology showing decreased separation performance at higher pressures (Almomani et al., 2021), causing the need for costly pressure reduction and compression, the Li-Cy is an option worth investigating for NG streams with low N_2 content in the hot section of the LNG plant, and **Table 6** summarizes the comparison between the different separation technologies discussed in this subsection.

Another chemical option is N_2 absorption by transition metal complexes/chelating agents, which shows a promising future, although much like gas-hydrate technology, very little research is done in this area. Much like other previously mentioned processes, it is preferred for the nitrogen component to be absorbed due to the high volume of methane gas in NG. This method was investigated by (Gilbertson et al., 2007) more than a decade ago, and while the authors report the technical feasibility of using *trans*-Fe(DMeOPrPE)$_2$Cl$_2$ complex for the absorption of N_2 from N_2/CH_4 mixtures, they do not elaborate on performance parameters and no selectivities/separation efficiencies were provided. On the other hand, (Z. Li et al., 2019)

report an N_2/CH_4 selectivity in the range of 1.7 – 2.4 by K-[Ru^{II}(EDTA)] depending on feed pressure at 30 ^oC and 3 – 30 bar. This technology's usage for nitrogen removal is severely hindered due to a seeming lack of interest by current research. Chelating agents are more commonly used for wastewater treatment purposes (Ahile et al., 2020; Nasef et al., 2014; K. Zhang et al., 2021) and medical applications (Amoroso et al., 2017; Sekhar et al., 2016). This problem is also encountered in lithium chemisorption, and this does hurt its appeal, but regardless, the results of absorption by chelating agents are promising, and more research work needs to be done to make any conclusions on which is more appealing for cold section UNR.

Table 6. Summary of the Different Technologies and Candidates for UNR

Technology	Description	TRL	Pros	Cons	Reported Performance	References
Cryogenic Distillation	• Extreme cooling of N_2/CH_4 mixture gas utilizing propane and mixed refrigerants to liquefy methane while keeping nitrogen gaseous	9*	• Efficient & Reliable • Well-established	• Energy-intensive • Investment demands are relatively higher • Process design is more complex ➔ must be given continuous care	-	-

Technology	Description	TRL	Pros	Cons	Reported Performance	References
Adsorption	• Selective attachment of a gaseous mixture component to the surface of an adsorbent due to weak van der Waals forces	5 – 9*	• Simpler regeneration of physical adsorption than that of chemical • can utilize cheap and/or natural adsorbents	• Most research done on CH_4 • Requires regeneration (no economic benefit) • Research favors its usage in coal mine gas treatment (low CH_4 content)	• CH_4/N_2 Selectivity: 1.2 – 28 • N_2/CH_4 Selectivity: 1.32 – 2.1	(Chang et al., 2021; Ghazi-MirSaeed & Matavos-Aramyan, 2020; L. Li et al., 2018; Ouyang et al., 2020; Pillai et al., 2017)
Membrane	• Selective rejection of a gaseous mixture component by a semipermeable barrier due to differences in molecular sizes	5 – 9*	• Increasingly gaining traction • Existing literature is oriented toward N_2 rejection • CO_2 gas removal capability ➔ can be used upstream to remove acid gas	• High N_2 selectivity is required to achieve a satisfactory product • Multi-stage units may be required ➔ higher installation costs • Gas recompression may be required proceeding with treatment to maintain high pressure	• CH_4/N_2 Selectivity: 1.62 – 3.1 • N_2/CH_4 Selectivity: 4.4 – 28	(Alam et al., 2020; Z. Gu et al., 2021; Yousef et al., 2021; Yu et al., 2021)

Technology	Description	TRL	Pros	Cons	Reported Performance	References
Gas Hydrate	• Primarily ice structures with gaseous molecules trapped in them upon formation by decreased temperature and/or increased pressure	4*	• Pressure requirements can be satisfied by high feed pressure • Regeneration is easy ➔ no need for a separate regeneration tank	• Relative Lack of research (novel subject for LNG plants) • Not enough promising results relevant to encountered NG • Too high a pressure could cause hydrate formation containing nitrogen impurities	• CH_4 molar fraction increased by 40 – 79%	(Cai et al., 2018; Dong et al., 2014; Sun, Chen, et al., 2019)
Absorption	• Selective absorption of nitrogen component by chelating agents containing ligands and a transition metal molecule(s)	1 – 3	• High N_2 selectivity due to chemical interactions • Current literature regarding CO_2 absorption was shown to have similar nature	• Requires regeneration • Severe lack of research on the subject • The solvent may experience losses which will increase costs	• N_2 selectivity: 1.7 – 5.8	(Z. Li et al., 2019; T et al., 2000)

Technology	Description	TRL	Pros	Cons	Reported Performance	References
Lithium Chemisorption	• Chemical nitridation of Li metal to form Li_3N upon contact with nitrogen under sufficiently moist conditions	1 – 3	• Highly selective towards N_2 • Significantly higher theoretical uptake rate (24 mmol/g) • The regeneration process produces ammonia	• Relatively novel for application of NG separation • Requires regeneration. • The reckless operation could lead to a hazardous reaction (violent exothermic reaction with H_2O)	• Uptake: 22 – 24 mmol/g	(Z. Li, 2018)

*Extracted from (Almomani et al., 2021)

CHAPTER 2: METHODOLOGY

2.1 Materials & Equipment

Granular lithium metal (≈ 300 mg) is used as the sorbent and is sourced from Sigma-Aldrich with a purity of 99% (metals basis) and containing high sodium. The granules were 4 – 10 mesh particle size (2 – 4.76 mm) and were kept in an isolated argon-filled environment due to their high reactivity with atmospheric air. For hydrolysis reaction tests, lithium nitride powder of mesh size 80 (177 microns) are also provided by Sigma-Aldrich of high purity (≥ 99.5%). Gas cylinders containing pure nitrogen and argon are both provided by Qatar's National Industrial Gas Plants. Argon gas with purity of 99.999% was used as purging gas to ensure no reactive gas remained in the tubes and as moisture carrying mobile medium ($O_2 \leq 2$ ppm, $N_2 \leq 5$ ppm, $H_2O \leq 2$ ppm, $CO_2 \leq 0.5$ ppm, Hydrocarbons ≤ 0.5 ppm), while nitrogen gas used as the reactant for nitridation of lithium was 99.999% pure ($O_2 \leq 3$ ppm, $H_2O \leq 2$ ppm, $CO+CO_2 \leq$ 0.5 ppm, Hydrocarbons ≤ 0.5 ppm). Although some of these impurities may in their nature be reactive with lithium metal, their quantities would prove to be too small to have any meaningful negative impacts on the samples. Distilled water is used as the moisture source, kept at room temperature (15 – 20 ^oC) and contained in an argon-filled environment.

All samples were kept inside an argon-filled glovebox manufactured by Korea Kiyon (2 port one-sided model: KK-011AS) where the oxygen and moisture content were always kept below 1 ppm. To confirm the unreactivity of the storing environment, a "sacrificial" lithium ribbon was freely placed outside of its container inside the glovebox, and in the case of its coloring changing from silver to either white or dark signifying formation of lithium oxide/hydroxide or nitride, respectively, the glovebox is purged until the environment is stable once more. The glovebox utilizes oxygen catalyst and molecular sieve purification system to ensure continuous cleaning of its environment from oxygen and moisture and operated at 1 – 2 atm pressure with the circulation blower speed set to 3. Additionally, the glovebox contained a Mettler Toledo analytical balance (Model: MS104S) with a maximum capacity of 120 g and readability of 0.1 mg for the purpose of weighing both the empty and the sample-loaded reactor in a non-reactive

environment. A second Mettler Toledo semi-micro balance (Model: XS105) with a maximum capacity and readability of 120 g and 0.01 mg, respectively, is also utilized for weighing of reactor after the experimental run is concluded to obtain the final weight. The reactor vessel housing the lithium sample is a tubular column (**Figure 5**) made of chemically and physically stable stainless steel (SS304) with an outer and inner diameters of 9.60 and 6.27 mm (thickness: 1.665 mm) and is 88.17 mm long, giving a total working volume of 0.0027 L. Meanwhile, fittings utilized in the fabricated experimental setup to connect the nitridation reactor to the influent/effluent stream tube were manufactured by Swagelok, and the stream tubes were also made of stainless steel. During the entirety of the reaction time, the column is housed inside a Daihan Scientific heating oven (Model: WON-32) to allow for temperature control, while the flow control was conducted with the combination of a valve and a flowmeter made from acrylic and PVC. The hydrolysis homemade reactor vessel was made of three parts, a bottom container for distilled water (**Figure 5**), a filter holder attachable to the bottom section and a top cover containing a gas outlet for ventilation and ensuring no pressure buildup. Both the bottom and top sections of the reactor were truncated cone-shaped, and the former had top & bottom radius, height, slant height and operating volume of 67 mm & 93 mm, 82 mm, 83 mm and 416 mL approximately, respectively, while the filter holding the sample was made of stainless steel and had a pore size of 100 microns. aside from the filter, all the components were made from unreactive aluminum composite material that can withstand temperatures much higher than the operating conditions. A Corning PC-420D stirring hot plate is used to maintain the hydrolysis reactor temperature, which is set to 40, 60 and 80 ^{o}C, close to the temperature range of the nitridation. The CHNS elemental analyzer Flash 2000 manufactured by Thermo Fisher Scientific Inc. (5x7") is utilized for nitrogen content analysis in Li_3N samples to measure conversion/extent of reaction.

Figure 5. Nitridation reaction column (a) and hydrolysis water container (b)

2.2 Experimental Procedure

2.2.1 Nitridation

The homemade experimental setup for the nitridation reaction is illustrated in **Figure 6**. The argon cylinder leads the gas to the pure water container to carry the moisture before arriving at the multipoint valve control intersection in which nitrogen stream is also connected to. The single valve effluent leads to a flow control device after which the gas stream travels to inside the oven where it passes through a long coil before entering the reactor column. The reason for the coil is to allow for heating of the entering gas which is kept under room temperature (15 – 20 ^{o}C) while the oven insides are often higher (e.g., 80 ^{o}C). The column effluent leads to a vent outlet to prevent accumulation of possibly disruptive gases in the setup and pressure buildup as well:

a) The column reactor is cleaned, dried and dry-heated in an oven at 105 ^{o}C to prevent any possibly remaining solids from previous trials or water to interfere with the next run.
b) Following complete evaporation of moisture in the column, the reactor is allowed to cool at room temperature (15 – 20 ^{o}C) before it is allowed inside the glovebox.
c) The dry, cooled reactor column, along with inlet/outlet caps, is transferred to the glovebox where the lithium samples are stored. Three cycles of refilling and vacuuming the antechamber were conducted to ensure complete removal of any contamination possibility.
d) Inside the glovebox, the weight of the reactor along with its caps is taken for later measurements before handling any samples.

e) Lithium granules are carefully loaded inside the column from the stock container. Only the granules that are entirely silver in color are placed inside the reactor to ensure purity of the reactant, and granules often came attached to each other which required manual cutting.

f) The weight of the sealed sample-loaded reactor column is taken for later measurements and the vessel is quickly transferred into the experimental setup.

g) The reactor column is quickly attached using the fittings to the inlet/outlet tubes. At this point, the oven has already reached target temperature as it is activated prior to the sample preparation steps. Additionally, moisture-carrying argon gas is flowing for the duration of sample loading to fill the oven inside with argon/moisture to minimize the chances of sample contamination as the column is fitted to the setup.

h) Moisture-carrying argon flows into the reactor for around 30 minutes at specified flow rates and a pressure of 1 atm for. This is the activation/moisture pretreatment step in which nitrogen flow is blocked by the valve and only the argon/moisture enters the column.

i) After the moisture pretreatment period, the argon cylinder is closed and its valve opening is blocked until the reading on the flowmeter is back to 0 (i.e., no argon flow), and the nitrogen cylinder/valve is opened for 2 hours (unless specified otherwise). This is the nitridation step in which lithium granules inside the column gradually shift color to dark, signifying conversion.

After the nitridation period ends, the nitrogen cylinder and valve opening is closed and the reactor column is quickly disassembled from the setup, covered with the caps and weighed at a nearby semi-micro balance. To ensure no contamination, the column is disassembled while nitrogen is still flowing to minimize any air from entering while opening the fittings.

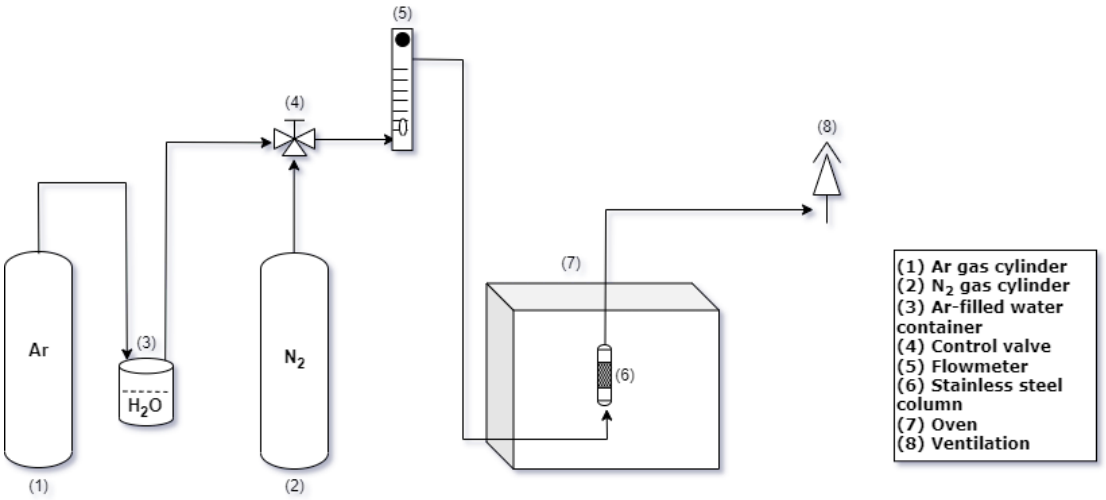

Figure 6. Nitridation experimental setup

2.2.2 Hydrolysis

Figure 7 illustrates the homemade hydrolysis reaction experimental setup utilized to investigate the regeneration of lithium. The stainless-steel mesh holds the Li_3N powder sample/reactant and can be seen positioned in the middle. After initiating heating, water vapor travels upwards to react with the dark red (almost black) lithium nitride, after which remaining excess vapor and gaseous by-products are immediately vented to prevent pressure buildup and/or accumulation of hazardous gases, so the entire experimental setup is installed inside a fume hood to ensure safety measures:

a) The sample holder is cleaned and dry-heated to remove all moisture before it is transferred into the glovebox where the sample is loaded into it and weighed and is covered by aluminum foil.

b) All reactor components are washed clean, dried and installed inside the fume hood beside the heater, and the stirring heater is turned on at the desired temperature.

c) Small plastic vials used to store the CHNS analyzer samples are weighed for later use (product sample analysis) and they are ensured to be clean and dry.

d) After the heater surface temperature is stabilized (20 – 30 minutes), the sample holder is taken outside of the glovebox, mounted into the reactor, which is then positioned on the heater.

e) After the reaction time passes, the heater is shut off, and the reactor is quickly disassembled to extract the consumed powder into the plastic vials for elemental analysis.

f) The loaded vials are weighed to determine the weight of the effective sample to undergo analysis for later measurements. It should be noted that very small (negligible) amounts of the powder are lost, and the powder is ensured to be homogenous before transfer.

g) CHNS elemental analysis is conducted, and the resulting N% and H% in the samples are used to calculate the conversion of the Li_3N by measuring its change via nitrogen content decrease.

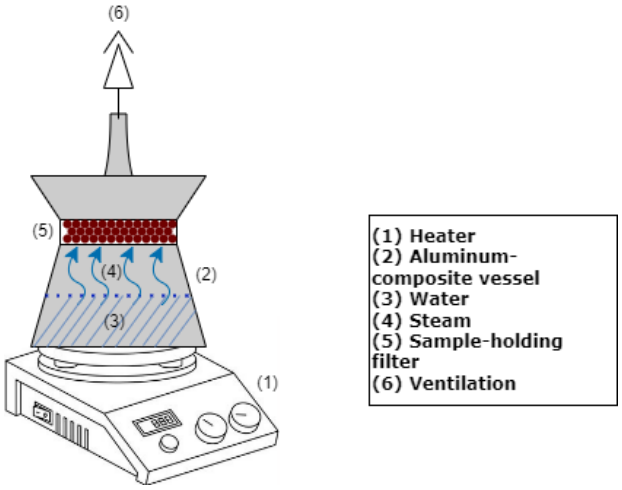

Figure 7. Hydrolysis experimental setup

2.3 Calculations & Analysis

Quantification of lithium conversion and nitrogen uptake rate are conducted via weight change measurements. One critical assumption made in this method is that all weight change occurs due to the formation of Li_3N, that is the addition of nitrogen molecules into the sorbent. This assumption may cause some degree of miscalculation, but it is deemed as negligible as visual observations on the consumed samples showed only dark/black layers on the lithium granules

with no white color in them, indicating only nitridation occurred and no meaningful amounts of lithium oxides and/or hydroxides are formed, thus the assumption that only Li_3N formation causes the weight change is safe. **Eq. 12** is used to calculate the nitrogen uptake rate (**N_2 UR**)

$$N_2\ \mathrm{UR} = \frac{(\mathrm{RSR}-\mathrm{RS})*\frac{1}{\mathrm{MW}_{N_2}}*\frac{1000\ \mathrm{mmol}}{1\ \mathrm{mol}}}{(\mathrm{RS}-\mathrm{R})} \tag{12}$$

where **R**, **RS** and **RSR** are the weights of the empty reactor column, the loaded reactor column and the consumed reactor column, respectively, in grams. **RS** is larger than **R** by the amount of sample added (which is often 300 mg), while **RSR** is larger than **RS** by the weight increase due to lithium nitride formation. $\mathbf{MW_{N_2}}$ is the molecular weight of nitrogen molecules (28.0134 g/mol), while the ratio/factor used in the equation above is for the purpose of quantifying the uptake rate in mmol/g. Similarly, the lithium conversion (**Li C%**) is calculated by **Eq. 13**

$$\mathrm{Li\ C\%} = \frac{(\mathrm{RSR}-\mathrm{RS})*\frac{1}{\mathrm{MW}_{N_2}}*\mathrm{SR}*\mathrm{MW}_{\mathrm{Li}}}{(\mathrm{RS}-\mathrm{R})} * 100\% \tag{13}$$

where **SR** is the molar stoichiometric ratio between lithium and nitrogen in the nitridation reaction seen in **Eq. 1**, which is 6, and $\mathbf{MW_{Li}}$ is the molecular weight of lithium metal (6.941 g/mol). These calculations are conducted for each experimental run to produce the figures in the results section correlating the lithium conversion and nitrogen uptake rate to the temperature, flow rate and reaction time.

The determination of hydrolysis conversion is less direct, though it too involved weight measurements. CHNS elemental analysis returns the carbon, hydrogen, nitrogen and sulfur species (not molecular) content by weight of the tested samples. The Li_3N conversion is calculated by weight change as can be seen in **Eq. 14**, but the final weight is indirectly determined from the N% (**Eq. 15**). Via a series of conversions, the N% is written in terms of Li_3N, which would be the final weight. The theoretical ammonia production rate is also calculated using stoichiometric ratios using **Eq. 17** of the hydrolysis reaction rather than directly captured

$$\mathrm{Li_3N\ C\%} = \frac{\mathrm{Li_3N_i}-\mathrm{Li_3N_f}}{\mathrm{Li_3N_i}} * 100\% \tag{14}$$

$$\mathrm{Li_3N_f} = \mathrm{W} * \mathrm{N\%} * \frac{1}{\mathrm{u_N}} * \mathrm{MR} * \mathrm{MW_{Li_3N}} \tag{15}$$

Where $\mathbf{Li_3N_i}$ and $\mathbf{Li_3N_f}$ are the initial and final samples weights, respectively (g or mg), **N%** is the nitrogen weight content from the elemental analysis, $\mathbf{u_N}$ is the atomic mass of nitrogen (14.0067 u), **MR** is the molar ratio between nitrogen and lithium nitride (1:1) and $\mathbf{MW_{Li_3N}}$ is the lithium nitride's molecular weight (34.83 g/mol). **W** is the weight of the sample extracted from the reactor (**Eq. 16**), not to be confused with $\mathbf{Li_3N_f}$ as the final powder product is expected to be a mixture of remaining Li_3N and LiOH, and it is calculated by the difference between the empty (**SH**) and the loaded CHNS vials (**SHS**)

$$W = SHS - S \tag{16}$$

$$P_{NH_3}\left(\frac{mmol}{g\ Li_3N}\right) = \left(\frac{Li_3N_i - Li_3N_f}{MW_{Li_3N}}\right) * \frac{1\ mol\ NH_3}{1\ mol\ Li_3N_i} * \frac{1000\ mmol\ NH_3}{1\ mol\ NH_3} * \frac{1}{Li_3N_i} \tag{17}$$

2.4 Kinetic Models

The investigation into the kinetics of the lithium cycle, despite its significant importance in diverse fields such as energy storage and pharmaceuticals and LNG industry, has received limited attention thus far. The investigation of the kinetics of lithium reactions is vital in order to enhance the efficiency and effectiveness of various technologies and processes. One of the primary difficulties encountered in the study of lithium kinetics is its inherent reactivity and the wide range of reactions that it can engage in.

Kinetic modelling is based on a novel approach that is employed for the analysis of reactions occurring between solid and gas phases. In contrast to homogeneous reactions, heterogeneous reactions, particularly gas-solid reactions, present difficulties arising from the heterogeneity of reaction intermediates and solid morphology. In order to tackle the intricacies involved, a novel methodology was suggested, taking into account the processes of nucleation, growth, diffusion, adsorption, and interfacial interactions. The concept of the pseudo-steady state approximation, which plays a critical role in the kinetic modeling of heterogeneous processes, was elucidated, with particular emphasis placed on its applicability under specific circumstances.

The conventional models, such as the Arrhenius equation (**Eq. 18**), exhibit limitations in their inclusivity as they fail to consider crucial aspects like as nucleation and anisotropic growth, and the impact of different thermodynamic and morphological variables on each other. The

comprehensive framework provided for the process kinetic incorporating both thermodynamic and morphological variables is presented in (**Eq. 19**). Where **Ø** (mol/m^2.s) is the growth reactivity and $\mathbf{S_m}$ (m^2/mol) is the morphological variable. The significance of the rate-determining step approximation in gas-solid reactions was emphasized, offering valuable insights into surface phenomena and interfacial reactions.

$$\frac{d\alpha}{dt} = Ae^{-\frac{E}{RT}}.f(\alpha) \tag{18}$$

$$\frac{d\alpha}{dt} = \emptyset S_m \tag{19}$$

CHAPTER 3: RESULTS & DISCUSSION

3.1 Nitridation of Lithium Metal

3.1.1 Ribbon-shaped Lithium Experiments

Prior to experimentation on granular lithium samples as illustrated in the methodology section of this study, lithium strips/ribbons were used as the samples to: a) Affirm the feasibility of nitrogen reaction with lithium at higher temperatures b) Observe the significance of some of the parameters, such as pressure, time and flow rate on the extent of conversion and c) Set a precedent/standard which will be later used to highlight the importance of surface area on the conversion of lithium to lithium nitride. The experimental procedure is very similar to the granular samples' conversion procedure, but the activation is initially conducted by partial exposure of the lithium ribbons to air for 15 minutes, and the samples (in the later "new" reactor volume) are approximately of width, length and surface area of 6 m, 88 m and 1056 mm^2, respectively.

Table 7 summarizes the results of the base experiment, along with 2 experiments conducted to get an idea on the effects of pressure and flow rate change. The base experiment showed a lithium conversion based on weight measurement change of 64%, which after observation of the consumed sample, was determined to be a corrupted result as the solid product was mostly white in color, which indicates high presence of lithium hydroxide and oxides rather than nitride. This would be proven to be the case in the following experiments as their conversion sits close to the others, all of which gave products of a dark purple layer (lithium nitride). Changes made to the pressure of the entering gas and its flow rate, which increased from 1 to 2 bar and decreased from 1.4 to 0.8 L/min respectively, showed very little effect on the extent of reaction between 10 – 13%. Generally, higher pressure is associated with higher conversion in gas-solid reactions, but in this case, the pressure increase had very little effect. This could mean that either further pressure increase is necessary to witness noticeable impact or that higher pressure is not necessary for near complete sorption of nitrogen, which would later turn out to be the case in granule experiments. Interestingly enough, decrease in flow rate of nitrogen had a positive impact on the conversion process, which might be counter intuitive since less

flow of nitrogen, a reactant, means less gas for the reaction. This could be because after a certain level, higher flow rates begin to hurt the reaction that relies on the sorption mechanisms of attachment, diffusion and reaction by "flushing"/removing the gas particles from the surface of the sample before they react to produce lithium nitride, thereby reducing the extent of reaction. This would prove an important realization for later experiments which will limit the flow rate to 0.05 – 0.15 L/min to prevent inhibition of the reaction.

Following these preliminary experiments, the reactor setup was slightly modified by adding an activation/moisture pretreatment mechanism by attaching the argon cylinder to a moisture containing glass container and into the reactor instead of partial activation in the air which consumes some of the sample as was seen in the form of white layers. Additionally, the reactor column was replaced with a larger one, almost 10 times in size, allowing for larger surface area. As can be seen from **Table 7**, higher conversion up to 22% was obtained by this larger reactor column, which is mostly due to the larger surface area for the ribbon sample. Moreover, changing activation time and reaction time led to the conclusion that activation times higher than 60 minutes and reaction times more than 3 hours have diminishing returns regarding the effect on the extent of reaction. It was concluded that nitridation does in fact occur but requires certain conditions.

Table 7. Preliminary Nitridation Experiments on Lithium Ribbons

Weight (mg)	Activation Time (min)	Oven Set Temperature (°C)	Pressure (bar)	Flow Rate (L/min)	Reaction Time (h)	Conversion
Old Reactor						
18.8	15	40	1	1.4	5	**64%**
24.6	15	40	2	1.4	5	**10%**
19.7	15	40	1	0.8	5	**13%**
New Reactor						
255	60	50	1	3.5	3	**18%**
226	120	50	1	1.5	4	**22%**

3.1.2 Granule-shaped Lithium Experiments

Following the investigation into the feasibility of nitridation, some conclusions were reached:

A. Nitridation is possible even under normal conditions achievable in the lab-scale. However, the lithium conversion (LiC%)/nitrogen uptake rate (NUR) is still unsatisfactory on ribbons. Thus, further optimization of parameters is required to obtain higher LiC%.
B. Although all of the aforementioned parameters have an impact to a certain extent, there is a hierarchy parameter importance: the most important parameters are temperature, reaction time and most importantly, sorbent surface area.
C. Pressure and flow rate values higher than 1 bar and 1 L/min may both be unnecessary and harmful to the LiC%, while moisture pretreatment period of 60 minutes is more than enough to activate the lithium samples.

From these previous experiments, lessons were applied in conducting nitrogen chemisorption experiments on granule-shaped lithium samples. The most important one being the limited LiC% obtained by using lithium ribbons which have a relatively low surface area, which were replaced by granular lithium that would later prove to achieve very high NURs. The effect of oven temperature on LiC% was investigated, ranging from a laboratory room temperature of 15 ^{o}C to 80 ^{o}C, while flow rates also varied between 0.05 and 0.15 L/min to determine the point in which higher flow rates begin to hamper nitridation if such exists. **Table 8** summarizes the results of 15 different experiments conducted for different temperatures and flow rates and their effect on both the LiC% and NUR. All experiments are conducted by the same procedure detailed in the methodology section with no changes to any step.

Table 8. LiC% and NUR With Temperature and Flow Rate Changes

T (^{o}C) \ F (L/min)	0.05	0.1	0.15
15	LiC%: **3.92%** NUR: **0.94 mmol/g**	LiC%: **3.29%** NUR: **0.79 mmol/g**	LiC%: **7.20%** NUR: **1.73 mmol/g**

T (°C) \ F (L/min)	0.05	0.1	0.15
30	LiC%: **1.53%** NUR: **0.37 mmol/g**	LiC%: **1.49%** NUR: **0.36 mmol/g**	LiC%: **2.80%** NUR: **0.67 mmol/g**
45	LiC%: **0.098%** NUR: **0.024 mmol/g**	LiC%: **2.86%** NUR: **0.69 mmol/g**	LiC%: **4.95%** NUR: **1.19 mmol/g**
60	LiC%: **42.30%** NUR: **10.16 mmol/g**	LiC%: **33.58%** NUR: **8.06 mmol/g**	LiC%: **28.91%** NUR: **6.94 mmol/g**
80	LiC%: **41.21%** NUR: **9.89 mmol/g**	LiC%: **29.75%** NUR: **7.14 mmol/g**	LiC%: **37.38%** NUR: **8.98 mmol/g**

Figure 8 & **Figure 9** visualize the effect of temperature on LiC% and NUR for different nitrogen flow rates. Both are related, mathematically speaking as illustrated in the methodology/calculation section, so it is natural they follow identical trends as responses to temperature/flow rate increase/decrease. For both LiC% and NUR, the values are very low and almost negligible at lower temperatures, fluctuating between 0 – 7% and 0 – 1.7 mmol/g, respectively in the temperature range of 15 – 45 °C. Interestingly, once the temperature is further increased beyond 45 °C, a sharp rise in the extent of reaction is witnessed, reaching a LiC% and NUR of 29 – 42% and 6.9 – 10.2 mmol/g, respectively for different flow rates. This not only confirms the unsurprising importance of temperature in the nitridation reaction, but also highlights its sheer significance as both LiC% and NUR increase 5 – 10 folds just by breaking the "temperature barrier". Before this temperature, the lithium metal can be exposed to air for several hours without any nitridation occurring, as demonstrated by DSC (Jain et al., 2017), and this temperature can be lowered by increasing pressure as increasing nitrogen pressure from 0.5 to 0.8 MPa was observed to compensate for preheating of lithium metal. The highest LiC% and NUR were 42.3% and 10.16 mmol/g respectively, and they were recorded at a temperature and flow rate of 60 °C and 0.05 L/min. Further increase of temperature had little

impact in the best-case scenario, and possibly negative effect in the worst scenario. The experimental results are consistent with thermodynamic studies proving the favorability of the nitridation reaction compared to reactions between lithium and other gases following moisture-pretreatment (Q. Gu et al., 2018).

It is difficult to exactly pinpoint the reason why higher temperature increase would lead to lower conversion rates, and it is believed that this supposed decline is caused by human and systemic errors made in the experimentation and calculation processes. Some of these errors include inaccuracies made by the microbalance instruments, which at some points did show some erratic behavior even when carefully recalibrated, and sample consumption/corruption during the points at which it is inserted into the reactor column, or the column is separated after the reaction completes for post-reaction weight measurement. Regardless, it is concluded that 60 – 80 ^{o}C is the ideal temperature range for NUR and further increase will lead to no noticeable improvements in the chemisorption. For this reason, further experimentation and kinetic studies for the nitridation of lithium for chemisorption of nitrogen from natural gas streams are recommended to be conducted at 60 – 80 ^{o}C. interestingly, other research (McEnaney et al., 2017) suggests that further increase in temperature up to 100 ^{o}C maintained higher conversions up to 80%, which is higher than the obtained experimental results, most likely due to greater solid surface area utilization.

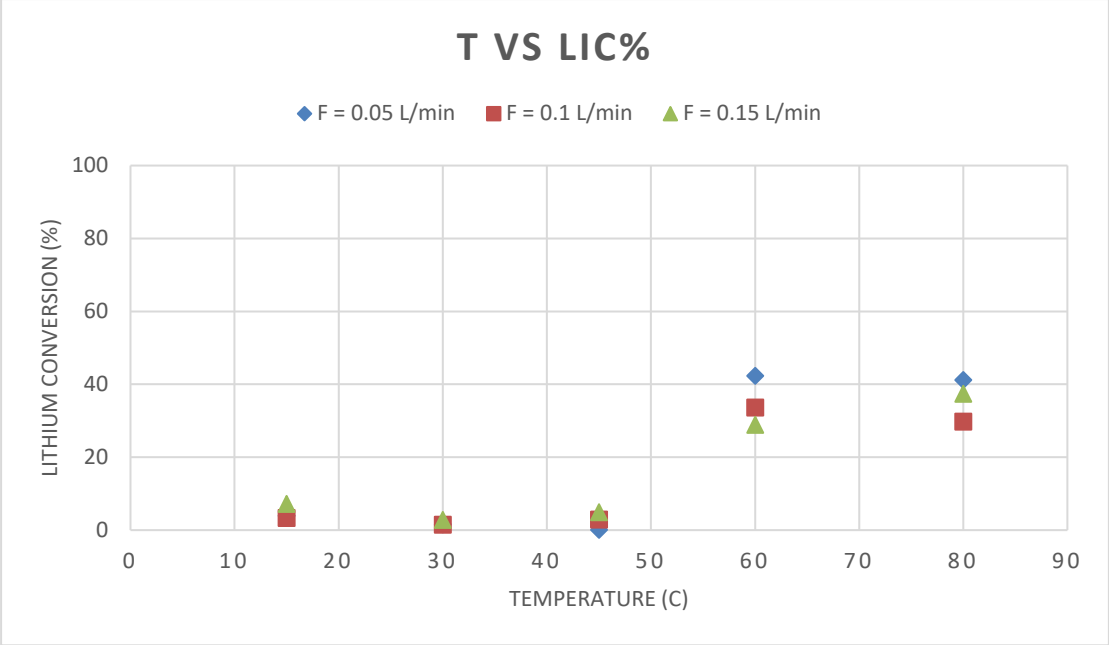

Figure 8. Effect of temperature on LiC% for different flow rates

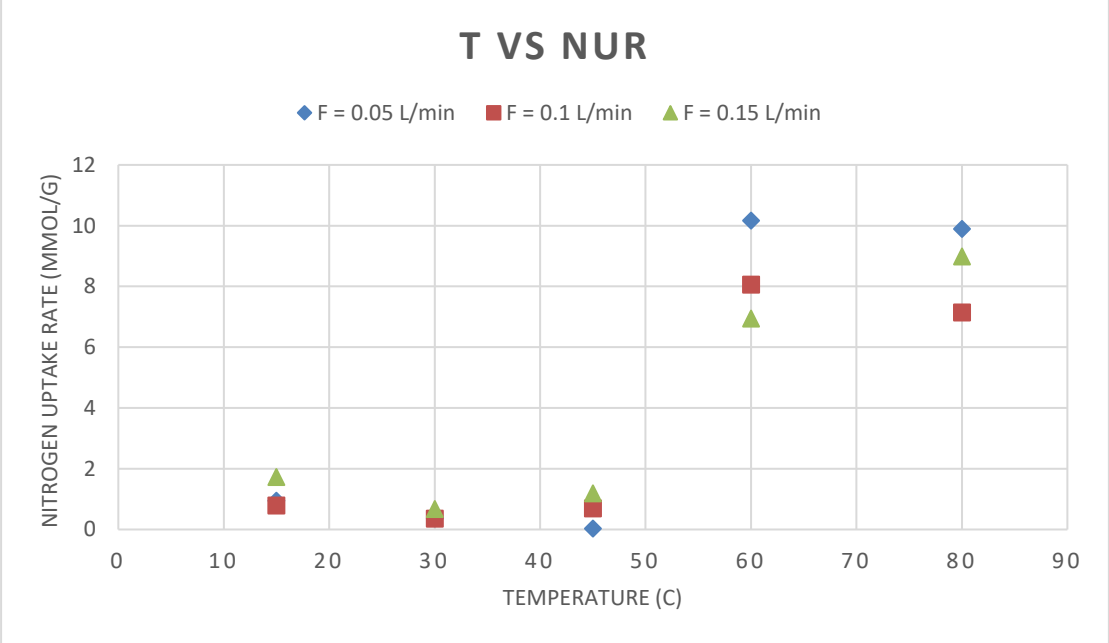

Figure 9. Effect of temperature on NUR for different flow rates

Figure 10 & **Figure 11** illustrate the same results but by fixing the temperature and showing the "isotherms" of chemisorption to allow us to visualize the effect of flow rate on LiC% and NUR for different temperatures. Two behaviors can be seen in the figures: at low temperatures where the extent of reaction is very low, flow rate has negligible effect on the reaction. This is

most likely due to the fact that reaction occurs at such a low rate in those conditions that no impact, whether positive or negative, is felt as the LiC% and NUR values are too low anyways. Interestingly, for both trends at 60 and 80 °C, the lower flow rate of 0.05 L/min improves the performance, and this can be explained by two reasons. Firstly, at lower flow rates, not enough nitrogen is supplied to the lithium sample, but the extent is still somewhat decent. Further increase provides more reactant gas and thus higher N_2 partial pressure/concentration inside the reactor without compromising or harming the attachment of nitrogen molecules/atoms at the metal surface. When the flow rate is too high, we start to observe the negative effects of excessive gas flow/speed, because the nitrogen concentration was already high enough such that the chemisorption is controlled/limited by the diffusion and reaction steps and not by any concentration gradients, and further increase in flow only increased the chance of molecules sweeping done by the bulk fluid, leading to more harm than good.

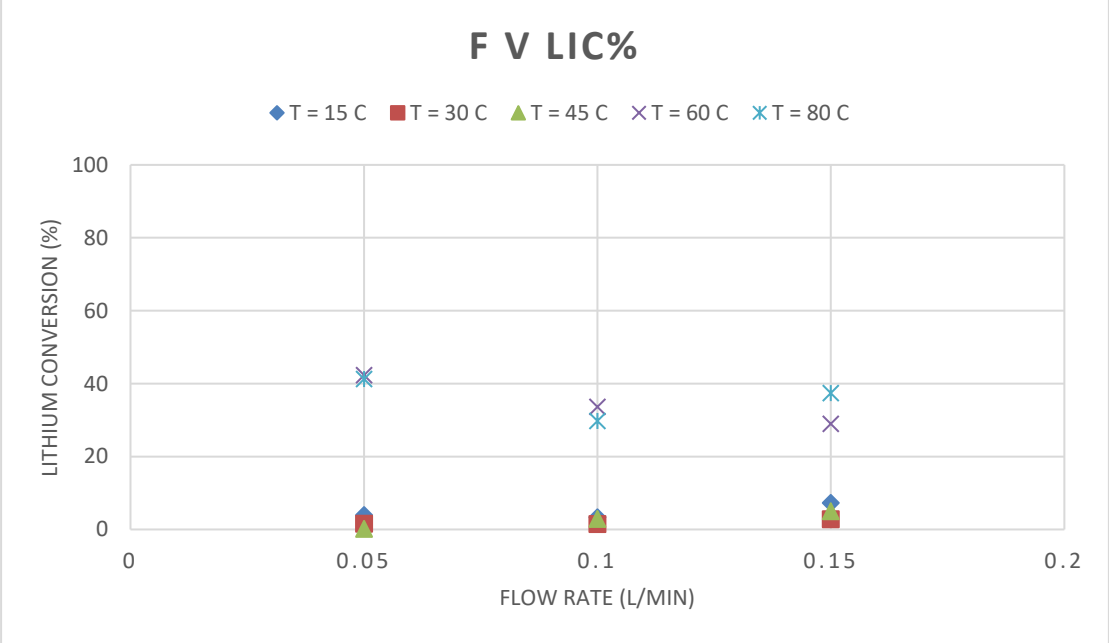

Figure 10. Effect of flow rate on LiC% for different temperatures

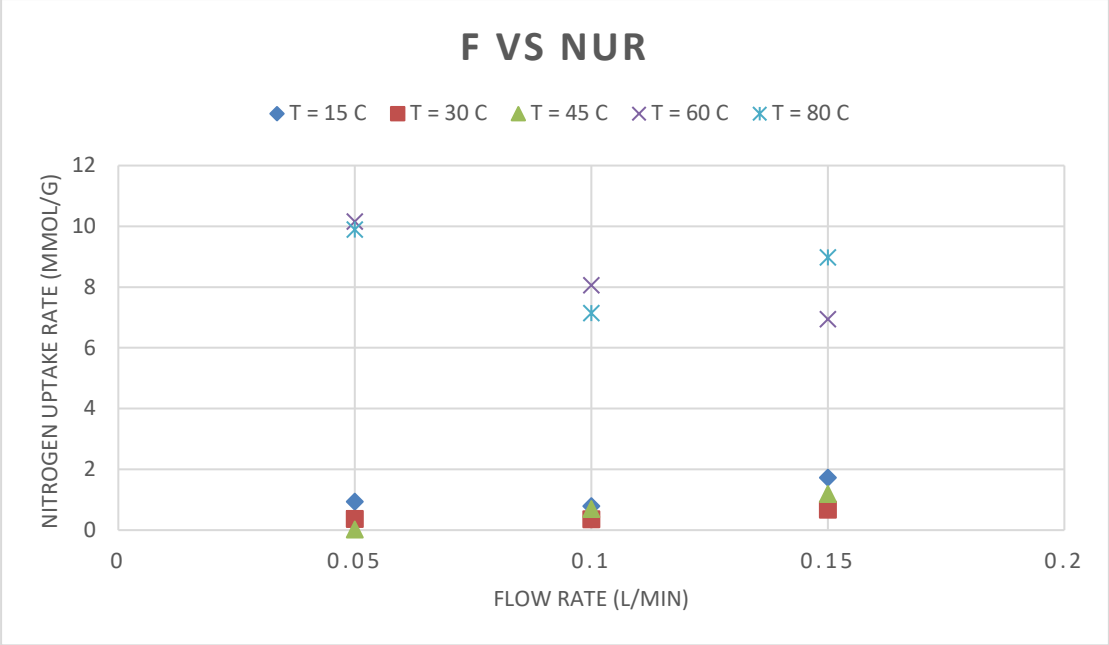

Figure 11. Effect of flow rate on NUR for different temperatures

Finally, it is worth touching on the subject of contact surface area and its impact on the chemisorption of nitrogen. Two experiments were conducted at a temperature, pressure, activation & reaction time and flow rate of 80 °C, 1 bar, 30 min & 2 hours and 0.1 L/min, respectively, with one difference in sample preparation. The 2 – 4.76 mm size lithium granules from the stock container are often attached to each other, that is, it is common to find clusters where three or even four granules are connected as one body. This essentially decreases their surface area, but it also seriously hinders gas-solid contact by randomly forming tunnels that divert or block the nitrogen flow inside the reactor column. Meanwhile, when such clusters are "sliced" to individual granules and each granules is manually inserted into the column, high surface area is achieved and the tunnelling across the reactor bed is uniform with no possibility of blockage. **Figure 12** & **Figure 13** demonstrate the impact this has on the extent of chemisorption, keeping in mind that dark granules are consumed lithium metal turned to lithium nitride and silver granules are unconsumed lithium metal. It can be seen that for the sliced granules, almost all reactant is consumed (black) while only some remain with one or more silver side, corresponding to a LiC% and NUR of 75% and 18 mmol/g, respectively. Meanwhile, the exact same experiment produced LiC% and NUR of 42% and 10 mmol/g

respectively, and it can be seen that silver granules are more common, owing up to lack of contact with nitrogen gas due to obstructed tunnel/pore flow.

(Q. Gu et al., 2018) showed the same trends where the nitridation of Lithium reaction slightly increases by increasing temperature of the reaction. However, their reported units (dehydration, NGL recovery, liquefaction) required much higher pressures (70 to 200 bar) (Netušil & Ditl, 2012). Moreover, the objective of most of the previous studies is the synthesis of ammonia. Most of the published work confirmed that the nitridation reaction exhibited a significant outcome in terms of the generation. The reasonable conversion of this reaction were observed to occur at three distinct temperatures (22, 50, and 100 ℃) and two alternative time durations (30 minutes and 12 hours) (McEnaney et al., 2017). In summary it was reported that increasing the temperature during the nitridation reaction resulted in enhanced conversion rates. Furthermore, subjecting the N_2 flow to a temperature of 100 ℃ for a duration of 30 minutes resulted in conversion ≥80%. On the other hand, when the N_2 flow was exposed for a duration of 12 hours, a 100% conversion was achieved. The Li_3N, ammonia as impurities of LiOH and Li_2O were formed during the process. Additionally, it was confirmed that the presence of oxygen (O_2) and water (H_2O) in the ambient air appeared to enhance the rate of the nitridation reaction.

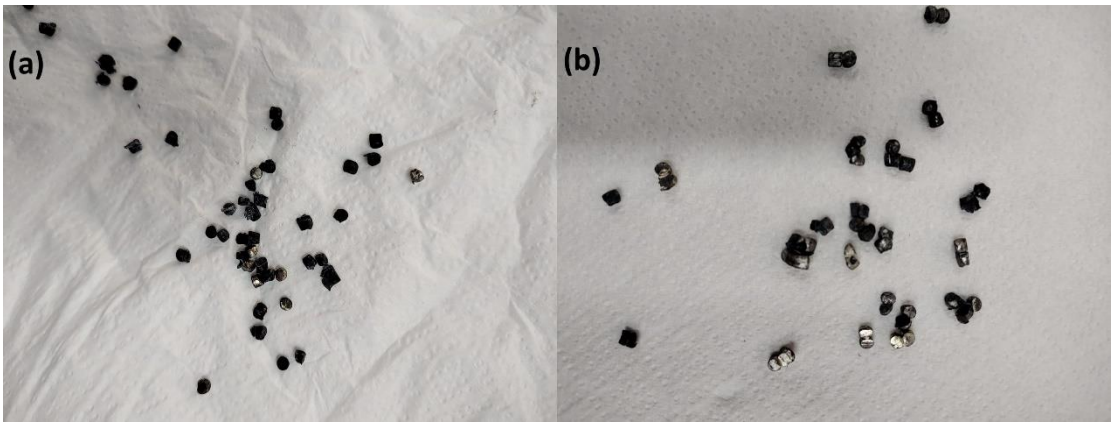

Figure 12. Extent of chemisorption demonstrated by lithium metal surface consumption for sliced (a) and clustered (b) granules

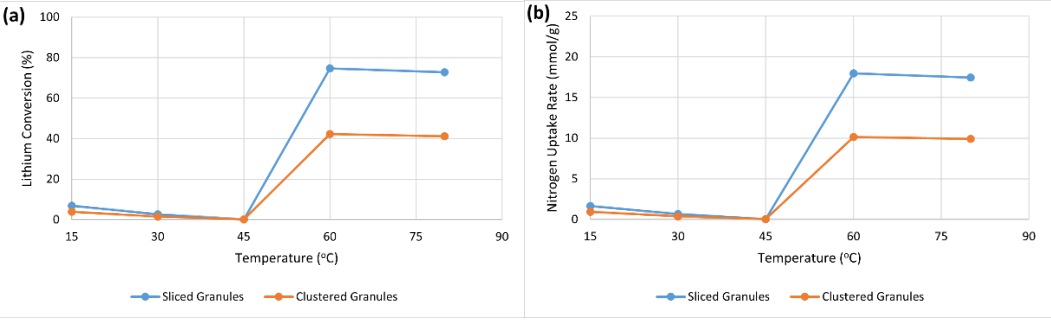

Figure 13. Effect of slicing lithium clusters into individual granules for chemisorption on lithium conversion (a) and nitrogen uptake rate (b)

Figure 14 below summarizes the results of nitridation trials investigating the effect of reaction time on the extent of reaction (LiC% and NUR) at temperatures of 60 and 80 °C. Interestingly, a similar pattern for the effect of time is observed as the effect of temperature, where initially, at a reaction time of only 1 hours, the LiC% and NUR are only 3% & 9% and 0.7 & 2.22 mmol/g respectively, which are unacceptable values, hence reaction time below 1 hour will not satisfy the required performance for nitrogen removal from NG streams. However, further increase of reaction time to 2 hours significantly improves the chemisorption, with the highest LiC% and NUR values recorded as 42% and 10 mmol/g at 60 °C. After this point, additional reaction time seems to have negligible effect on nitrogen sorption as it sees diminishing returns.

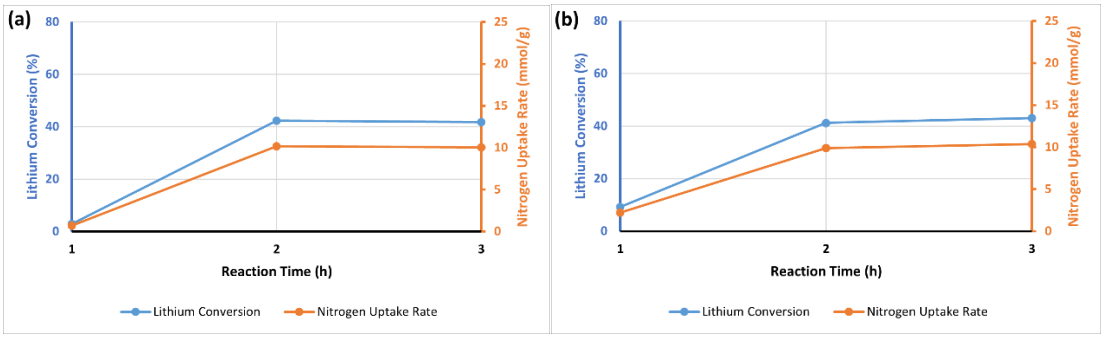

Figure 14. Reaction time trials for the flow rate of 0.05 L/min and T = 60 °C (a) and 80 °C (b)

Further experimentation concerning the effect of reaction time on the nitridation reaction visualized in **Figure 15** yielded results with important conclusions. Firstly, consistent testing

showed 80 °C to be the optimal temperature for nitridation at a flow rate and pressure of 0.1 L/min and 1 atm, respectively, with LiC% and NUR reaching consistent values of around 79% and 19 mmol/g, respectively. Secondly, higher temperatures (100 °C) not only had no positive effect on the reaction rate, but it actually led to decreased conversion and uptake rate, and this might be explained by the fact that the reaction rate-temperature relationship has reached its "upper limits", that is, temperature increase above 80 °C causes the reacting molecules to be too unstable for settling down and forming new nuclei. However, a better explanation might be the effect of increased temperature on the formation of a LiOH layer as illustrated by **Figure 16**. It is determined that a certain thickness of LiOH layer is necessary to facilitate nucleation of Li_3N molecules on the solid phase, but this layer can be too thick to the point that it prevents contact between the nitrogen and lithium. At 60 °C, the granules are either partially dark (low conversion due to thermal conditions) or silver (unreacted), but little to no presence of gray/white layer is detected. Increasing the temperature further to 80 °C causes appearance of gray layers on the granules, which is associated with the sudden jump in LiC% and NUR, demonstrating the importance of moisture pretreatment/metal activation. Further increase of temperature, however, accelerates the rate of LiOH formation such that the lithium conversion is reduced from 80% to around 60%, owing to handicapped nitridation. It is reasonable then to question whether or not the calculated conversion via weight changes can actually be attributed to nitridation or activation, and to answer this, we can simply simultaneously consider the effect of activation time (t_A) on the reaction as illustrated by **Figure 17**, and the previous results of the nitridation time experiments shown in **Figure 15**. Initially, the observer might be misled to conclude that the weight change occurs due to activation, this does not make sense considering that at a nitridation reaction time (t_{Rxn}) of less than 60 minutes, little to no weight change occurs despite 30 minutes of activation in the time experiments, meaning the weight change actually occurs with nitridation time increase, though it is a bit more complicated than that. These results do in fact confirm the reliance of nitridation reaction on the activation pretreatment together, rather than the importance of each of them separately. At low/no activation times, even two hours or nitridation lead to little to no weight change because no nucleation occurs as no LiOH

works as a precursor to it, while high activation times causes meaningful weight change at low nitridation times.

The moisture pretreatment/activation trials make important conclusions regarding two points brought about earlier:

1) The presence of water moisture does in fact initiate a reaction on the surface of lithium, resulting in the formation of lithium hydroxide and lithium hydride, which may appear as white to gray in color as claimed by (Shang & Shirazian, 2018). The presence of moisture in the reaction has two advantages. Firstly, it leads to the formation of a lithium hydroxide layer, which enhances the reactivity of the edge site, facilitating the nitridation process (Z. Li, 2018). Secondly, the interaction with moisture releases energy, specifically 375 kJ/mol, which serves as the activation energy for the nitridation reaction (Q. Gu et al., 2018).
2) The matter of conflicting in the literature findings regarding the probability of lithium interacting with nitrogen under dry conditions is resolved. The experimental results prove Irvine's findings indicate that the application of moisture pre-treatment has a substantial impact on the rate of response (Wayne Ronald Irvine, 1961) as opposed to (Mcfarlane & Tompkins, 1962) and (Meyer M. Markowitz & Boryta, 2002) claim that such enhancement is possible at best and unlikely at worst.

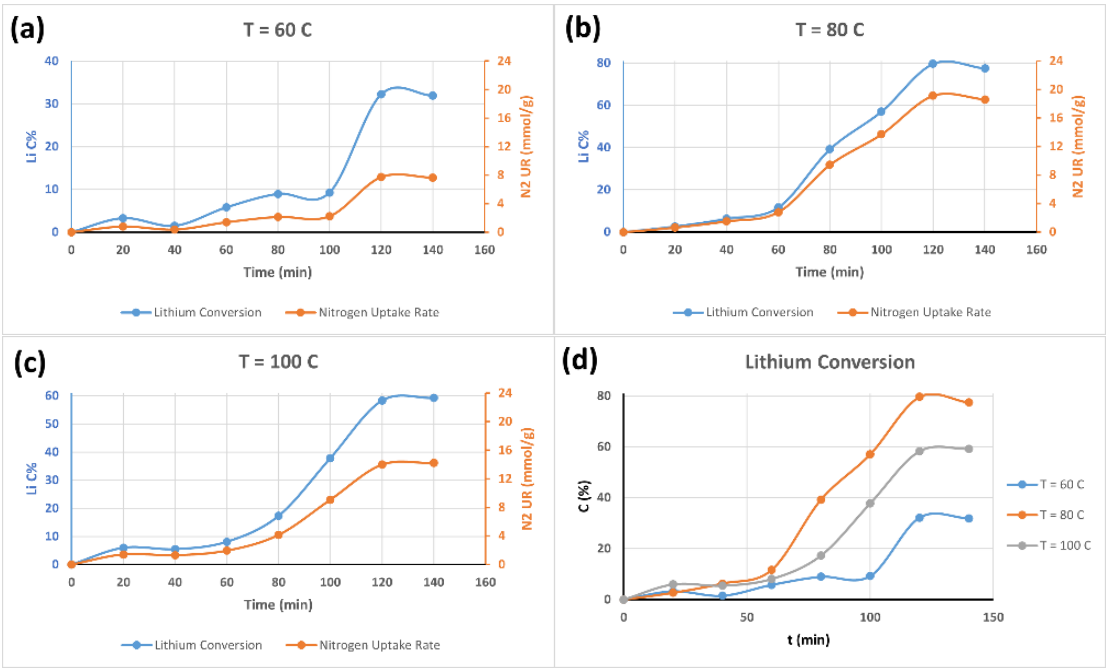

Figure 15. Nitridation time experiments at 60 ºC (a), 80 ºC (b) and 100 ºC (c) (P: 1 bar, F: 0.1 L/min, t_A: 30 minutes), and all compared (d)

Finally, at the relatively low temperature of 60 ºC, it can be seen that the least LiC% and NUR are achieved by the lithium metal. In light of the previously discussed phenomena, this is most likely due to slow nitridation reaction rate caused by low collision frequencies and the lack of enough LiOH layer to simulate the nucleation of Li_3N molecules, leading to an overall low chemisorption.

The literature extensively documents the nitridation reaction, particularly in the presence of moisture, which is mostly conducted by chemists. However, its application for nitrogen removal from natural gas streams is rather infrequent. The viability of this procedure was recently emphasized by a combination of experimental and theoretical testing (Z. Li, 2018). The confirmation of the thermodynamic favorability of the reaction was also provided by (Q. Gu et al., 2018). Furthermore, patents have been filed for the utilization of lithium in the chemical sorption of nitrogen from natural gas (NG) (CHIE et al., 2012; V & SAI, 2018).

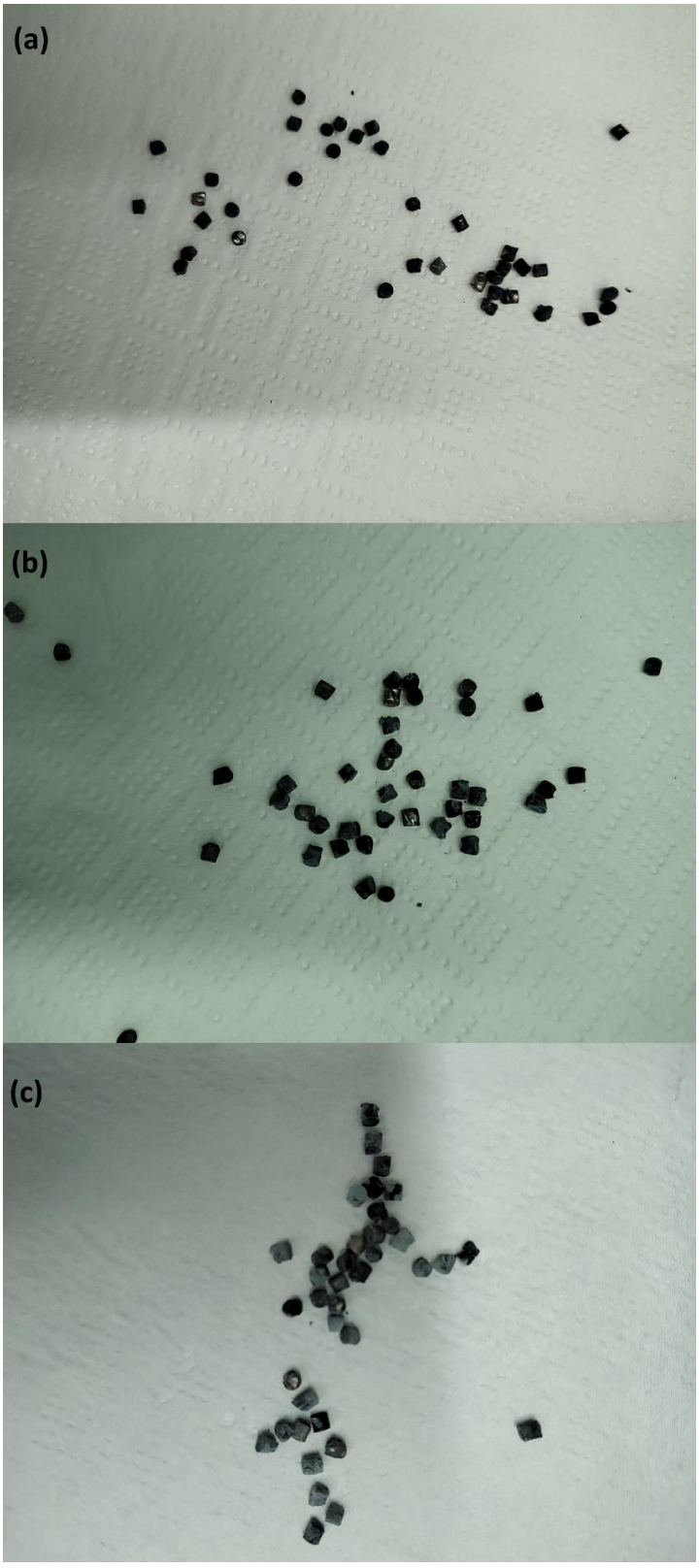

Figure 16. Effect of reaction temperature of 60 (a), 80 (b) and 100 (c) ^{o}C on formation of LiOH layer (F: 0.1 L/min, t_A: 30 minutes, t_{Rxn}: 140 minutes, P: 1 bar)

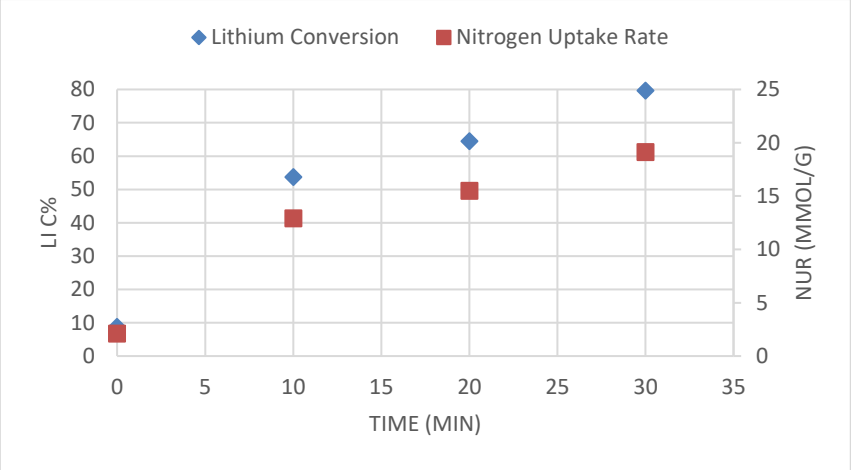

Figure 17. Effect of sample activation time on the lithium conversion to Li_3N (T: 80 ^oC, P: 1 atm, F: 0.1 L/min, t_{Rxn}: 120 minutes)

3.1.3 Kinetic Model

This research will apply the new proposed kinetic modelling approach presented by (Pijolat & Favergeon, 2018) to analyze solid-gas phase reactions. Chemical kinetics cannot be utilized for heterogeneous reactions the same way they are for homogenous reactions due to differences in mechanisms of reaction intermediates. Oxidation reactions approaches are lacking due to not accounting for the various solid shapes other than planar type and negligence of the nucleation step. For these reasons, it was deemed crucial that a new approach must be put forward that is general for all gas-solid reactions regardless of solid morphology and the reaction nature. Two assumptions are critical to initiate this systemic process: 1) all gas-solid reactions consist of the two phenomena of nucleation and growth (inward/outward); 2) diffusion, adsorption or interfacial reaction are some of the possible options for the one elementary step that makes the growth step. Modelling of the gas-solid reaction kinetics can either consider one of the previously mentioned process (slow/rate determining step) or both simultaneously which would complicate the study. This approach would be superior to the traditional Arrhenius modelling which rarely accounted for the effect of the solid morphologies on the reaction and the assumption of a constant activation energy with time, temperature and morphology changes.

One crucial condition for the kinetic modelling of heterogenous reactions is the pseudo-steady

state approximation, which concerns the reaction intermediates and their impact on its rate. In homogeneous reactions, the term $\frac{d(V[i])}{dt}$, which is a rewritten form of the change in moles by relating it to concentration (of intermediate species **i**) and volume, can be further simplified by taking out the volume variable as it is considered fixed, and the change in the intermediate species is assumed to be zero (i.e., steady state assumption). However, in the case of heterogenous reactions, the reactional zones volume may change with time (as with morphological variables), and as such, the pseudo-steady state approximation is only valid when the steady state assumption is valid AND the reactional zones volume is changing very slowly, which is true for reactions that take up to hours to reach near completion such as those concerned in this paper. Only under the pseudo-steady state approximation can we conclude that the change in the extent of reaction ζ with respect to time for both the reactant A and the product B are equal $\left(\frac{d\zeta_A}{dt} = \frac{d\zeta_B}{dt}\right)$.

The Arrhenius model was traditionally utilized in kinetics analysis of most heterogenous reactions, but this approach does not answer questions regarding the mechanism of nucleation and growth, and the popular Avrami model which became popular for well representation of sigmoidal curves makes some assumptions that are questionable such as the nucleation at the bulk as opposed to the surface, meaning the area for nucleation is not theoretically limited (infinite). Following nucleation, growth can either proceed inwards or outwards, something that is also not accounted for in the Arrhenius models. Additionally, it could be either isotropic (equal growth rate in all directions) or anisotropic (infinitely higher in direction tangential to surface than radially). All of these possible scenarios should have a profound impact on the formulation of reaction kinetic models, and yet they cannot be seen in the conventional Arrhenius model described by **Eq. 18**. The only relevant variable seen is the temperature and a function f(α) varying with fractional conversion, while the activation energy is assumed to be constant and the effect of solid morphology is imbedded in the pre-exponential factor as a fixed parameter, and not only are both changing variables with extent of the reaction, but the impact different variables have on each other is not considered. The rate equation can therefore be

separated into thermodynamic and morphological halves, one describing the impact of temperature & pressure and another the solid dimensions, respectively.

The general reaction rate equation demands that the rate-determining step approximation be accepted as it proved itself valuable for many gas-solid reactions (e.g., oxidation, chain reactions, etc.,). Some of the options for the rate-determining step include surface processes including adsorption & desorption and interfacial processes such as diffusion. Regardless of which is selected, a general expression is described by **Eq. 19**, in which the growth areic reactivity **Ø** (mol/m^2.s) denotes the thermodynamic variable which changes with temperature and partial pressure of reacting gases, and $\mathbf{S_m}$ (m^2/mol) is the morphological variable which changes with time only as the reaction proceeds and is not affected by thermodynamic parameters. For the scenario of adsorption, the thermodynamic variable is equivalent to the areic rate of adsorption/desorption $\mathbf{v_s}$ (mol/m^2.s), whereas it corresponds to the diffusion flux **J** (mol/m^2.s) in the case of diffusion-controlled determining step, and in both cases, there is a morphology variable. In order to derive the kinetic rate law for both the nitridation and hydrolysis reactions, the growth mechanism must be determined to obtain **Ø** and the morphological expression must be settled depending on the specifications of the solid material. The specific expression of the reaction rate constant above can be derived after determining 3 factors regarding the nature of the reaction that is characterized by instantaneous nucleation and slow growth: 1) whether the spread of the new product phase is inward or outward 2) what the rate-limiting step is (adsorption/diffusion/reaction) and 3) what the symmetry of the reactant particles is (spherical/planar/cylindrical).

Table 9 summarizes the solutions for the reaction rate expression from **Eq. 19** according to the different assumptions made regarding the solid particle geometry, nature of growth and direction of growth, resulting in 18 different expressions as extracted from (Pijolat & Favergeon, 2018). The derivation of each expression can be found in the original works of the authors and will not be discussed in this work, and **Table 10** explains the meaning of different symbols in the reaction rate expressions.

Table 9. The Reaction Rate Expression (dα/dt) for The 18 Different Scenarios

		Spherical	Cylindrical	Plate
Internal Interface	Inward Growth	$\frac{3ØV_{mA}}{r_0}(1-\alpha)^{\frac{2}{3}}$	$\frac{2ØV_{mA}}{r_0}(1-\alpha)^{\frac{1}{2}}$	$\frac{ØV_{mA}}{e_0}$
	Outward Growth	$\frac{3ØV_{mA}}{r_0}$	$\frac{2ØV_{mA}}{r_0}$	$\frac{ØV_{mA}}{e_0}$
External Interface	Inward Growth	$\frac{3ØV_{mA}}{r_0}(1+(z-1)\alpha)^{\frac{2}{3}}$	$\frac{2ØV_{mA}}{r_0}(1+(z-1)\alpha)^{\frac{1}{2}}$	$\frac{ØV_{mA}}{e_0}$
	Outward Growth	$\frac{3ØV_{mA}}{r_0}(1+z\alpha)^{\frac{2}{3}}$	$\frac{2ØV_{mA}}{r_0}(1+z\alpha)^{\frac{1}{2}}$	$\frac{ØV_{mA}}{e_0}$
Diffusion	Inward Growth	$\frac{4\pi l_0 r_0(1-\alpha)^{\frac{1}{3}}[1+(z-1)\alpha]^{\frac{1}{3}}}{n_0\left[(1+(z-1)\alpha)^{\frac{1}{3}}-(1-\alpha)^{\frac{1}{3}}\right]}$	$\frac{4V_{mA}l_0Ø}{r_0^2\ln\left(\frac{1+(z-1)\alpha}{1-\alpha}\right)}$	$\frac{Øl_0V_{mA}}{ze_0^2\alpha}$
	Outward Growth	$\frac{3ØV_{mA}l_0(1+z\alpha)^{\frac{1}{3}}}{r_0^2\left[(1+z\alpha)^{\frac{1}{3}}-1\right]}$	$\frac{4V_{mA}l_0Ø}{r_0^2\ln(1+z\alpha)}$	$\frac{Øl_0V_{mA}}{ze_0^2\alpha}$

Table 10. Notations for The Reaction Rate Law Expressions

Symbol	Description
Ø	The areic reactivity of growth (mol/m^2.s)
V_{mA}	The reactant solid phase's molar volume (m^3/mol)
r_0	The initial reactant solid phase particle/granule radius (m)
α	The fractional conversion (0 – 1)
e_0	The initial reactant solid phase plate particle half-thickness
z	The volume expansion coefficient
l_0	Constant length parameter equal to 1 m
n_0	The reactant phase's initial number of moles

Using the rate law expressions discussed earlier, the obtained kinetic data will be fitted into each expression to see which one's trend the data follow more closely. However, a few notes must be mentioned:

1- The expressions for the plate symmetry will not be considered as the Li metal solid phase used was granular in shape. This shape, however, depending on each granule could be

approximated to either be a cylinder or spherical to a degree for the naked eye as the granules display an irregular shape, so both cylindrical and spherical geometries are considered.

2- Diffusion-controlled gas-solid reaction expressions are also deemed to be inappropriate as many attempts to fit the reaction data have resulted in failure to obtain linear models as described by the expression

3- Reaction rate expressions for scenarios where the anisotropic growth occurs outwardly and at the internal interface are, according to the authors, not dependent on the conversion, and as such, the reaction data obtained in this study are not useful for it

Ultimately, this leaves us with only 6 rate law expressions describing the inward growth-controlled rate at the internal/external interface of the spherical/cylindrical particles (4) and the outward growth-controlled rate at the external interface of the spherical/cylindrical particles (2).

For example consider the first scenario: the gas-solid heterogeneous reaction of the nitridation of lithium can be described as inward growth-controlled and occurring at the internal interface of a spherical lithium metal particle. The reaction rate expression for such a scenario would then be the following:

$$\frac{\mathrm{d}\alpha}{\mathrm{dt}} = \frac{3\text{Ø}\mathrm{V_{mA}}}{\mathrm{r_0}}(1-\alpha)^{\frac{2}{3}}$$

$$\ln\left(\frac{\mathrm{d}\alpha}{\mathrm{dt}}\right) = \ln\left(\frac{3\text{Ø}\mathrm{V_{mA}}}{\mathrm{r_0}}\right) + \frac{2}{3}\ln(1-\alpha)$$

Where Ø is the thermodynamic variable, which should be constant for a set of reactions conducted at a fixed temperature and pressure such as those in this work, V_{mA} is the molar volume of lithium ($\approx 1.31\text{x}10^{-5}$ m^3/mol), r_0 is the radius of the lithium particle (0.00338 m) and α is the conversion. We can simply linearize the rate expression by assigning $\ln\left(\frac{d\alpha}{dt}\right)$ to be the Y-axis value and $\ln(1-\alpha)$ to be the X-axis, with Ø being the "constant" embedded in the value of the Y-intercept obtained. The slope for the $\mathrm{Y} = \mathrm{mX} + \mathrm{c}$ equation should then around 2/3, and this should be valid if the R^2 value is close 1, implying the obtained experimental data

does in fact obey the behavior of the proposed rate expression. **Table 11** summarizes the results of this model fitting for the set of experimental data conducted at 80 ^{o}C.

Table 11. Experimental Results of Lithium Nitridation (T: 80 ^{o}C, P: 1 atm)

t (min)	α	dα/dt (min-1)	Y=ln(dα/dt)	$\bar{\alpha}$	X = ln(1-α)
0	0	-	-	-	-
20	0.0268	0.001340	6.615085665	0.01340	0.013490590
40	0.0633	0.001825	6.306175292	0.04505	0.046096296
60	0.1167	0.002670	5.925676807	0.09000	0.094310679
80	0.3928	0.013805	4.282724434	0.25475	0.294035546
100	0.5713	0.008925	4.718898951	0.48205	0.657876566
120	0.7968	0.011275	4.485167394	0.68405	1.152171306

Figure 18 visualizes the model describing the Spherical-Inward Growth-Internal Interface scenario fitted into the obtained experimental results, and the data seem to conform decently, with the determination coefficient being around 0.8938, close to acceptable levels (0.9+). However, this is only an example of one scenario, and **Figure 19** contains all the 6 different models fitted into the experimental data to determine the most accurate, or at least the least inaccurate, one to explain our results.

As can be seen, all models show a generally good fit to the kinetic data, with R^2 ranging from 0.8938 – 0.9638. It should be noted that these are obtained by overlooking one of the data points (X = 0.294035546) which was deemed unusual/corrupt due to its significant effect on an otherwise consistent trend. Nevertheless, it is interesting to note that the scenarios of external interface-outward growth seems to lead to the highest R^2 value of 0.9638. This makes sense with observations made to the samples of lithium both before and after the reaction as most granules looked closer to cylindrical shape than spherical as can be seen in **Figure 12** & **Figure 16**. Additionally, in all the time experiment, the dark lithium nitride layer was observed to start from the external surface and grow outwardly which was confirmed by slicing the granules and

finding silver (unreacted) cores. Both the spherical and cylindrical models containing the same Y and X values share similar trends and the cylindrical model is selected due to the irregular cylindrical-like shape of the granules.

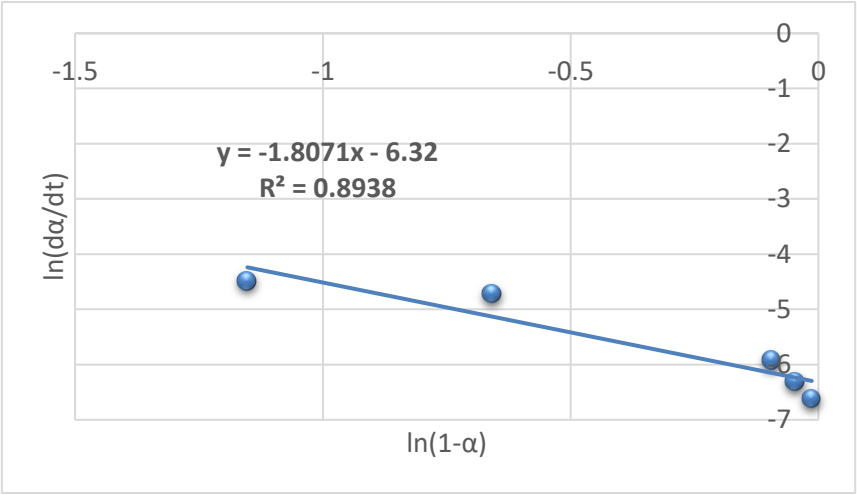

Figure 18. Fitted kinetic model of spherical particles with inward growth-controlled rate at the internal interface (T: 80 °C, P: 1 atm)

Interestingly, although the models describing inward growth at the internal interface have the lowest fit coefficient, the value of the obtained slope (-1.8) is technically "closer", albeit negative, to that in the proposed models for spherical (2/3) and cylindrical scenarios (1/2) than for the outward growth at the external interface (5.4). The latter is considered to be more accurate due to the better fit, and the expression rate is modified according to the obtained slope to describe the nature of this reaction most accurately Although not accurately predictive to a satisfactory degree, the following equation is concluded to be the "most fitting" reaction rate expression amidst the different scenarios presented for nitridation at 80 °C and 1 atm:

$$\frac{d\alpha}{dt} = \frac{2\emptyset V_{mA}}{r_0}(1 + z\alpha)^{\frac{1}{2}}$$

$$\mathbf{\frac{d\alpha}{dt} = \frac{5.3E-06(1+0.698\alpha)^{5.4}}{r_o}}$$

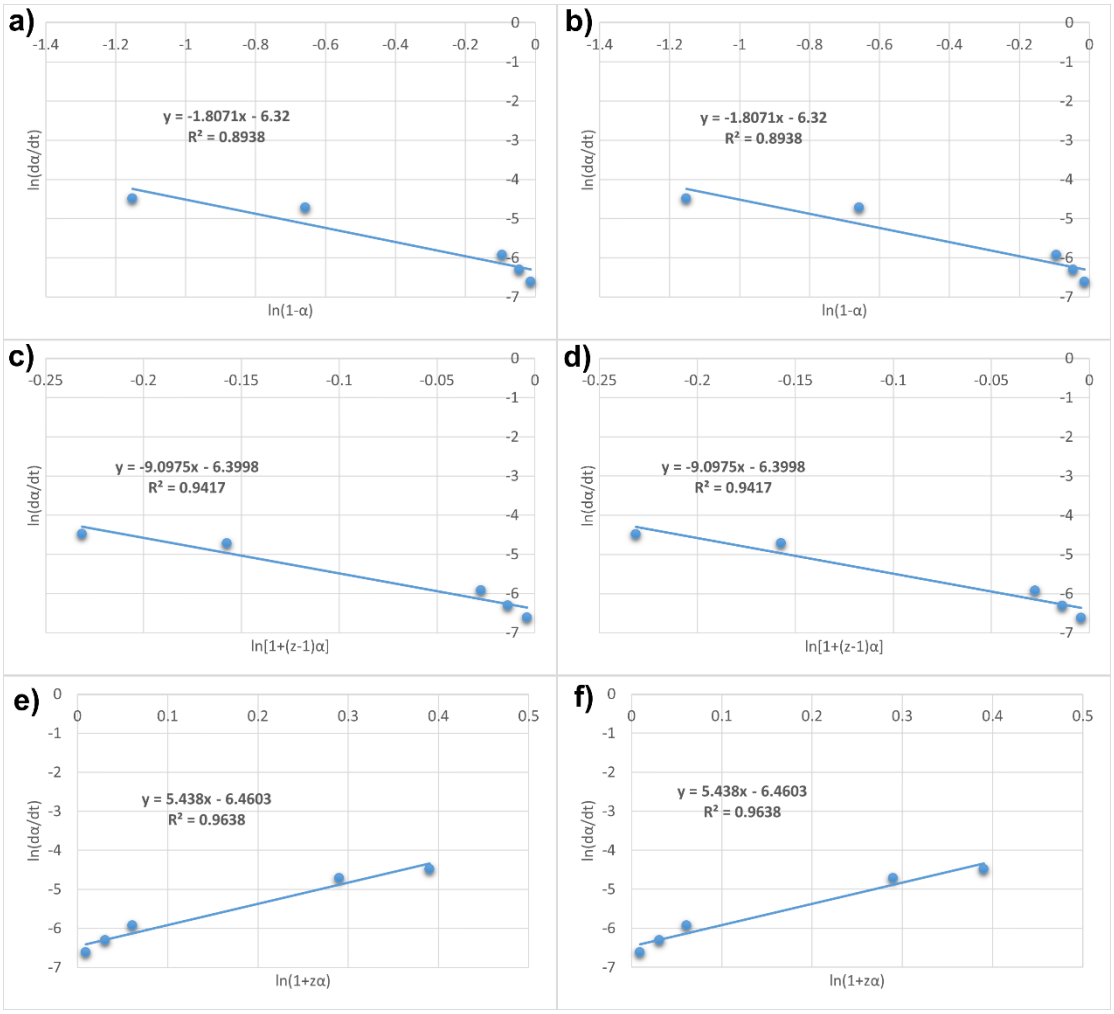

Figure 19. Kinetic model fitting into nitridation experimental data at 80 °C and 1 atm under the assumptions of a) spehrical-internal interface-inward growth b) cylindrical-internal interface-inward growth c) spherical-external interface-inward growth d) cylindrical-external inerface-inward growth e) spherical-external interface-outward growth f) cylindrical-external interface-outward growth.

3.2 Hydrolysis of Lithium Hydroxide

3.2.1 Temperature & Heating Rate Experiments

The temperature, duration of heating, number of filters and extent of reaction are strongly correlated to each other. To better understand this, consider an experiment conducted with just 1 filter holding the sample with the heater set to 60 °C and a reaction time of 40 minutes. Noticeable amounts of vapor shortly started evolving out of the reactor, indicating a violent reaction, and further examination of the water vapor source, which was now white-ish in color,

showed that some of the solid reactant fell into the liquid phase upon interacting with the vapor in addition to most solid in the filter turning to lithium hydroxide (conversion occurred). To remedy this, a second filter was installed to prevent lithium nitride ever touching the water phase and ensure the solid only reactor with the vapor phase. Interestingly, when conducting the same experiment with two filters for 30 minutes, no change in the powder color occurred, and when left further for 30 more minutes and the temperature raised to 80 ^{o}C, the sample turned white. This could imply a second filter hindered the movement of moisture which prevented the conversion, a problem that could either be solved by longer reaction times to allow vapor build in the bottom half of the reactor until it forces its way through the filters, or increased set temperature to achieve a similar outcome. Additionally, this investigation prompted another important question, whether or not to preheat the liquid phase prior to initiating the experiment. Twin experiments were conducted at 80 ^{o}C for 30 minutes, with the first having no preheating step and the second containing the preheating of water up to the reaction temperature prior to sample installation and reaction start. In the first experiment, almost all powder was dark in color, containing only a faint trace of white layer after only 30 minutes, while for the second experiment, not only did most of react with the water vapor, but the filter also showed burn signs as can be seen in **Figure 20**. It is thus concluded that gradual heating of water is more ideal, not only for safety purposes, but also because reacting the solid sample with hot vapor instantly causes an immediate, quick and violent reaction that could damage the equipment and ruin the sample itself. From thereafter, experiments would be conducted such that reaction times include the gradual heating of water. For example, a 40-minute hydrolysis at 80 ^{o}C does NOT mean solid samples reactor with water vapor at 80 ^{o}C for 40 minutes, rather the experiment setup was assembled at room temperature and then mounted on the heater at 80 ^{o}C for 40 minutes. This distinction is important because for this approach, one must consider the rate of heating inside the reactor, and **Figure 21** highlights the change in temperature with time for the heater set temperatures of 40, 60 and 80 ^{o}C, matching the conditions of the next three experiments. As can be seen in the heating rate figure below, it takes around 30 minutes for the temperature inside the reactor to reach a stable value after

which the cooling effect from the surrounding environment equals the heating rate, and the actual temperatures corresponding to the heater's set temperatures of 40, 60 and 80 ºC are 32, 45 and 58 ºC, respectively. For future knowledge, the temperature points will be referenced by the set temperature (ST) of each trial, and the heating curve can be used to identify the actual temperature of the water.

Figure 20. Burned filter and sample

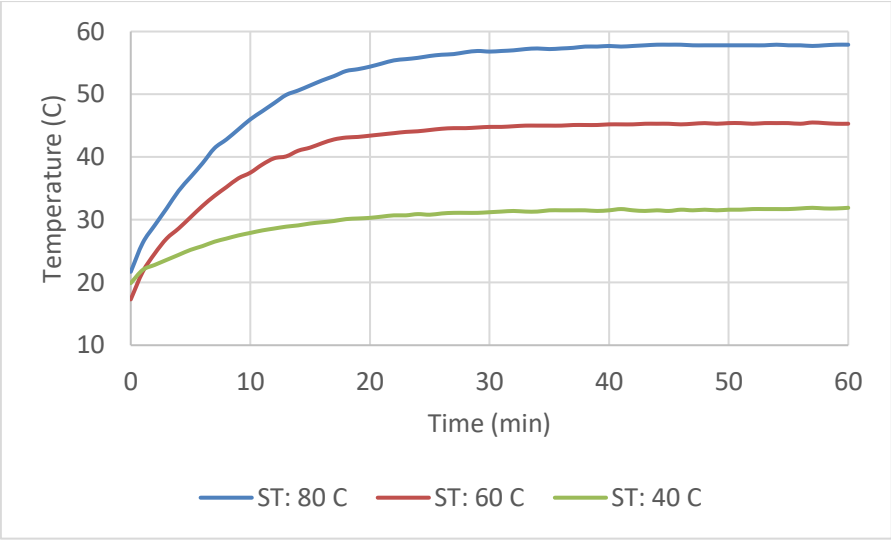

Figure 21. Reactor gradual temperature increase (ST: heater's set temperature)

Following observation of the heating curves' behaviors, hydrolysis experiments were conducted for the three different set temperatures, and the CHNS analysis results are summarized in **Table 12**. The main reasoning behind investigating the lithium nitride conversion and ammonia production at the different temperatures has to do with the fact that optimum nitridation conversion/performance often occurs after passing the 2 hours mark as seen in previous results. In the context of designing a fully integrated process that combines all the different steps of the Li-Cy, the operation time of each step is not a free variable but is rather restricted by the time of the other steps along with some operational parameters such as the number of reactor beds/columns. For practical purposes, it is important that the ideal temperature selected of the regeneration step is one such that the solid is almost entirely converted by the time the flow of natural gas containing nitrogen is redirected to it once again in the cycling between the different consumed/fresh beds. Since nitridation experiments showed the 2-hour mark to be an important one, and since regeneration is consisted of two steps: the hydrolysis and electrolysis, a 1-hour period was initially selected as the reaction time to observe the extent of hydrolysis reaction for the different STs of 40, 60 and 80 ^{o}C. the nitrogen (N) and hydrogen (H) content (wt%), lithium nitride conversion (LNC%) and theoretical ammonia production (AP) are included in the table below, and we can conclude some important statements from them. Firstly, a ST of 40 ^{o}C is too low for any meaningful conversion to occur since only around 15% is witnessed after 1 hour, and while increasing the reaction time to 2 hours is expected to improve it, it would not do so to a satisfactory extent. In a way, the same can be said for 60 ^{o}C, albeit it gives more acceptable results. On the other hand, ST value of 80 ^{o}C achieved high conversions in the 60 – 70% range, which means we can expect conversion at this temperature point to reach near complete with doubling of reaction time, implying it is the ideal temperature for hydrolysis. Secondly, looking at the uniformity/deviation of nitrogen and hydrogen content measurements, we can see that selection of nitrogen as an indirect indicator of reaction extent was the right choice because its values are higher and easily distinguishable from different others at different temperatures, leaving little room for error, and the different nitrogen measurements for multiple replicates of the same sample/trial show little

variation compared to their values. Additionally, hydrogen measurements seem to be erratic and unpredictable, as can be seen in the hydrogen contents of replicates R2 and R3 of experiment #2 and R1 and R2 of experiment #3 where H% varies to a greater relative extent than N%. The simplest explanation for the unreliability of H% measurements is the interruption caused by moisture in the sample, which always existed to a very small extent regardless of how dry the product was. Nitrogen in the sample, on the other hand, can only exist in the form of lithium nitride (Li_3N), and hence it is more reliable. It is interesting to note that a sudden jump in the extent of reaction is most notable from 40 to 60 °C, implying the temperature "barrier" earlier discussed could be somewhere in that temperature range.

Table 12. Hydrolysis Results of Temperature Trials by CHNS Analysis

Experiment	Weight (mg)		Replicate		N (%)	H (%)	LNC (%)	AP (mmol/g)
	Initial	Final	Code	Weight (mg)				
#1			R1	2.002	28.02	1.97	15.02%	4.31
ST: 40 °C	132	161	R2	6.522	28.00	1.97	15.08%	4.33
t: 1 hour			R3	3.037	27.91	2.10	15.35%	4.41
#2			R1	3.453	19.86	2.52	46.29%	13.29
ST: 60 °C	137	149	R2	3.489	19.65	2.51	46.86%	13.45
t: 1 hour			R3	2.685	19.81	2.21	46.42%	13.33
#3			R1	3.248	10.10	3.13	66.90%	19.21
ST: 80 °C	129	170	R2	6.341	10.30	2.90	66.25%	19.02
t: 1 hour			R3	5.493	10.00	2.98	67.23%	19.30

3.2.2 Reaction Time Experiments

As 80 °C was determined as the ideal temperature point for hydrolysis of lithium nitride to lithium hydroxide (LiOH), reaction time experiments were conducted on this temperature to study the extent of lithium generation given the time constraints in future reactor designs. Fortunately, the hydrolysis reached near completion (98%) after only 2 hours of reaction time, which is around the same time for nitridation, but the conversion is much higher. The detailed results are summarized in **Table 13**, which shows the determined nitrogen and hydrogen

content in the consumed Li_3N samples after hydrolysis at different times (0 – 120 minutes). A similar trend is observed for time and conversion, with progressively lower nitrogen content and higher hydrogen content detected by CHNS analysis with higher hydrolysis times. Again hydrogen cannot be relied upon for calculation of conversion as seen from the relatively significant margin of error calculated from multiple sample replicates compared to the content value. Initially, nitrogen content in a pure Li_3N sample is around 40 wt%, and it is detected at around 26 wt% after only 20 minutes of reaction, indicating the presence of LiOH molecules in the sample even if they cannot be visually seen in **Figure 22**, which shows the change in Li_3N powder surface color with increased hydrolysis time. After 2 hours, LNC% and AP reach near the maximum values of 98% and 28 mmol/g, respectively.

Table 13. Summary of Analysis Results, LNC% and AP for The Time Trials

Time (min)	Weight (mg)		N%	H%	LNC (%)	AP (mmol/g)
	Initial	Final				
20	121	139	26.1 ± 0.2	1.9 ± 0.5	25.4 ± 0.5	7.3 ± 0.1
40	122	162	16.1 ± 0.4	2.6 ± 0.4	46.7 ± 1.2	13.4 ± 0.3
60	122	193	8.7 ± 0.0	3.1 ± 0.8	65.7 ± 0.1	18.9 ± 0.0
80	119	201	4.9 ± 0.2	3.7 ± 0.9	79.3 ± 1.0	22.8 ± 0.3
100	121	222	1.5 ± 0.1	4.4 ± 0.5	93.0 ± 0.6	26.7 ± 0.2
120	122	250	0.4 ± 0.2	4.8 ± 0.3	97.8 ± 1.0	28.1 ± 0.3

One interesting fact to note is the nature of nucleation and growth of LiOH molecules on the Li_3N sample, which appears to start from the surface as can be concluded from the similarity in colors between the 80- and 120-minutes samples despite the 20% conversion difference, implying the growth mechanism is most likely inward rather than outwards which will be confirmed shortly.

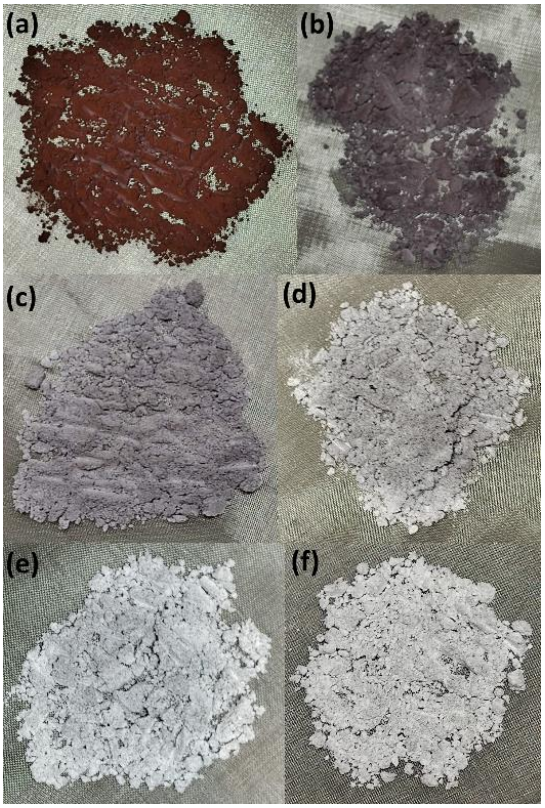

Figure 22. Change in Li_3N powder's color to LiOH for 20 (a), 40 (b), 60 (c), 80 (d), 100 (e) and 120 (f) minutes

3.2.3 Kinetic Model

A simpler approach is utilized for the hydrolysis reaction for two reasons. Firstly, we are certain of the solid phase particle's shape which is a powder, and secondly, the experimental data is more consistent, more likely due to the lower sensitivity of the samples which led to lower degree of error in obtaining the reaction kinetics. This further restricts the "viable" kinetic models to one derived from Pijolat and Favergeon's work(Pijolat & Favergeon, 2018) for powdered samples:

$$\frac{d\xi}{dt} = Ø4\pi r_0^2(1-\alpha)^{\frac{2}{3}}$$

$$\frac{d\alpha}{dt} = \frac{Ø4\pi r_0^2(1-\alpha)^{\frac{2}{3}}}{n_0}$$

$$\ln\left(\frac{d\alpha}{dt}\right) = \frac{2}{3}\ln(1-\alpha) + \ln\left(\frac{4Ø\pi {r_o}^2}{n_o}\right)$$

Fitting this model into the experimental results yields a fairly accurate predictive model for the hydrolysis of lithium nitride as can be seen in **Figure 23**, with a determination coefficient of 0.9959. The slope of the curve from the experimental results, which according to the kinetic model should be 2/3 (0.6667) is found to actually be 0.5698. The deviation of the coefficient of determination and the slope, albeit occurring, is still small considering human and systemic errors encountered in reaction experiments.

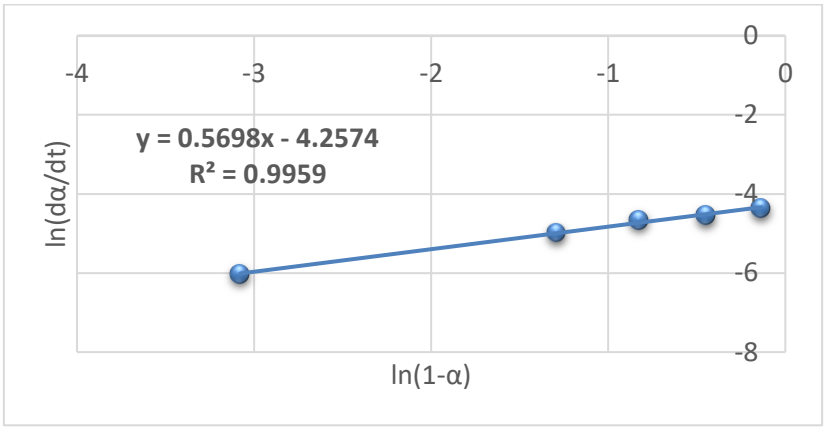

Figure 23. Fitted kinetic model for powdered samples for the hydrolysis of lithium nitride at 80 ^{o}C and 1 atm

Using the Y-intercept value, we can then simply find the value of the thermodynamic variable (i.e., the areic reactivity of growth) which is determined to equal approximately 126 mol/m^2.min, and the reaction rate expression is as follows:

$$\ln\left(\frac{4\emptyset\pi {r_o}^2}{n_o}\right) = -4.2574 \rightarrow \emptyset = \frac{n_o e^{-4.2574}}{4\pi {r_o}^2} = \frac{\frac{0.121\ g}{34.83\frac{g}{mol}} * e^{-4.2574}}{4\pi * (0.000177\ m)^2} \approx 125\frac{mol}{m^2.min}$$

$$\mathbf{\frac{d\xi}{dt} = 1570 r_0^2 (1-\alpha)^{0.57}}$$

CHAPTER 4: ECONOMIC CONSIDERATIONS

The primary appeal of the proposed Li-Cy is the upfront nitrogen removal in the LNG production line. Liquefaction occurs in the cold section of conventional LNG plants. In this section, the gas stream is mostly composed of nitrogen and methane. The gas stream is cooled by a complex web of heat exchangers, pumps and compressors, fractionation units and phase separation units which use the propane and refrigerant cycles. According to (Pal et al., 2021), the energy cost of the cold section is reported to be approximately 60%. However, the cost can be optimized with improved resource management, structural design changes, and mathematical optimization techniques.

After designing a basic conventional cold section of an LNG plant, the researchers attempted to optimize the specific power consumption (SPC) of the section, which was a variable defined as the total amount of power (MW) needed for LNG production (MTPA). The researchers used the commercial simulation software Aspen HYSYS for the process design and the programming language MATLAB in which a particle swarm optimization (PSO) code was developed to maximize the SPC value of the plant. This program considered 27 parameters, including flow rate, temperature, pressure, and split fractions inside the section. The optimal model improved the LNG production capacity by 16 KTA and decreased the total power consumption and SPC by 4.83% and 5.52%, respectively. Additionally, the optimized model reduced the compression power requirements for fuel gas and mixed refrigerants by 56.1% and 2.1%, respectively.

While these results are promising for the cryogenic distillation process, the potential energy savings are limited. In contrast, employing an NRU to remove nitrogen from the hot section could reduce the load needed for the expensive refrigerant and propane cycles, which are the main sources of the high energy requirements. As nitrogen is present throughout the entire cold section in high quantities, it significantly adds to the load in the cold section. Removing the nitrogen almost entirely or partially before entering the cold section removes the dead volume that it occupies and increases the LNG capacity of the plant. For example, (Almomani et al.,

2021) reported preliminary engineering calculations that exemplified a removal of 70% of N_2 upfront at the hot section decreases the energy required for the propane/refrigerant cycle by 6.1%. According to the thermodynamic calculations, the required compression work (30% efficiency) for the upfront removal of nitrogen (70%) would require 55% of the energy. The researchers also highlighted how the modification to the process would lower the boil-off gas (BOG) in the storage and shipping stages without impairing the fuel requirements in the plant. (Mkacher et al., 2022) conducted a thorough experiment in which LNG optimization for cost PSO was performed. In the seven experimental scenarios there was a corresponding upfront nitrogen removal of 12.5%, 25%, 37.5%, 50%, 62.5%, 75%, and 87.5%. In each of these scenarios 11 variables including flow rate, temperature, pressure, and split fraction were isolated to reduce the SPC and maintain the LNG production rate and high heating value (HHV) to satisfactory industrial specifications. The optimization technique indicated that removing 87.5% of the nitrogen in the NG stream upfront would lower the total power requirement and exergy losses by 0.24% and 0.23%, respectively. Additionally, at optimal conditions, the plant can produce a 4.4% more LNG flow rate with an HHV of 1105 Btu/Scf.

Rather than replacing the conventional cryogenic distillation with a new method, using upfront removal before the cold section decreases the energy load. (Ohs et al., 2016) provides an example of an upfront NRU using selective membranes. The researchers conducted an economic analysis based on the mathematical optimization (integer programming) of methane selective and nitrogen selective membranes. The reported cost savings were 40% under optimal conditions in comparison to conventional plants. However, membrane technology has a few disadvantages such as fouling, low selectivity, and inverse selectivity. Adsorption is also an option, though it has similar problems with selectivity. In particular, most adsorbents are methane selective, which would require large quantities of adsorbent for the NG stream and drastically increase costs. Lithium chemisorption has also been proposed and experimentally shown to achieve maximum nitrogen uptake rates (Z. Li, 2018) according to the reaction's stoichiometry at significantly lower costs because the reaction can be initiated at or below 100 ℃ (hot section) following the moisture pre-treatment. Currently, there is minimal research on

the economic feasibility and challenges associated with operating a lithium-based NRU on a large scale as well as incorporating the process into an overall cycle that includes metal regeneration. However, this paper aims to address these issues.

Figure 24 illustrates the appeal of the upfront removal of nitrogen. The savings obtained in the cold section are more than enough to accommodate the upfront nitrogen removal with a net profit. For the Li-Cy, the upfront nitrogen removal unit also produces ammonia, which increases the economic value of the process but is not exhibited in the diagram.

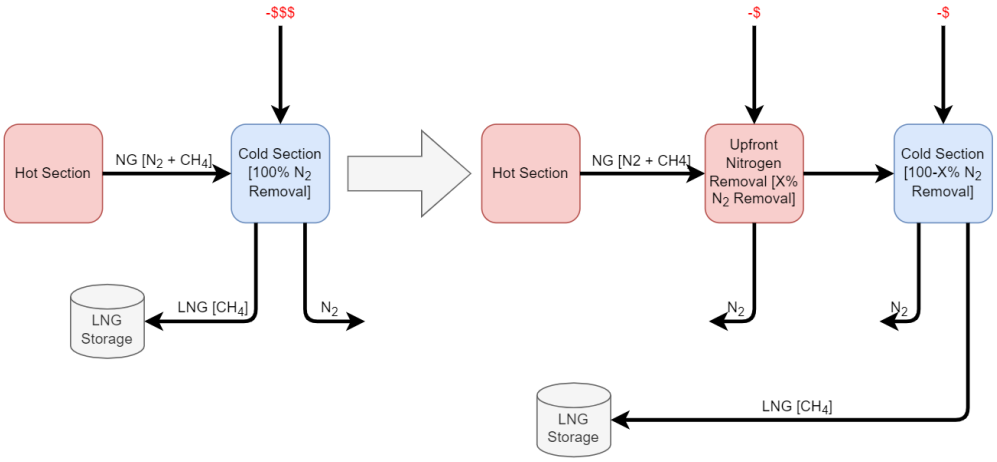

Figure 24. Block diagram visualizing the economic benefit of upfront nitrogen removal

Reaction conditions for the nitridation and hydrolysis steps in the proposed Li-Cy are not extreme. Neither step exerts pressure on the energy load. However, the opposite is true for electrolysis as costs are expected to increase for three main reasons. First, the feed flow to the electrolytic cell must be at a high temperature of up to 400 ℃, which requires heating energy. Second, the electrodes must either be replaced as the anode experiences corrosion or extracted as the cathode must have the solid deposits (i.e., layer) scraped off. Both of these procedures add to the maintenance cost and suggest that there is a need for more than one electrolytic cell to ensure continuous operation. Third, electrolysis requires a continuous supply of energy in the form of electricity to initiate the RedOx reactions, which produce lithium metal. As such, energy losses generated by Faraday/current efficiencies must be considered.

One common way to quantify the economic impact of the electrolytic cell is by determining the process energy demand, which is defined as the amount of energy (kWh) required to produce the lithium metal (kg). For example, (Takeda et al., 2014) performed LiOH electrolysis in their cycle of hydrogen storage which included hydrogenation of lithium to produce LiH, and hydrolysis of lithium hydride to produce hydrogen and LiOH, and electrolysis of LiOH. The researchers conducted four experiments with different temperatures, initial LiOH added (mols), and electrolytic baths used (LiCl-KCl vs LiCl-KCl-CsCl). The temperature, amount of LiOH, electricity passed, and current efficiency (η_c) of the cathode for the four experiments were 673, 673, 573 ^oK, 0.0194, 0.0297, 0.0196, 0.0301 mol, 1871, 2866, 1893, 2904 °C, and 84.5, 84.2, 83.8, 85.5%, respectively. The voltage for the two temperature points was 2.8 V for 673 ^oK and approximately 2.9 V for 573 ^oK. Additionally, it is important to note that the reaction stoichiometry states that for each mol of LiOH used, 1 mol of Li is deposited. The energy demand for the electrolytic cell can be calculated using **Eq. 20** provided by (Takeda et al., 2014)

$$\text{Energy Demand} = \frac{\text{Energy Used}}{\text{Lithium Deposited}} = \frac{V*Q*\frac{1\ \text{kWh}}{3.6*10^6\ \text{J}}}{\eta_c*n_{Li}*M_{Li}*\frac{1\ \text{kg}}{1000\ \text{g}}} \quad (20)$$

After conducting these four experiments, the energy demand values were 12.79, 12.84, 13.38, and 13.10 kWh/kg Li, respectively. As expected, the energy demand is less at higher temperatures because higher temperatures have been reported to decrease the reaction potential required (Takeda et al., 2014).

Beyond exhibiting high theoretical nitrogen uptake rates, the proposed lithium cycle outperforms the competition by producing ammonia as a side product through the reaction of Li_3N hydrolysis. The produced ammonia could be directed towards another process to convert it into useful products that can be sold. However, this is a low priority for the LNG plant. Instead, produced ammonia can be directly sold to other manufacturers. Though, it is difficult to precisely calculate the expected value of ammonia and ammonia-based fertilizer as market prices have exhibited significant fluctuations over the years. At the time of writing data on ammonia for Qatar was not available, though Jiang from (*Ammonia Prices Maintain Peak in Saudi, Strong Demand Pushes Up the Cost Curve*, n.d.) reports that the FOB price (Jebel Ali)

in Saudi Arabia spiked to 870 USD/T as of 17 December 2021. This price is significantly higher than the average for the past two decades. The sudden rise in ammonia prices has been attributed to the arrival of the winter season and the decline in NG storage. Moreover, as of 16 December 2020 the ammonia prices from the US Gulf Coast, Middle East, and the Far East had estimated values of 1090, 1000, and 1020 USD/T, respectively (Garg, 2021). According to (Schnitkey et al., 2021), the price of ammonia (anhydrous) has increased by 278 USD/T as of July 2021. Identical patterns were observed for ammonia-based products such as fertilizers and urea. The cost for all upfront nitrogen removal technologies can be offset by a portion of the energy savings in the propane/refrigerant cycle and the Li-Cy. Further, the production of ammonia can compensate for the cost of the electrolysis without the need to redirect the cold section costs.

A quick preliminary calculation can exemplify this point. In this scenario, we will assume the electrolysis energy demand is 13 kWh/kg Li (Takeda et al., 2014) and the electricity price is 0.036 USD/kWh according to Qatar's standards for businesses, which yields an electrolysis cost of 0.468 USD/kg Li deposited in the cathode. To calculate the economic benefit of ammonia, the price is assumed to be approximately 800 USD/T (*Global Ammonia Prices Rise in August as Supply Tightens | S&P Global Commodity Insights*, n.d.). For the stoichiometric values, **Eq. 1** and **Eq. 5** will be used.

$$\text{Ammonia Return (USD/kg Li)} = \frac{800\ \text{USD}}{1\ \text{T NH}_3} * \frac{1\ \text{T NH}_3}{10^6\ \text{g NH}_3} * \frac{17.031\ \text{g NH}_3}{1\ \text{mol NH}_3} * \frac{1\ \text{mol NH}_3}{1\ \text{mol Li}_3\text{N}} * \frac{2\ \text{mol Li}_3\text{N}}{6\ \text{mol Li}} * \frac{1\ \text{mol Li}}{6.941\ \text{g Li}} * \frac{1000\ \text{g Li}}{1\ \text{kg Li}} = 0.654$$

As the calculations exemplify, the economic value of the produced ammonia (0.654 USD/kg Li) exceeds the cost of the electricity supply for the electrolysis process (0.468 USD/kg Li). These calculations are made with the assumption of complete conversion for nitridation and hydrolysis reactions. Considering the experimentally obtained nitridation and hydrolysis conversions of 80% and 98.5%, the ammonia return is 0.515 USD/kg Li, which is still noticeably higher than the electrolysis cost energy cost. The price of ammonia can also fluctuate

over weeks, months, or years. Thus, the exact value for the net profit is difficult to pinpoint.

Figure 25 highlights a cycle with an additional step that is similar to the one proposed in this paper. (Z. Li, 2018) provided a summarized economic analysis of the proposed regeneration loop. It consisted of the nitridation of lithium to lithium nitride, followed by the hydrolysis of lithium nitride to lithium hydroxide. Thereafter, lithium hydroxide is reacted with hydrochloric acid to produce lithium chloride. Then, it is electrolyzed to obtain lithium metal for reuse to close the loop. The author made a few assumptions to make the calculation possible, including NRU feed specifications of $10N_2/90CH_4$ mol%, outlet gas specifications of $1N_2/99CH_4$ mol%, and an LNG production capacity of 5 MTPA. The nitrogen removal rate and the corresponding lithium requirement (from stoichiometry) were 99 and 149 ton/h which required three separate adsorption columns each containing 447 tons of lithium. The cycle operated for 3 hours and regenerated for 6 hours. Additionally, a one-time purchase of industrial-grade lithium metal for all the towers would cost USD 147 million assuming the price of the pure material is USD 110,000 per ton. Moreover, the hydrolysis of Li_3N requires water, but this cost is negligible because water can be supplied internally from produced water in the LNG plant (e.g., dehydration). Ammonia is expected to be produced at a quantity of 1.05 MTPA, which would generate annual revenue of USD 421 million. HC1 must also react with LiOH to form LiC1, though the cost is negligible because chloride is generated later in the electrolytic cell after which it can be made to react with excess produced water to generate HC1.

More important to this process is the cost of the electrolysis cell which is manifested in the electricity demand. With a process energy demand of 8 kWh/kg for the electrolysis of LiC1 and an electricity unit price of 0.033 USD/kWh with a methane gas turbine, the annual cost of the electrolysis is estimated to be USD 344 million for approximately 1.3 MT of lithium metal produced. The net annual profit using this Li-Cy is estimated to be around USD 77 million with the profit made from ammonia production and the cost associated with electrolysis considered. However, it should be stressed that these are preliminary calculations, and a more comprehensive economic assessment is expected to differ in many ways. For example, (Z. Li, 2018) assumes conversion in all reaction steps to be 100% as the values are extracted from

stoichiometric relations. While this assumption can be somewhat validated by laboratory experiments, large-scale application of this technology would likely show that such high values are difficult to achieve. Additionally, the price values can differ by location (i.e., a country's economy) and time (i.e., inflation). As of June 2021, the electricity price for businesses in Qatar was 0.036 USD/kWh and the average world electricity price was reported to be 0.124 USD/kWh. Considering Qatari prices is of greater relevance to this paper. As such, the electrolysis of LiC1 would cost approximately USD 375 million, which would lower the annual net profit to USD 46 million. The ammonia market price has also increased in value which correspondingly increases the appeal of this process. The process is especially appealing if the market price continues to trend upwards or stabilize above 400 USD/T. Lastly, the regeneration cycle proposed by (Z. Li, 2018) differs from the one proposed in this paper. It includes the reaction of LiOH with HC1 to produce LiC1 to be electrolyzed. In comparison, the proposed cycle electrolyzes LiOH directly which is more economical. This difference also leads to different process energy demands, which as previously noted would be 13 kWh/kg Li as reported by Takeda et al.(Takeda et al., 2014).

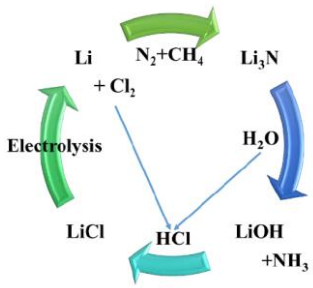

Figure 25. Lithium regeneration loop

According to the rough calculations by (Z. Li, 2018), there is an expected yearly ammonia production rate of 1.05 MT and a yearly lithium electrolysis demand of 1.3 MT. However, with more realistic numbers related to the type of electrolysis (13 kWh/kg Li), Qatar's electricity price (0.036 USD/kWh), and the current ammonia market price (800 USD/T), the annual electricity cost is expected to be USD 609 million with ammonia revenue of USD 840 million.

This equals a net profit of USD 231 million.

Error! Reference source not found. summarizes the main economic costs and benefits that have b een calculated from preliminary calculations of the annual revenue and costs of ammonia production and lithium hydroxide electrolysis respectively. These results are obtained from the hypothetical scenarios corresponding to LNG plant capacities of 1 – 5 MTPA. The conversions for all three reactions are assumed to be complete and the influent to the Li-Cy contains 5 mol% N_2 and 95 mol% CH_4, while the effluent specification is 99 mol% CH_4. Other than the complete conversion assumption, it should be noted that these numbers do not represent the ultimate profit value for the entire plant as doing so would require a more in-depth techno-economic analysis of equipment capital cost, operation and maintenance requirements and adjusting to inflation for both basic scenarios (traditional liquefaction) and upfront nitrogen removal, while also calculating the energy savings made in the liquefaction section, which was done recently by (Pal et al., 2023). These results merely represent the attractiveness of ammonia production as a side product when compared to electrolysis economic losses. Even if one were to assume other costs associated with equipment installation and maintenance of Li-Cy would offset revenue made by selling ammonia, the main benefit of this proposed cycle remains to be the profits made in the liquefaction section in which high volumes of nitrogen no longer exists, which leads to lower costs of mechanical energy requirements in the refrigerant/propane cycle due to the decrease of the volume nitrogen previously occupied.

Table 14. Summary of The Main Economic Benefits of Ammonia

LNG Capacity (MTPA)	Ammonia Production (TPA)	Ammonia Revenue (USD)	Lithium Consumption (TPA)	Electrolysis Cost (USD)	Net Profit (USD)
1	9.0E04	$72MM	1.1E05	$51MM	$21MM
2	1.8E05	$144MM	2.2E05	$103MM	$41MM
3	2.7E05	$216MM	3.3E05	$154MM	$62MM
4	3.6E05	$288MM	4.4E05	$206MM	$79MM
5	4.5E05	$360MM	5.5E05	$257MM	$103MM

A more detailed techno-economic analysis of using the Li-Cy was recently conducted by (Pal et al., 2023) and their findings are summarized in Error! Reference source not found. which i ncludes the profits calculated when the UNR achieved is 12.5 – 87.5% compared to the basic scenario where the stream is directly fed to the liquefaction cycle for different LNG prices. Information on the detailed cost analysis conducted by the authors can be found in their work and the process parameters they used for the Li-Cy were extracted from other previous sources (Afzal & Sharma, 2018; Jeppson et al., 1978; Kherdekar et al., 2021; Z. Li, 2018; McEnaney et al., 2017; Stinn & Allanore, 2020; Takeda et al., 2014). While their results do confirm the positive effect of the Li-Cy on the plant, some criticisms are in order. Firstly, some of the process parameters such as the lithium bed L/D ratio and porosity are assumed to be equal to that of beds from studies that do not involve the use of lithium, let alone the formation of lithium nitride by reacting with nitrogen from NG. (Kherdekar et al., 2021) determined the optimum L/D ratio for a catalytic water gas shift (WGS) reaction bed, while (Afzal & Sharma, 2018) assume the bed porosity to be 0.5 for a Ti bed for hydrogen storage which is more forgivable for the lithium nitridation reactor due both being metals despite the differences in properties. Additionally, process parameters obtained from (Z. Li, 2018) such as ammonia prices and electricity costs are not based on the value reflected in Qatar, which would require modifications as previously stated, and the electrowinning electricity demands were for the electrolysis of LiCl and not LiOH. The author also specifies 3 fixed bed reactors (FBRs) to be used; each 3 hours operation and 6 for regeneration, but they never explain the reason for such selection and whether or not 3 beds are necessary compared to 2 beds for example. Finally, the results in Error! Reference source not found. are obtained under the same assumption made in t his section and previous source papers on the subject, which is the complete conversion of lithium-to-lithium nitride. If the complete conversion is deemed impractical in large-scale applications of this technology, then additional lithium must be supplied to maintain the same nitrogen removal rates, and lower quantities of ammonia are expected to arise which would lead to lower returning revenue from their sale.

Table 15. Percentage Increase in Annual Profits

UNR	LNG Price ($/MBTU)				
	7	9	11	13	15
12.5%	0.10%	0.16%	0.20%	0.23%	0.25%
25.0%	0.94%	1.00%	1.04%	1.07%	1.09%
37.5%	0.87%	1.02%	1.11%	1.18%	1.22%
50.0%	1.89%	2.09%	2.21%	2.29%	2.35%
62.5%	1.87%	2.15%	2.32%	2.44%	2.53%
75.0%	3.51%	3.62%	3.68%	3.73%	3.76%
87.5%	3.92%	4.07%	4.16%	4.22%	4.27%

CHAPTER 5: PROSPECTS, LIMITATIONS AND FUTURE CHALLENGES

The performance of the proposed lithium-based cycle must be tested to ensure its reliability. This is accomplished by analyzing potential approaches and examining the strengths, limitations, and challenges. As such, this section summarizes the relevant research outlined in **Table 3**, including setup designs, outcomes based on the reaction conditions, useful analysis, calculation approaches, issues that should be avoided, and challenges to overcome.

5.1 Nitridation

For the nitridation of lithium reaction, the theoretical work exhibited a binary mixture stream containing 10% nitrogen and methane, which can be effectively separated within 70 minutes at 35 °C and 0.1 MPa by lithium (moisture-pretreated) with Li_3N received as a solid (Q. Gu et al., 2018). According to (Jain et al., 2017) the reaction can also be conducted at 55°C and 0.8 MPa and completed within 15 minutes. Another experimental work conducted at atmospheric pressure indicated more than 80% conversion from lithium to ammonia, which can be achieved after 30 minutes at 100 °C (McEnaney et al., 2017). Moreover, 100% conversion can be achieved after 12 h at 22 °C (McEnaney et al., 2017).

The reaction can thermodynamically proceed with 0.1 MPa, however, it needs to be initiated by a high pressure because it has an activation barrier (Jain et al., 2017). Conversely, the lithium can be heated to a higher temperature, which reduces the needed pressure (Jain et al., 2017). The temperature and pressure play a significant role in the reaction and the time it takes to complete. Thus, a decision must be made regarding the pressure and temperature range that should be experimentally tested. Though it is preferable for the reaction to occur at a moderate temperature and pressure as this requires less time and exhibits high values of conversion. A set of experimental trails can be started from an experiment conducted at atmospheric pressure and room temperature. Then, the conditions of the next experiment should have one parameter (e.g., pressure) that is constantly maintained and the other (e.g., temperature) increased by small intervals while observing the conversion values and the time required for complete conversion. Thereafter, the effect of the previously constant parameter (e.g., pressure) should be studied by

varying it and keeping the other parameter (e.g., temperature) constant. Again, the conversion time and values should be recorded.

The theoretical calculations and models can be conducted in parallel with the performed experiments to gain reliable insights into the accuracy of the experiments. The DFT is an example of theoretical work that can be conducted and used for reactivity analysis. The temperature-programmed kinetic Monte Carlo calculation method can also be used for analyzing lithium separation from nitrogen in the NG stream (Q. Gu et al., 2018). Beyond theoretical methods, experimental analysis techniques are equally beneficial and essential for the confirmation of the lithium transition to lithium nitride. The effect of different reaction conditions on the nitridation reaction can be obtained using DSC and the product of the reaction can be identified using XRD.

The moisture pre-treatment of lithium can support the nitridation step for the needed activation energy. The pre-treatment step avoids the requirement for a high temperature and pressure by releasing the required energy to overcome the activation barrier (Q. Gu et al., 2018). The moisture pre-treatment also creates active sites for the reaction to occur (Z. Li, 2018). For the experimental setup, the nitridation of lithium reaction can be conducted in a differential scanning calorimetry (Jain et al., 2017) or a purged tube furnace under the atmosphere of nitrogen (McEnaney et al., 2017).

5.2 Hydrolysis

For the hydrolysis of the lithium nitride reaction, (Jain et al., 2017) showed that the most optimized conditions were 80 ℃ and 0.1 Pa with a 95% consumption of lithium nitride after 2 hours. More than 80% of the conversion from the lithium sample to ammonia can be achieved after 30 minutes when the nitridation reaction is conducted at a temperature of 100 ℃ under an atmospheric pressure nitrogen stream (McEnaney et al., 2017). Additionally, an experimental setup can act as a reactor system with a closed chamber and vacuum pressure of 0.1 Pa, which produces water vapor to react with the lithium nitride placed above it (Jain et al., 2017). A scintillation vial that contains 10 mL of de-ionized water can also be used (McEnaney et al., 2017).

However, both setup configurations need further modification because they seem to be impractical. For instance, vacuum pressure is energy-demanding and the reaction of lithium nitride with water is not advisable. Using liquid water in the hydrolysis reaction causes an immediate dissociation of the ammonia formed in situ and the remaining ammonia is dissolved in water because the reaction is highly exothermic (Jain et al., 2017). As such, the hydrolysis reaction requires more work as the setup and conditions cannot be confirmed. Additionally, the authors mention the pressure inside the reactor increased significantly from 0.1 Pa to 0.8 MPa, which when considering the application in an LNG plant where the dehydration unit before the Li-Cy can vary between 70 – 200 bar (Netušil & Ditl, 2012) is very worrying. This increase in pressure is explained by the evolution of large amounts of hydrogen gas besides ammonia in the product inside the closed reactor chamber which the authors suggest is the result of water reacting with pure lithium, but given the sample, they performed the reaction on is almost pure lithium nitride ($\geq$ 99.5%), it is still odd and yet unexplained how such quantities of hydrogen gas were detected by gas chromatography. Nevertheless, because the pressure increase is caused by the production of gaseous products, such pressure changes inside the reactor in the proposed cycle could easily be controlled by continuous extraction of the evolved gases to maintain operating pressure at acceptable levels, and in the rare case of an emergency (pressure build-up) by pressure relief valves. While not the goal of the proposed cycle, if the production of hydrogen is confirmed to be inevitable under this pressure, it could serve as an additional economic benefit, seeing how hydrogen as a source of alternative fuel is picking up speed (Manoharan et al., 2019; Singla et al., 2021). Although in this work the hydrolysis of lithium nitride reaction is proposed by reacting lithium nitride with water, other research has highlighted the reaction between lithium nitride and other sources of protons such as sulfuric acid (Kim et al., 2018) and ethanol (Lazouski et al., 2019). Furthermore, H_2 was used to react with lithium nitride to produce ammonia (Goshome et al., 2015; Yamaguchi et al., 2020). However, the other product from the reaction was not lithium hydroxide, consequently, the third step in the cycle was quite different than the electrolysis of lithium hydroxide. For future research, the hydrolysis reaction requires greater analysis as well as the examination of possible

alternatives to water as the source of protons for the hydrolysis reaction.

Two analysis approaches can be used for this reaction including a gas chromatography system connected to the experimental setup to analyze the reaction products, and XRD analysis to identify the products after the reaction (Jain et al., 2017). Two analysis techniques can be conducted at this stage. First, UV-Vis spectroscopy is used to detect and verify the presence of ammonia. Second, FTIR spectroscopy helps to confirm that the generated ammonia comes from the nitrogen provided in the experiment and not from other sources (McEnaney et al., 2017). Further research should be carried out to understand the possibility of applying these techniques to identify the presence of ammonia and lithium as well as to confirm the source of nitrogen is the one supplied for the experiment. Additionally, as a safety precaution, reaming lithium in the lithium nitride sample used for hydrolysis can cause a violent reaction (McEnaney et al., 2017). Before the hydrolysis reaction, ensuring the full conversion of lithium-to-lithium nitride is essential.

5.3 Electrolysis

For the electrolysis of the lithium hydroxide reaction, the potential diagram was constructed for a Li-O-H system depending on the thermodynamic data (Barin, 1995), as shown in **Figure 26**. It showed that obtaining lithium from lithium hydroxide requires no direct contact between them because the deposited lithium reacts with the lithium hydroxide to generate lithium oxide and hydrogen (Sato & Takeda, 2013). As described by **Eq. 11**, the lithium oxide precipitates on the cathode which affects the normal accumulations of produced lithium on the cathode (Tang & Guan, 2021). To explain, for the experimental setup the lithium hydroxide must only be placed on the anode to ensure there is no interference with the lithium deposition on the cathode. Additionally, there is concern regarding the handling of lithium hydroxide as it can easily absorb carbon dioxide from the atmosphere (Sato & Takeda, 2013).

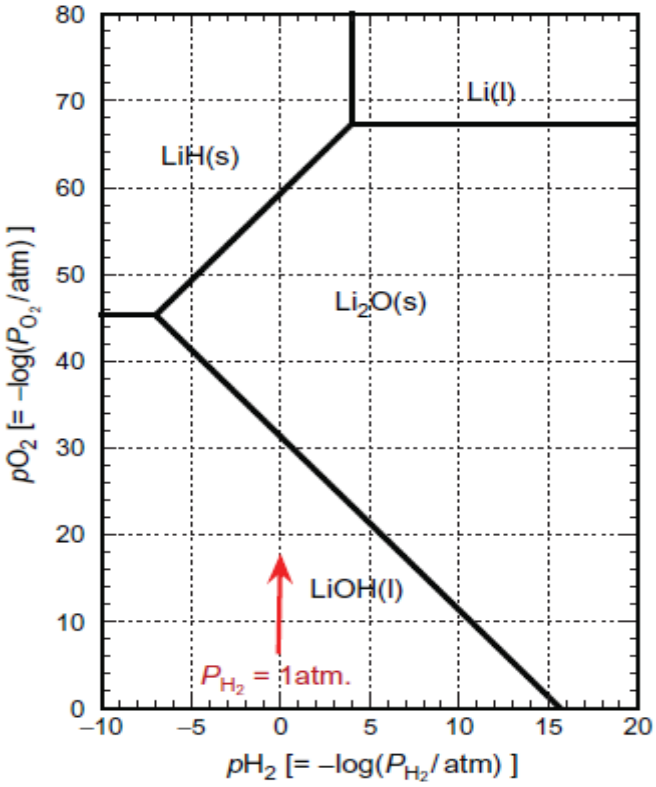

Figure 26. Li-O-H system's potential diagram

For the obtained outcomes, a current efficiency of 37.9% was achieved by the lithium hydroxide electrolysis at 380 °C using the molten salt LiOH–LiCl (70% – 30% mol ± 1%) mixture (Laude et al., 2010). In comparison, a cathode current efficiency of 84 – 86% was obtained using LiCl−41 mol% KCl or LiCl–17mol% KCl–26 mol% CsCl as the molten salt, which has a high decomposition potential for the electrolysis of lithium hydroxide at 548–673 °K (274.85–399.85 °C) (Takeda et al., 2014). Although the molten salt mixture of LiCl–KCl/LiOH–LiCl has lithium hydroxide as a component, an 88.5% current efficiency was achieved for the lithium yield, while the lithium hydroxide electrolysis held between 400-450 °C (McEnaney et al., 2017). This occurred because the experimental setup was designed to effectively separate the lithium product from other components in the electrolysis cell to avoid potential side reactions. The molten salt mixture used for electrolysis that does not contain lithium hydroxide can mitigate undesirable side reactions and produce a relatively high current efficiency. However, the current efficiency may be higher if there is the addition of lithium hydroxide in the molten

salt mixture. This would ensure there is no direct contact between the produced lithium and lithium hydroxide.

For the experimental preparation, the molten salt preparation is highly dependent on the molten salt mixture, which each has a unique melting point. The melting points for LiOH–LiCl (70%–30% mol ± 1%), LiCl−41 mol% KCl, and LiCl–17mol% KCl–26 mol% CsCl are 325 (Levin & McMurdie, 1975), 355 and 260 (Sato & Takeda, 2013) ºC, respectively. The molar ratio for the molten salt LiOH–LiCl (63%-37% mol) has a melting point of 275 ºC (Z. Chen et al., 2021). The complete dehydration of lithium hydroxide must also be ensured (Laude et al., 2010), as it may negatively affect the electrolysis, which can be verified by XRD analysis (Takeda et al., 2014). Additionally, the experimental setup plays a vital role in the electrolysis reaction. It can be a quartz reactor surrounded by an electric furnace with an alumina crucible inside it to contain the molten salt (Laude et al., 2010; Takeda et al., 2014). It can also be an alumina crucible inserted into a heating tape or mantle in a cylindrical shape containing all the parts (McEnaney et al., 2017).

Moreover, an essential part of the electrolysis cell is the electrode, which is primarily comprised of three electrodes, including the cathode, the anode, and the reference electrode. Some electrode materials may be cause for concern such as nickel and graphite anode electrodes, which may cause corrosion when working with molten hydroxide (McEnaney et al., 2017). A graphite anode can also produce carbon dioxide emissions (Takeda et al., 2014). There are multiple analysis and measurement techniques that can be used, including cyclic voltammetry measurement to measure the potential between the electrodes, reacting lithium with water to determine the amount of lithium produced from the hydrogen generated, $Ba(OH)_2$ solution test, and/or gas chromatography to assess the generation of CO_2 (if needed), XRD analysis to measure the product phase, KI solution test to ensure there is no decomposition of the LiC1, and DSC to observe the formation of lithium around the cathode (Laude et al., 2010; Takeda et al., 2014).

Several strategies, conditions, and analysis techniques have been identified for future research, though further investigation is required to determine whether they are appropriate for

implementation, and what, if any, substitutions or modifications are required. Challenges and limitations within the three steps have also been clarified. A summary of these important points is provided in **Table 16**. Moreover, future research should focus on approaches and techniques that can be applied to achieve continuous operating cycles. Primarily, attention should be given to the transportation and preparation of the product from one step to the next. For example, experimental work by (McEnaney et al., 2017) detailed the preparation required for lithium produced from the electrolysis step to be suitable for the nitridation step. Then, designing an experimental setup that connects the three steps and collects the side products for continuous operation should be considered. The researchers also created an experimental setup for the three steps, as shown in **Figure 27**, but it needs some modification as it currently supports the reaction of lithium with water, which can cause violent reactions. Lastly, achieving a setup for the three steps would help to determine how it could be transferred to a large-scale operation.

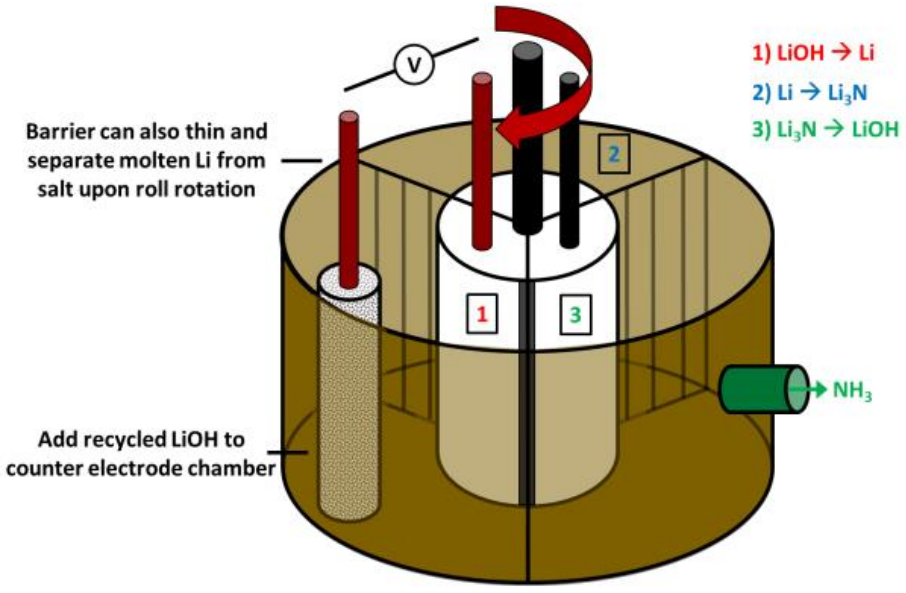

Figure 27. Potential setup considering connecting the three-cycle steps for continuous operation

Table 16. Summarized points for future work

	Reaction conditions	Setup	Possible Analysis methods or calculations	Challenges	Limitations
Nitridation	• Start with moderate values, and increase by small intervals, while observing the time and the conversion values. • Experimental setup for moisture pre-treatment.	• Differential scanning calorimetry or N_2 purged tube furnace.	• Theoretical: DFT and (TP-KMC) • Experimental: DSC and XRD	• Lithium surface activation. • Preheating lithium if it was exposed to air for a long time and no moisture pre-treatment applied.	• The activation energy of the reaction if no moisture pre-treatment for lithium. • Handling moisture-pretreated lithium.
Hydrolysis	• Reaction with water vapor instead of water under a controlled atmosphere or using another source of protons. (not confirmed)	• Reactor system with closed chamber or Scintillation vials. (not suitable setups and need modifications)	• Gas chromatography system analysis. • XRD analysis • (UV-Vis) and (FTIR). (not confirmed if suitable and needed or not)	• Suitable experimental setup. • Give attention to lithium hydroxide rather than ammonia. • Confirm the usage of water vapor if water is the source of protons.	• If the only way suitable found for hydrolysis is to apply vacuum pressure. • No lithium can remain in the lithium nitride sample

	Reaction conditions	Setup	Possible Analysis methods or calculations	Challenges	Limitations
Electrolysis	• LiCl–KCl or LiCl–KCl–CsCl (at lower temperatures) molten salt mixtures. • Investigate if the molten salt mixture of LiCl–KCl/LiOH–LiCl would produce higher current efficiency or not. • The temperature held through the electrolysis depends on the molten salt mixture used.	• Quartz reactor surrounded by an electric furnace or alumina crucible inserted in heating tape or mantle. • Electrodes choice that does not cause any or have very minimal corrosion or carbon dioxide emissions. • Molten salt preparation according to the melting temperature of the molten salt mixture.	• XRD analysis to confirm no moisture available in the preparation steps. • XRD analysis for the phases of the product. • Reacting lithium with water to know the amount of lithium produced from the water generated. • $Ba(OH)_2$ solution test evaluation CO_2 emissions. • Gas chromatography to check for CO_2 emissions. • KI solution test to check the decomposition for LiCl. • Differential scanning calorimetry (DSC) for observing the lithium disposition.	• Ensuring no direct contact between produced lithium and lithium hydroxide. • Preparing mixtures with no remaining moisture • Possible Cl_2 evolution. • Possible CO_2 emissions. • Li_2O precipitate on the cathode.	• High-temperature demand for the reaction and the molten salt preparation. • Corrosion by nickel and graphite concern. • Handling of LiOH.

CONCLUSION

The upfront removal of nitrogen gas from NG streams via the proposed lithium cycle is promising, as shown by the very high nitrogen uptake rates and ease of solid regeneration. However, more research needs to be conducted on the technical challenges and limitations of an integrated setup that connects the full cycle in one continuous mode of operation. Additionally, scaling up of this technology is bound to raise some issues, particularly surrounding the consistency of the high conversion results in a real pilot or large-scale reactor and the added economic challenges associated with them. Preliminary economic evaluation of the cost of electrolysis and the anticipated profit from ammonia production paint a positive image on the economic appeal of the Li-Cy along with the reduced energy costs in the liquefaction cycle and overall production capacity, but a detailed Life Cycle Assessment (LCA) and Techno-Economic Analysis (TEA) are needed before making any definitive statements. Finally, although this study proves the chemical affinity lithium metal has towards nitrogen gas, a thorough kinetic study of the solid-gas interaction that includes methane as well is necessary to be able to fully predict the chemical nature of this chemi-sorption in a realistic setting. Overall, this work successfully experimentally demonstrates the feasibility of the Li-Cy by showing the high chemical conversions obtainable from simply laboratory equipment and it is hoped that it serves as an asset for future work in this area.

REFERENCES

Afzal, M., & Sharma, P. (2018). Design of a large-scale metal hydride based hydrogen storage reactor: Simulation and heat transfer optimization. *International Journal of Hydrogen Energy*, *43*(29), 13356–13372. https://doi.org/10.1016/J.IJHYDENE.2018.05.084

Ahile, U. J., Wuana, R. A., Itodo, A. U., Sha'Ato, R., & Dantas, R. F. (2020). A review on the use of chelating agents as an alternative to promote photo-Fenton at neutral pH: Current trends, knowledge gap and future studies. *Science of The Total Environment*, *710*, 134872. https://doi.org/10.1016/J.SCITOTENV.2019.134872

Alam, S. F., Kim, M. Z., Kim, Y. J., Rehman, A. ur, Devipriyanka, A., Sharma, P., Yeo, J. G., Lee, J. S., Kim, H., & Cho, C. H. (2020). A new seeding method, dry rolling applied to synthesize SAPO-34 zeolite membrane for nitrogen/methane separation. *Journal of Membrane Science*, *602*, 117825. https://doi.org/10.1016/J.MEMSCI.2020.117825

Almomani, F., Othman, A., Pal, A., Al-Musleh, E. I., & Karimi, I. A. (2021). Prospective of Upfront Nitrogen (N2) Removal in LNG Plants: Technical Communication. *Energies*, *14*(12), 3616. https://doi.org/10.3390/en14123616

Ammonia Prices Maintain Peak in Saudi, Strong Demand Pushes Up the Cost Curve. (n.d.). Retrieved March 3, 2022, from https://www.chemanalyst.com/NewsAndDeals/NewsDetails/ammonia-prices-maintain-peak-in-saudi-strong-demand-pushes-up-the-cost-curve-8990

Amoroso, A. J., Fallis, I. A., & Pope, S. J. A. (2017). Chelating agents for radiolanthanides: Applications to imaging and therapy. *Coordination Chemistry Reviews*, *340*, 198–219. https://doi.org/10.1016/J.CCR.2017.01.010

Baker, R. W., & Lokhandwala, K. (2008). Natural Gas Processing with Membranes: An Overview. *Industrial and Engineering Chemistry Research*, *47*(7), 2109–2121. https://doi.org/10.1021/IE071083W

Ballard, A. L., & Sloan, J. D. (2002). The Next Generation of Hydrate Prediction: An Overview. *Journal of Supramolecular Chemistry*, *2*(4–5), 385–392. https://doi.org/10.1016/S1472-7862(03)00063-7

Banger, S., Nayak, V., & Verma, U. P. (2018). Hydrogen storage in lithium hydride: A theoretical approach. *Journal of Physics and Chemistry of Solids*, *115*, 6–17. https://doi.org/10.1016/J.JPCS.2017.11.027

Barin, I. (1995). Thermochemical Data of Pure Substances. *Thermochemical Data of Pure Substances*. https://doi.org/10.1002/9783527619825

Brockhinke, A., Koppmann, J., Brockhinke, R., Kellermann, R., Eckert, H., Taroata, D., & Schmid, G. (2014). Spectroscopic characterization of lithium combustion. *MRS Online Proceedings Library 2014 1644:1*, *1644*(1), 1–7. https://doi.org/10.1557/OPL.2014.316

Cai, J., Xu, C. G., Chen, Z. Y., & Li, X. Sen. (2018). Recovery of methane from coal-bed methane gas mixture via hydrate-based methane separation method by adding anionic surfactants. *Https://Doi.Org/10.1080/15567036.2013.820233*, *40*(9), 1019–1026. https://doi.org/10.1080/15567036.2013.820233

Chang, M., Ren, J., Yang, Q., & Liu, D. (2021). A robust calcium-based microporous metal-organic framework for efficient CH4/N2 separation. *Chemical Engineering Journal*, *408*, 127294. https://doi.org/10.1016/J.CEJ.2020.127294

Chatti, I., Delahaye, A., Fournaison, L., & Petitet, J. P. (2005). Benefits and drawbacks of clathrate hydrates: a review of their areas of interest. *Energy Conversion and Management*, *46*(9–10), 1333–1343. https://doi.org/10.1016/J.ENCONMAN.2004.06.032

Chen, C., Yuan, H., Bi, R., Wang, N., Li, Y., He, Y., & Wang, F. (2022). A novel conceptual design of LNG-sourced natural gas peak-shaving with gas hydrates as the medium. *Energy*, *253*, 124169. https://doi.org/10.1016/J.ENERGY.2022.124169

Chen, Z., Wang, T., Yu, H., Guo, J., Zhong, H., Hu, C., Zhao, R., & Chen, H. (2021). Closed-Loop Utilization of Molten Salts in Layered Material Preparation for Lithium-Ion Batteries. *Frontiers in Energy Research*, *8*, 254. https://doi.org/10.3389/FENRG.2020.587449/BIBTEX

CHIE, H., KAZUTAKA, U., AKIKO, Y., AKIHIRO, N., HIDEYUKI, O., KEIICHI, I., & EIJI, Y. (2012). *Gas-Absorbing Substance, Gas-Absorbing Alloy and Gas-Absorbing Material*

(Issue US 2009/0169869 A9). https://lens.org/100-976-431-424-404

Deal, B. E., & Svec, H. J. (1953). Metal-Water Reactions. II. Kinetics of the Reaction between Lithium and Water Vapor. *Journal of the American Chemical Society*, *75*(24), 6173–6175. https://doi.org/10.1021/ja01120a019

Dong, Q., Su, W., Liu, X., Liu, J., & Sun, Y. (2014). Separation of the N 2 /CH 4 Mixture through Hydrate Formation in Ordered Mesoporous Carbon. *Adsorption Science & Technology*, *32*.

Economides, M. J., & Wood, D. A. (2009). The state of natural gas. *Journal of Natural Gas Science and Engineering*, *1*(1–2), 1–13. https://doi.org/10.1016/J.JNGSE.2009.03.005

Faraday's laws of electrolysis | Definition, Example, & Facts | Britannica. (n.d.). Retrieved November 22, 2023, from https://www.britannica.com/science/Faradays-laws-of-electrolysis

Friesen, D., Babcock, W., Edlund, D., & Lyon, D. (2000). *Liquid absorbent solutions for separating nitrogen from natural gas*. https://www.osti.gov/biblio/873042

Garg, V. (2021). *Global ammonia prices surge on European natural gas cost push*. https://www.spglobal.com/commodity-insights/en/market-insights/latest-news/energy-transition/121621-global-ammonia-prices-surge-on-european-natural-gas-cost-push

Ge, B. Bin, Li, X. Y., Zhong, D. L., & Lu, Y. Y. (2022). Investigation of natural gas storage and transportation by gas hydrate formation in the presence of bio-surfactant sulfonated lignin. *Energy*, *244*, 122665. https://doi.org/10.1016/J.ENERGY.2021.122665

Ghazi-MirSaeed, M., & Matavos-Aramyan, S. (2020). Gaseous Mixtures Separation via Chemically-Activated Nano Silica-Modified Carbon Molecular Sieves. *Silicon 2020 13:5*, *13*(5), 1331–1345. https://doi.org/10.1007/S12633-020-00529-8

Gilbertson, J. D., Szymczak, N. K., Crossland, J. L., Miller, W. K., Lyon, D. K., Foxman, B. M., Davis, J., & Tyler, D. R. (2007). *Coordination Chemistry of H2 and N2 in Aqueous Solution. Reactivity and Mechanistic Studies Using trans-Fe II (P 2) 2 X 2-Type Complexes (P 2) a Chelating, Water-Solubilizing Phosphine)*. https://doi.org/10.1021/ic061570o

Global ammonia prices rise in August as supply tightens | S&P Global Commodity Insights. (n.d.). Retrieved September 21, 2023, from https://www.spglobal.com/commodityinsights/en/market-insights/latest-news/electric-power/091923-global-ammonia-prices-rise-in-august-as-supply-tightens

Goshome, K., Miyaoka, H., Yamamoto, H., Ichikawa, T., Ichikawa, T., & Kojima, Y. (2015). Ammonia Synthesis via Non-Equilibrium Reaction of Lithium Nitride in Hydrogen Flow Condition. *MATERIALS TRANSACTIONS*, *56*(3), 410–414. https://doi.org/10.2320/MATERTRANS.M2014382

Gu, Q., Shang, J., Hanif, A., Li, G., & Shirazian, S. (2018). Theoretical Study of Moisture-Pretreated Lithium as Potential Material for Natural Gas Upgrading. *Industrial and Engineering Chemistry Research*, *57*(45), 15512–15521. https://doi.org/10.1021/acs.iecr.8b03120

Gu, Z., Yang, Z., Guo, X., Qiao, Z., & Zhong, C. (2021). Vacuum resistance treated ZIF-8 mixed matrix membrane for effective CH4/N2 separation. *Separation and Purification Technology*, *272*, 118845. https://doi.org/10.1016/J.SEPPUR.2021.118845

Hafezi, R., Akhavan, A. N., Pakseresht, S., & A. Wood, D. (2021). Global natural gas demand to 2025: A learning scenario development model. *Energy*, *224*, 120167. https://doi.org/10.1016/J.ENERGY.2021.120167

Hales, J. M., & Drewes, D. R. (1979). Solubility of ammonia in water at low concentrations. *Atmospheric Environment (1967)*, *13*(8), 1133–1147. https://doi.org/10.1016/0004-6981(79)90037-4

Hu, J., Wu, F., Gu, C., & Liu, J. (2021). Computational Design of Porous Framework Materials with Transition-Metal Alkoxide Ligands for Highly Selective Separation of N2 over CH4. *Industrial and Engineering Chemistry Research*, *60*(1), 378–386. https://doi.org/10.1021/ACS.IECR.0C05546/SUPPL_FILE/IE0C05546_SI_001.PDF

Ichikawa, T., Isobe, S., Hanada, N., & Fujii, H. (2004). Lithium nitride for reversible hydrogen storage. *Journal of Alloys and Compounds*, *365*(1–2), 271–276. https://doi.org/10.1016/S0925-8388(03)00637-6

Irvine, W. R., & Lund, J. A. (1963). The Reaction of Lithium with Water Vapor. *Journal of The Electrochemical Society*, *110*(2), 141. https://doi.org/10.1149/1.2425691

Jain, A., Miyaoka, H., Kumar, S., Ichikawa, T., & Kojima, Y. (2017). A new synthesis route of ammonia production through hydrolysis of metal – Nitrides. *International Journal of Hydrogen Energy*, *42*(39), 24897–24903. https://doi.org/10.1016/j.ijhydene.2017.08.027

Jeppson, D. W., Ballif, J. L., Yuan, W. W., & Chou, B. E. (1978). *Lithium literature review: lithium's properties and interactions*. http://inis.iaea.org/Search/search.aspx?orig_q=RN:9410560

Jhaveri, J., & Robinson, D. B. (1965). Hydrates in the methane-nitrogen system. *The Canadian Journal of Chemical Engineering*, *43*(2), 75–78. https://doi.org/10.1002/CJCE.5450430207

Kencana, K. S., Min, J. G., Kemp, K. C., & Hong, S. B. (2022). Nanocrystalline Ag-ZK-5 zeolite for selective CH4/N2 separation. *Separation and Purification Technology*, *282*, 120027. https://doi.org/10.1016/J.SEPPUR.2021.120027

Kennedy, D. A., & Tezel, F. H. (2018). Cation exchange modification of clinoptilolite – Screening analysis for potential equilibrium and kinetic adsorption separations involving methane, nitrogen, and carbon dioxide. *Microporous and Mesoporous Materials*, *262*, 235–250. https://doi.org/10.1016/J.MICROMESO.2017.11.054

Kherdekar, P. V., Roy, S., & Bhatia, D. (2021). Dynamic Modeling and Optimization of a Fixed-Bed Reactor for the Partial Water-Gas Shift Reaction. *Industrial and Engineering Chemistry Research*, *60*(25), 9022–9036. https://doi.org/10.1021/ACS.IECR.0C06042/ASSET/IMAGES/MEDIUM/IE0C06042_M048.GIF

Kim, K., Lee, S. J., Kim, D. Y., Yoo, C. Y., Choi, J. W., Kim, J. N., Woo, Y., Yoon, H. C., & Han, J. I. (2018). Electrochemical Synthesis of Ammonia from Water and Nitrogen: A Lithium-Mediated Approach Using Lithium-Ion Conducting Glass Ceramics. *ChemSusChem*, *11*(1), 120–124. https://doi.org/10.1002/CSSC.201701975

Krishna, R., & Van Baten, J. M. (2021). How Reliable Is the Ideal Adsorbed Solution Theory

for the Estimation of Mixture Separation Selectivities in Microporous Crystalline Adsorbents? *ACS Omega*, *6*(23), 15499–15513. https://doi.org/10.1021/ACSOMEGA.1C02136/ASSET/IMAGES/LARGE/AO1C02136_0014.JPEG

Kuo, J. C., Wang, K. H., & Chen, C. (2012). Pros and cons of different Nitrogen Removal Unit (NRU) technology. *Journal of Natural Gas Science and Engineering*, *7*, 52–59. https://doi.org/10.1016/J.JNGSE.2012.02.004

Laude, T., Kobayashi, T., & Sato, Y. (2010). Electrolysis of LiOH for hydrogen supply. *International Journal of Hydrogen Energy*, *35*(2), 585–588. https://doi.org/10.1016/J.IJHYDENE.2009.11.028

Lazouski, N., Schiffer, Z. J., Williams, K., & Manthiram, K. (2019). Understanding Continuous Lithium-Mediated Electrochemical Nitrogen Reduction. *Joule*, *3*(4), 1127–1139. https://doi.org/10.1016/J.JOULE.2019.02.003/ATTACHMENT/4360F83D-4D59-495F-BB6C-D965C7F87A65/MMC1.PDF

Levin, E. M., & McMurdie, H. F. (1975). *Phase diagrams for ceramists, 1975 supplement*. https://doi.org/10.2172/5784138

Li, L., Yang, L., Wang, J., Zhang, Z., Yang, Q., Yang, Y., Ren, Q., & Bao, Z. (2018). Highly efficient separation of methane from nitrogen on a squarate-based metal-organic framework. *AIChE Journal*, *64*(10), 3681–3689. https://doi.org/10.1002/AIC.16335

Li, X., Yang, S., Feng, N., He, P., & Zhou, H. (2016). Progress in research on Li–CO2 batteries: Mechanism, catalyst and performance. *Chinese Journal of Catalysis*, *37*(7), 1016–1024. https://doi.org/10.1016/S1872-2067(15)61125-1

Li, Yanmei, He, S., Shu, C., Li, X., Liu, B., Zhou, R., & Lai, Z. (2021). A facile approach to synthesize SSZ-13 membranes with ultrahigh N2 permeances for efficient N2/CH4 separations. *Journal of Membrane Science*, *632*, 119349. https://doi.org/10.1016/J.MEMSCI.2021.119349

Li, Yao, Xu, R., Wang, B., Wei, J., Wang, L., Shen, M., & Yang, J. (2019). Enhanced N-doped Porous Carbon Derived from KOH-Activated Waste Wool: A Promising Material for

Selective Adsorption of CO2/CH4 and CH4/N2. *Nanomaterials 2019, Vol. 9, Page 266*, *9*(2), 266. https://doi.org/10.3390/NANO9020266

Li, Z. (2018). *Separation of Nitrogen from Natural Gas: Conventional and Emerging Technologies*. 10–21. https://api.research-repository.uwa.edu.au/portalfiles/portal/32927788/THESIS_DOCTOR_OF_PHILOSOPHY_LI_Zhikao_2018.pdf

Li, Z., Xiao, G., Graham, B., Li, G., & May, E. F. (2019). Nitrogen Sorption in a Transition Metal Complex Solution for N2 Rejection from Methane. *Industrial & Engineering Chemistry Research*, *58*(29), 13284–13293. https://doi.org/10.1021/ACS.IECR.9B01356

Lim, W., Choi, K., & Moon, I. (2013). Current status and perspectives of Liquefied Natural Gas (LNG) plant design. *Industrial and Engineering Chemistry Research*, *52*(9), 3065–3088. https://doi.org/10.1021/IE302877G/ASSET/IMAGES/LARGE/IE-2012-02877G_0029.JPEG

Lokhandwala, K. A., Pinnau, I., He, Z., Amo, K. D., DaCosta, A. R., Wijmans, J. G., & Baker, R. W. (2010). Membrane separation of nitrogen from natural gas: A case study from membrane synthesis to commercial deployment. *Journal of Membrane Science*, *346*(2), 270–279. https://doi.org/10.1016/J.MEMSCI.2009.09.046

Lokhandwala, K., Pinnau, I., He, Z., … K. A.-J. of M., & 2010, undefined. (n.d.). Membrane separation of nitrogen from natural gas: A case study from membrane synthesis to commercial deployment. *Elsevier*. Retrieved February 26, 2022, from https://www.sciencedirect.com/science/article/pii/S0376738809007030?casa_token=vXc5Drq-vNkAAAAA:CNgBBoUpGnllWDLru42vmy2P7A4kymVZz6_byZC-B6-dqmH_i9wVTVRIaIZgbpTjayvysx3pHQ

Manoharan, Y., Hosseini, S. E., Butler, B., Alzhahrani, H., Senior, B. T. F., Ashuri, T., & Krohn, J. (2019). Hydrogen Fuel Cell Vehicles; Current Status and Future Prospect. *Applied Sciences 2019, Vol. 9, Page 2296*, *9*(11), 2296. https://doi.org/10.3390/APP9112296

Markowitz, M. M., & Boryta, D. A. (1962). Lithium Metal-Gas Reactions. *Journal of Chemical*

& Engineering Data, *7*(4), 586–591. https://doi.org/10.1021/je60015a047

Markowitz, Meyer M., & Boryta, D. A. (2002). Lithium Metal-Gas Reactions. *Journal of Chemical and Engineering Data*, *7*(4), 586–591. https://doi.org/10.1021/JE60015A047

Maroni, V. A., Beatty, R. A., Brown, H. L., Coleman, L. F., Foose, R. M., McPheeters, C. C., Slawecki, M., Smith, D. L., Van Deventer, E. H., & Weston, J. R. (1981). *Analysis of the October 5, 1979 lithium spill and fire in the Lithium Processing Test Loop*. https://doi.org/10.2172/5396630

McEnaney, J. M., Singh, A. R., Schwalbe, J. A., Kibsgaard, J., Lin, J. C., Cargnello, M., Jaramillo, T. F., & Nørskov, J. K. (2017). Ammonia synthesis from N2 and H2O using a lithium cycling electrification strategy at atmospheric pressure. *Energy & Environmental Science*, *10*(7), 1621–1630. https://doi.org/10.1039/C7EE01126A

Mcfarlane, E. F., & Tompkins, F. C. (1962). Nitridation of lithium. *Transactions of the Faraday Society*, *58*(0), 997–1007. https://doi.org/10.1039/TF9625800997

Michle, P., Loïc, F., & Michel, S. (2011). From the drawbacks of the Arrhenius-f(α) rate equation towards a more general formalism and new models for the kinetic analysis of solid-gas reactions. *Thermochimica Acta*, *525*(1–2), 93–102. https://doi.org/10.1016/j.tca.2011.07.026

Mkacher, H., AlMomani, F., Pal, A., Karimi, I. A., & Al-musleh, E. I. (2022). Roadmap toward energy-positive upfront nitrogen removal process in baseload LNG plant. *International Journal of Energy Research*. https://doi.org/10.1002/ER.7749

Montes Luna, A. de J., Fuentes López, N. C., Castruita de León, G., Pérez Camacho, O., Yeverino Miranda, C. Y., & Perera Mercado, Y. A. (2021). PBI/Clinoptilolite mixed-matrix membranes for binary (N2/CH4) and ternary (CO2/N2/CH4) mixed gas separation. *Journal of Applied Polymer Science*, *138*(14), 50155. https://doi.org/10.1002/APP.50155

Nagesh Rao, H., & Karimi, I. A. (2017). A superstructure-based model for multistream heat exchanger design within flow sheet optimization. *AIChE Journal*, *63*(9), 3764–3777. https://doi.org/10.1002/AIC.15714

Napán, R., & Peltzer Y Blancá, E. L. (2012). First-principles studies of lithium hydride series

for hydrogen storage. *International Journal of Hydrogen Energy*, *37*(7), 5784–5789. https://doi.org/10.1016/J.IJHYDENE.2011.12.117

Nasef, M. M., Nallappan, M., & Ujang, Z. (2014). Polymer-based chelating adsorbents for the selective removal of boron from water and wastewater: A review. *Reactive and Functional Polymers*, *85*, 54–68. https://doi.org/10.1016/J.REACTFUNCTPOLYM.2014.10.007

Netušil, M., & Ditl, P. (2012). Natural Gas Dehydration. *Natural Gas - Extraction to End Use*. https://doi.org/10.5772/45802

NIST Chemistry WebBook. (n.d.). Retrieved February 14, 2022, from https://webbook.nist.gov/chemistry/

Ohs, B., Lohaus, J., & Wessling, M. (2016). Optimization of membrane based nitrogen removal from natural gas. *Journal of Membrane Science*, *498*, 291–301. https://doi.org/10.1016/J.MEMSCI.2015.10.007

Ouyang, T., Zhai, C., Sun, J., Panezai, H., & Bai, S. (2020). Nanosol precursor as structural promoter for clinoptilolite via hydrothermal synthesis and resulting effects on selective adsorption of CH4 and N2. *Microporous and Mesoporous Materials*, *294*, 109913. https://doi.org/10.1016/J.MICROMESO.2019.109913

Pal, A., Al-Musleh, E. I., & Karimi, I. A. (2021). Reducing Power Use in the Cold Section of LNG Plants. *ACS Sustainable Chemistry and Engineering*, *9*(38), 13056–13067. https://doi.org/10.1021/ACSSUSCHEMENG.1C04866/SUPPL_FILE/SC1C04866_SI_001.PDF

Pal, A., Mkacher, H., AlMomani, F., Karimi, I. A., & Al-musleh, E. I. (2023). Techno-economic assessment of upfront nitrogen removal in a baseload LNG plant. *Fuel*, *331*, 125535. https://doi.org/10.1016/J.FUEL.2022.125535

Perth, Z. L.-T. U. of W. A., & 2018, undefined. (2018). Separation of Nitrogen from Natural Gas: Conventional and Emerging Technologies. *Research-Repository.Uwa.Edu.Au*. https://research-repository.uwa.edu.au/files/32927788/THESIS_DOCTOR_OF_PHILOSOPHY_LI_Zhi

kao_2018.pdf

Pijolat, M., & Favergeon, L. (2018). Kinetics and Mechanisms of Solid-Gas Reactions. *Handbook of Thermal Analysis and Calorimetry*, *6*, 173–212. https://doi.org/10.1016/B978-0-444-64062-8.00011-5

Pillai, R. S., Yoon, J. W., Lee, S. J., Hwang, Y. K., Bae, Y. S., Chang, J. S., & Maurin, G. (2017). N2 Capture Performances of the Hybrid Porous MIL-101(Cr): From Prediction toward Experimental Testing. *Journal of Physical Chemistry C*, *121*(40), 22130–22138. https://doi.org/10.1021/ACS.JPCC.7B07029/SUPPL_FILE/JP7B07029_SI_001.PDF

Qiao, Y., Yi, J., Wu, S., Liu, Y., Yang, S., He, P., & Zhou, H. (2017). Li-CO2 Electrochemistry: A New Strategy for CO2 Fixation and Energy Storage. *Joule*, *1*(2), 359–370. https://doi.org/10.1016/J.JOULE.2017.07.001

Sato, Y., & Takeda, O. (2013). Hydrogen Storage and Transportation System through Lithium Hydride Using Molten Salt Technology. *Molten Salts Chemistry*, 451–470. https://doi.org/10.1016/B978-0-12-398538-5.00022-6

Schnitkey, G., Paulson, N., Swanson, K., & Zulauf, C. (2021). *Management Decisions Relative to High Nitrogen Fertilizer Prices*. https://farmdocdaily.illinois.edu/2021/10/management-decisions-relative-to-high-nitrogen-fertilizer-prices.html#:~:text=The average anhydrous ammonia price,nitrogen above university recommended levels.

Sekhar, M. S., Unnikrishnan, M. K., Rodrigues, G. S., & Vyas, N. (2016). Chelating agents and antioxidants: Pragmatic approaches for management of Buerger's disease. *Reviews in Vascular Medicine*, *4–5*, 23–25. https://doi.org/10.1016/J.RVM.2016.04.003

Shang, J., & Shirazian, S. (2018). Facilitated Dissociation of Water in the Presence of Lithium Metal at Ambient Temperature as a Requisite for Lithium–Gas Reactions. *The Journal of Physical Chemistry C*, *122*(28), 16016–16022. https://doi.org/10.1021/ACS.JPCC.8B01817

Singla, M. K., Nijhawan, P., & Oberoi, A. S. (2021). Hydrogen fuel and fuel cell technology for cleaner future: a review. *Environmental Science and Pollution Research*, *28*(13),

15607–15626. https://doi.org/10.1007/S11356-020-12231-8/FIGURES/13

Stinn, C., & Allanore, A. (2020). Estimating the capital costs of electrowinning processes. *Electrochemical Society Interface*, *29*(2), 44–49. https://doi.org/10.1149/2.F06202IF/XML

Sun, Q., Azamat, A., Chen, B., Guo, X., & Yang, L. (2019). The effects of alkyl polyglucosides on the formation of CH4 hydrate and separation of CH4/N2 via hydrates formation. *Https://Doi.Org/10.1080/01496395.2018.1559857*, *55*(1), 81–87. https://doi.org/10.1080/01496395.2018.1559857

Sun, Q., Chen, B., Li, Y., Yuan, G., Xu, Z., Guo, X., Li, X., Lan, W., & Yang, L. (2019). Enhanced separation of coal bed methane via bioclathrates formation. *Fuel*, *243*, 10–14. https://doi.org/10.1016/J.FUEL.2019.01.045

T, F. D., C, B. W., J, E. D., K, L. D., & K, M. W. (2000). *Liquid absorbent solutions for separating nitrogen from natural gas* (Issue US 6136222 A). https://lens.org/085-293-715-272-954

Takeda, O., Li, M., Toma, T., Sugiyama, K., Hoshi, M., & Sato, Y. (2014). Electrowinning of Lithium from LiOH in Molten Chloride. *Journal of The Electrochemical Society*, *161*(14), D820–D823. https://doi.org/10.1149/2.0871414JES/XML

Tang, Z., & Guan, X. (2021). Lithium Extraction from Molten LiOH by Using a Liquid Tin Cathode. *Journal of Sustainable Metallurgy*, *7*(1), 203–214. https://doi.org/10.1007/S40831-021-00339-1/FIGURES/6

Tang, Z., Meng, X., Shi, Y., & Guan, X. (2021). Lithium-based Loop for Ambient-Pressure Ammonia Synthesis in a Liquid Alloy-Salt Catalytic System. *ChemSusChem*, *14*(21), 4697–4707. https://doi.org/10.1002/CSSC.202101571

Tu, S., Yu, L., Lin, D., Chen, Y., Wu, Y., Zhou, X., Li, Z., & Xia, Q. (2022). Robust Nickel-Based Metal–Organic Framework for Highly Efficient Methane Purification and Capture. *ACS Applied Materials and Interfaces*, *14*(3), 4242–4250. https://doi.org/10.1021/ACSAMI.1C23249/ASSET/IMAGES/LARGE/AM1C23249_0012.JPEG

V, J. A., & SAI, B. (2018). *Process for removal of nitrogen from natural gas* (Issue US 9988587 B2). https://lens.org/043-482-845-981-600

Wang, S., Guo, Q., Liang, S., Li, P., Li, X., & Luo, J. (2018). [Ni3(HCOO)6]/Poly(styrene-b-butadiene-b-styrene) Mixed-Matrix Membranes for CH4/N2 Gas Separation. *Chemical Engineering & Technology*, *41*(2), 353–366. https://doi.org/10.1002/CEAT.201700317

Wayne Ronald Irvine, by. (1961). *The reactions of lithium with nitrogen and water vapour*. https://doi.org/10.14288/1.0106079

Wu, S., Li, X., Liu, B., Wang, B., & Zhou, R. (2020). An effective approach to synthesize high-performance SSZ-13 membranes using the steam-assisted conversion method for N2/ CH4 separation. *Energy and Fuels*, *34*(12), 16502–16511. https://doi.org/10.1021/ACS.ENERGYFUELS.0C03494/SUPPL_FILE/EF0C03494_SI_001.PDF

Wu, Y. J., Yang, Y., Kong, X. M., Li, P., Yu, J. G., Ribeiro, A. M., & Rodrigues, A. E. (2015). Adsorption of Pure and Binary CO2, CH4, and N2 Gas Components on Activated Carbon Beads. *Journal of Chemical and Engineering Data*, *60*(9), 2684–2693. https://doi.org/10.1021/ACS.JCED.5B00321/SUPPL_FILE/JE5B00321_SI_001.PDF

Wu, Y., Yuan, D., Zeng, S., Yang, L., Dong, X., Zhang, Q., Xu, Y., & Liu, Z. (2021). Significant enhancement in CH4/N2 separation with amine-modified zeolite Y. *Fuel*, *301*, 121077. https://doi.org/10.1016/J.FUEL.2021.121077

Yamaguchi, T., Shinzato, K., Yamamoto, K., Wang, Y., Nakagawa, Y., Isobe, S., Ichikawa, T., Miyaoka, H., & Ichikawa, T. (2020). Pseudo catalytic ammonia synthesis by lithium–tin alloy. *International Journal of Hydrogen Energy*, *45*(11), 6806–6812. https://doi.org/10.1016/J.IJHYDENE.2019.12.190

Yousef, S., Tuckute, S., Tonkonogovas, A., Stankevičius, A., & Mohamed, A. (2021). Ultra-permeable CNTs/PES membranes with a very low CNTs content and high H2/N2 and CH4/N2 selectivity for clean energy extraction applications. *Journal of Materials Research and Technology*, *15*, 5114–5127. https://doi.org/10.1016/J.JMRT.2021.10.125

Yu, H. J., Shin, J. H., Lee, A. S., Hwang, S. S., Kim, J. H., Back, S., & Lee, J. S. (2021).

Tailoring selective pores of carbon molecular sieve membranes towards enhanced N2/CH4 separation efficiency. *Journal of Membrane Science*, *620*, 118814. https://doi.org/10.1016/J.MEMSCI.2020.118814

Zhang, C., Chen, Y., Wu, H., Li, H., Li, X., Tu, S., Qiao, Z., An, D., & Xia, Q. (2022). Mechanochemical synthesis of a robust cobalt-based metal–organic framework for adsorption separation methane from nitrogen. *Chemical Engineering Journal*, *435*, 133876. https://doi.org/10.1016/J.CEJ.2021.133876

Zhang, K., Dai, Z., Zhang, W., Gao, Q., Dai, Y., Xia, F., & Zhang, X. (2021). EDTA-based adsorbents for the removal of metal ions in wastewater. *Coordination Chemistry Reviews*, *434*, 213809. https://doi.org/10.1016/J.CCR.2021.213809

Zhang, Q., Zheng, J., Zhang, B., & Linga, P. (2021). Coal mine gas separation of methane via clathrate hydrate process aided by tetrahydrofuran and amino acids. *Applied Energy*, *287*, 116576. https://doi.org/10.1016/J.APENERGY.2021.116576

Zheng, F., Chen, L., Chen, R., Zhang, Z., Yang, Q., Yang, Y., Su, B., Ren, Q., & Bao, Z. (2022). A robust two–dimensional layered metal–organic framework for efficient separation of methane from nitrogen. *Separation and Purification Technology*, *281*, 119911. https://doi.org/10.1016/J.SEPPUR.2021.119911